USING CHEMICAL TRACERS TO ASSESS OCEAN MODELS

Matthew H. England
Centre for Environmental Modelling and Prediction
School of Mathematics
University of New South Wales
Sydney, New South Wales, Australia

Ernst Maier-Reimer
Max Planck Institute for Meteorology
Hamburg, Germany

Abstract. Chemical tracers can be used to assess the simulated circulation in ocean models. Tracers that have been used in this context include tritium, chlorofluorocarbons, natural and bomb-produced radiocarbon, and to a lesser extent, oxygen, silicate, phosphate, isotopes of organic and inorganic carbon compounds, and certain noble gases (e.g., helium and argon). This paper reviews the use of chemical tracers in assessing the circulation and flow patterns in global and regional ocean models. It will be shown that crucial information can be derived from chemcial tracers that cannot be obtained from temperature-salinity (T-S) alone. In fact, it turns out that a model with a good representation of T-S can have significant errors in simulated circulation, so checking a model's ability to capture chemical tracer patterns is vital. Natural chemical tracers such as isotopes of carbon, argon, and oxygen are useful for examining the model representation of old water masses, such as North Pacific and Circumpolar Deep Water. Anthropogenic or transient tracers, such as tritium, chlorofluorocarbons, and bomb-produced ^{14}C, are best suited for analyzing model circulation over decadal timescales, such as thermocline ventilation, the renewal of Antarctic Intermediate Water, and the ventilation pathways of North Atlantic Deep Water and Antarctic Bottom Water. Tracer model studies have helped to reveal inadequacies in the model representation of certain water mass formation processes, for example, convection, downslope flows, and deep ocean currents. They show how coarse models can chronically exaggerate the spatial scales of open-ocean convection and deep currents while underestimating deep flow rates and diffusing downslope flows with excessive lateral mixing. Higher-resolution models typically only resolve thermocline ventilation because of shorter integration times, and most resort to high-latitude T-S restoring to simulate reasonable interior water mass characteristics. This can be seen to result in spuriously weak chemical tracer uptake at high latitudes due to suppressed convective overturn and vertical motion. Overall, the simulation of chemical tracers is strongly recommended in model assessment studies and as a tool for analyzing water mass mixing and transformation in ocean models. We argue that a cost-effective approach is to simulate natural radiocarbon to assess long-timescale processes, and CFCs for decadal to interdecadal ocean ventilation.

1. INTRODUCTION

The oceans form a key component of the Earth's climate system. They have an enormous capacity to store and transport heat, absorbing vast quantities of warmth in the tropics and releasing heat at higher latitudes. They dominate the global hydrological cycle, providing reservoirs of moisture and transporting salt in vast ocean currents. The oceans also play a vital role in the regulation of atmospheric gases such as carbon dioxide, absorbing gaseous compounds at the sea surface and consuming some of them in biological processes.

To understand the role of the oceans in our climate system, computational *ocean circulation models* (terms in italic are defined in the glossary, after the main text) have been developed that predict ocean currents, temperature, and salinity (see reviews by *Bryan* [1979], *Marotzke* [1994], and *McWilliams* [1996]). These numerical ocean models are derived from the laws of conservation of mass, momentum, heat, and salt. They form a key component of coupled climate models [see, e.g., *Manabe et al.*, 1991, 1992; *Gordon and O'Farrell*, 1997; *Guilyardi and Madec*, 1997, *Johns et al.*, 1997]. Traditionally, ocean models only included temperature and salinity as tracers since these are required to determine density, which in turn influences ocean circulation. More recently, *chemical tracers* have been incorporated into ocean models for a variety of applications. These include ocean model validation efforts (e.g., CFCs, tritium, radiocarbon), studies of the *ocean carbon cycle* (e.g., carbon compounds, oxygen, phosphate, nitrate), diagnosis of model circulation mechanisms (e.g., argon), data assimilation studies (e.g., CFCs, tritium), and paleoceanographic considerations (carbon-13, oxygen-18). In this paper we review the use of chemical tracers in assessing ocean model simulations.

The rate of *ocean ventilation* associated with *water mass* formation is among the most important properties relevant to the ocean's role in climate. Rapid ventilation occurs when surface waters are removed to depth via

wind-driven or thermohaline overturning. A rapidly ventilating ocean can thereby sequester excess heat and carbon from the atmosphere by mixing these properties downward, therefore retarding climate change [e.g., *Stouffer et al.*, 1989; *Sarmiento and Le Quéré*, 1996]. Despite the importance of ocean ventilation to the global climate system, there remains uncertainty in the nature and timing of ocean renewal and how to represent this in general circulation models of the system. Geochemical tracer data provide a novel means for understanding the ocean's ventilation processes [*Jenkins and Smethie*, 1996] and how well these are reproduced in models.

Ocean modelers strive to develop and refine circulation models of the ocean. A key aspect of this is the representation of water mass formation, since this controls the removal of surface waters to greater depth and determines poleward heat and freshwater transports. Evaluating a model's ability to capture water mass formation processes relies on ocean measurements and is fundamentally limited in certain ways. For example, many processes that are linked with water mass formation, such as convection, mixing, and deep currents, are extremely difficult to measure directly. Most modelers rely on traditional hydrographic parameters, such as temperature-salinity (T-S), to provide a "proxy" means for assessment of the water mass formation processes operating in models [e.g., *Bryan and Lewis*, 1979; *England*, 1993; *Hirst and Cai*, 1994]. This is in part because temperature and salinity are prognostic variables in global ocean models and intrinsic in any definition of a water mass, so it is tempting to rely solely on them in the assessment of model water mass formation. However, they are not ideal diagnostics of model ocean ventilation. This is because they can provide only limited information on water mass formation processes, such as indicating the depth of rapid ventilation associated with surface mixing.

Chemical tracers can provide detailed information on the pathways and rates of water mass renewal beneath the surface mixed layer. Seawater carries signatures of dissolved chemical tracers, such as silicate, oxygen, phosphate, CFCs, and isotopes of carbon. The concentration of these tracers can be quite distinct for different water masses and different times [see, e.g., *Broecker and Peng*, 1982; *Libes*, 1992; *Poole and Tomczak*, 1998]. Both observationalists and modelers can exploit these properties in assessing measured and simulated oceanic circulation.

Chemical tracers that have been used to assess ocean models include tritium, chlorofluorocarbons, natural and bomb-produced radiocarbon, and to a lesser extent, oxygen, phosphate, isotopes of organic and inorganic carbon, and certain noble gases (e.g., helium and argon). The choice of tracer depends partly on the timescales of interest. For example, natural carbon isotopes, oxygen, and phosphate are useful for examining old water masses, such as North Pacific and Circumpolar Deep Water. Anthropogenic tracers, such as tritium and chlo-

rofluorocarbons, are best suited for analyzing model ventilation over decadal timescales, such as thermocline ventilation and the renewal of Antarctic Intermediate Water (AAIW). Factors determining which tracer is best suited for a given problem include the timescale of ocean entry/decay of the tracer, whether this is well known, whether the tracer is involved in biological processes, and whether the tracer is easy to measure and indeed that there are sufficient observations in the region of interest. A comprehensive summary of chemical tracers used in ocean models is given in Table 1.

The remainder of this paper is divided into seven sections. In sections 2–4 we examine the use of natural and bomb-produced radiocarbon, tritium, and chlorofluorocarbons in the assessment of model circulation and water mass formation. In section 5 we review the use of natural seawater chemistry in this context, and in section 6 we cover more exotic chemical tracers, such as inert gases and mantle helium. It will be seen that substantially more information can be derived from chemical tracers than from T-S alone. Finally, in section 7 we give an overview of the uncertainties and limitations in chemical tracer modeling, and in section 8 we offer a summary and conclusions.

2. RADIOCARBON

Radiocarbon (^{14}C) is a *radioisotope* (or *radionuclide*) of carbon. Because it is created in the atmosphere, both naturally and through human activities, and subsequently dissolved in the surface mixed layer, its natural radioactive decay in the ocean leads to a gradual differentiation of content in water masses. The longer a given water mass has been out of contact with the atmosphere, the more depleted the ^{14}C content becomes (in proportion to the concentration of ^{12}C). The half-life of ^{14}C is 5730 years, making it suitable for differentiating ocean ventilation rates over very long timescales. In addition, bomb tests during the 1950s dramatically increased the atmospheric concentration of ^{14}C, and this can be used to study shorter timescale ventilation processes.

Natural radiocarbon provides the best estimate of deep ocean ventilation rates over long timescales, say, century timescales and beyond. Modern anthropogenic tracers (e.g., CFCs, bomb-produced tritium) only resolve the decadal to interdecadal timescale. As such, radiocarbon observations provide the most stringent test of model behavior over long timescales. To date, a number of researchers have exploited ^{14}C in assessing the circulation and water mass formation in ocean models (e.g., *Maier-Reimer and Hasselmann* [1987]; *Toggweiler et al.* [1989a, 1989b] (hereinafter referred to as TDBa and TDBb; *Duffy et al.* [1995a, 1995b, 1997]; and *England and Rahmstorf* [1999]).

By convention the radiocarbon content of the ocean or atmosphere is expressed as the deviation of the ^{14}C/^{12}C ratio (in parts per thousand) from the preindustrial

TABLE 1. Chemical Tracers Used to Assess Ocean Circulation Models and/or Those Incorporated Into Biogeochemical Models[a]

Tracer	Chemical Formula	Main Sources	Properties	Measurability,[b] L	Applications	Key References
Radiocarbon	^{14}C	natural isotope and bomb-produced	5730-year half-life	0.250	natural and transient	Toggweiler et al. [1989a, 1989b]
Tritium	^{3}H	bomb-produced radionuclide	12.43-year half-life	2.5	transient (favors NH)	Sarmiento [1983]
Chlorofluorocarbons	CCl_NF_M	refrigerants, foams, solvents	stable, inert	0.030	transient	England et al. [1994]
Argon-39	^{39}Ar	natural radioactive isotope of ^{40}Ar	269-year half-life	200–1200	model diagnosis	Maier-Reimer [1993b]
Helium-3	^{3}He	seafloor volcanism, ^{3}H by-product	stable	0.100	deep-water flows	Farley et al. [1995]
Silicon-32	^{32}Si	natural radioactive isotope of ^{28}Si	120-year half-life	1000[c]	model diagnosis[c]	Peng et al. [1993]
Krypton-85	^{85}Kr	bomb-produced radionuclide	10.6-year half-life	200–1200	North Atlantic	Smethie et al. [1986]
Cesium-137	^{137}Cs	bomb-produced, Chernobyl	30-year half-life	0.030	regional models	Staneva et al. [1999]
Sulphur hexafluoride	SF_6	deliberate tracer release experiments	stable, inert	0.350	mixing estimates	Ledwell et al. [1998]
Oxygen-18	$\delta^{18}O$	natural stable isotope of ^{16}O	T/state fractionation	0.015	paleoceanographic	Schmidt [1998]
Carbon-13	$\delta^{13}C$	natural stable isotope of ^{12}C	T/productivity fractionation	0.250	paleoceanographic	Maier-Reimer [1993a, 1993b]
Phosphate	PO_4	naturally occurring nutrient	biogeochemical	0.010	carbon cycle models	Maier-Reimer [1993a, 1993b]
Nitrate	NO_3	naturally occurring nutrient	biogeochemical	0.010	carbon cycle models	Maier-Reimer [1993a, 1993b]
Silicate	SiO_2	naturally occurring nutrient	biogeochemical	0.010	carbon cycle models	Maier-Reimer [1993a, 1993b]
Oxygen	O_2	air-sea flux of gaseous oxygen	biogeochemical	0.150	carbon cycle models	Maier-Reimer [1993a, 1993b]

[a]Chemical formulae indicate the modeled isotope, compound, or ion. Chlorofluorocarbons cover a variety of species (CFC-11 (CCl_3F) and CFC-12 (CCl_2F_2) are the most common). NH refers to the Northern Hemisphere. Natural radioactive isotopes are created by cosmic rays in the atmosphere, then radioactively decay once dissolved in seawater. The stable isotope ($\delta^{18}O$, $\delta^{13}C$) fractionation effects are dependent on temperature (T), changes in state such as precipitation, evaporation and ice formation (state), and/or productivity. Key citations listed are those that describe the method of including the various tracers into ocean models, normally the first reported use of the given chemical tracer.

[b]The measurability indicator is simply the required volume of seawater to detect the chemical tracer to reasonable levels of accuracy; it should be noted that some tracers require sophisticated equipment to make such measurements.

[c]Silicon-32 is barely detectable to typical oceanic concentrations.
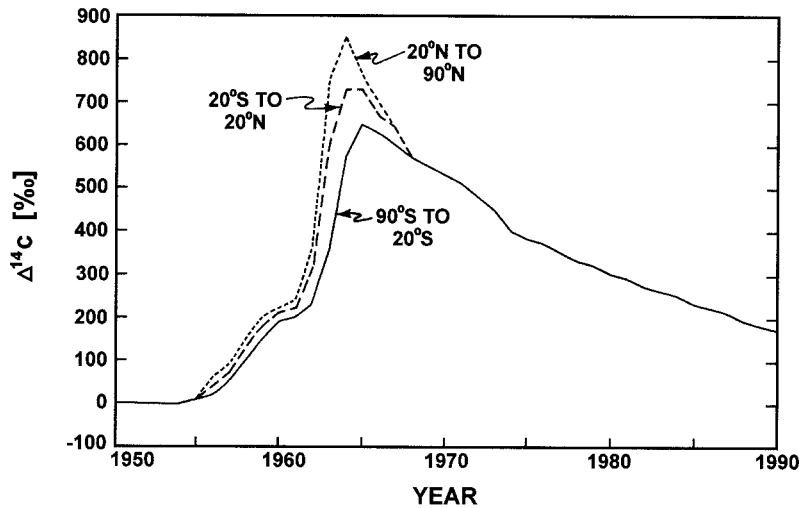
Figure 1. Time history of atmospheric $\Delta^{14}C$ (per mil) used in radiocarbon simulations.

^{14}C isotopic standard. The notation used for this difference is $\Delta^{14}C$, which is normally negative in the deep ocean as the ^{14}C isotope decays beneath the surface mixed layer:

$$\Delta^{14}C = [^{14}C/^{12}C]_{ocean} - [^{14}C/^{12}C]_{ref}$$

The more negative the value of $\Delta^{14}C$, the more time has elapsed since the water mass was last in contact with the atmosphere. The $\Delta^{14}C$ ratio is the quantity simulated in ocean models, not the absolute concentration of ^{14}C. This means that biological conversion processes can be largely ignored (within 10% error) [*Fiadiero*, 1982] because they affect ^{12}C and ^{14}C compounds in the same manner. Because $\Delta^{14}C$ simulations do not predict gas transfer on the basis of actual $^{12}CO_2$ and $^{14}CO_2$ concentration levels, isotopic fractionation between gaseous and dissolved CO_2 phases is neglected. However, measured $\Delta^{14}C$ is corrected for fractionation effects, so direct model-observation comparisons are possible.

Natural radiocarbon is therefore treated like a tracer concentration in ocean models, with the prebomb cycle of $\Delta^{14}C$ forced toward a time-independent atmospheric value of zero, typically at a rate that is wind speed–dependent and calibrated to match observed global mean gas exchange rates (e.g., experiment P′ of TDBa). Interior $\Delta^{14}C$ values then get transported by the model circulation, convection, and mixing processes, and undergo natural radioactive decay with a ^{14}C half-life of 5730 years. When simulating bomb-produced ^{14}C uptake, atmospheric $\Delta^{14}C$ is increased from zero to the estimated values resulting from nuclear weapons testing during the 1950s and 1960s (see, e.g., Figure 1). In addition, a small ($\sim25\%o$) decrease in atmospheric ^{14}C prior to the time of weapons testing can be included to take account of fossil fuel burning (which releases $^{12}CO_2$ to the atmosphere but no $^{14}CO_2$). This is known as the "Suess effect," and while it is substantially smaller than the bomb signal (up to $1000\%o$), it may be important for waters formed in the period just prior to nuclear weapons testing [see, e.g., *Toggweiler et al.*, 1991].

An example of natural $\Delta^{14}C$ simulations is shown in Figure 2, which shows the measured $\Delta^{14}C$ in the western Pacific during 1974 in the Geochemical Ocean Sections Study (GEOSECS) [*Ostlund et al.*, 1987] as well as that simulated in three natural radiocarbon simulations. Experiments C14B and C14C are from two robust diagnostic experiments wherein the interior model T-S are continuously restored toward climatological data. They differ only in that experiment C14B treats vertical diffusion rates with a depth-dependent profile (weak in the upper ocean and stronger at depth), whereas C14C adopts a constant vertical diffusivity of 1.0 cm^2 s^{-1}. Experiment P is identical to experiment C14B, except there is no interior restoring of T-S. Experiment P is therefore prognostic in its treatment of water masses; they form at the surface due to convection and vertical motions and spread laterally due to interior currents and mixing. In contrast, cases C14B and C14C artificially generate interior sources of heat and salt, so that water masses need not necessarily form at the sea surface. They can instead be created by the model's interior restoration of T-S to climatological data.

Apparent in the upper kilometer of the GEOSECS observations is the penetration of high concentrations of ^{14}C due to bomb influx of this radioactive isotope. This higher invasion of ^{14}C is simulated by TDBb (Figure 3) by running the natural $\Delta^{14}C$ simulations from 1950 onward using the atmospheric $\Delta^{14}C$ concentrations of Figure 1. Below 1 km, however, much of the observed $\Delta^{14}C$ is derived from prebomb atmospheric forcing. North Pacific Deep Water (NPDW), for example, has no traces of bomb-produced ^{14}C at the time of the GEOSECS observations. Clearly apparent in Figure 2 is the relative success of the prognostic experiment in simulating the ventilation of NPDW in contrast to the robust-diagnostic experiments. TDBa find similar results in the Atlantic Ocean, namely, that experiment P is superior to the robust-diagnostic cases. This is related to the way convection and vertical motions are suppressed in the diagnostic integrations, because water masses can be created
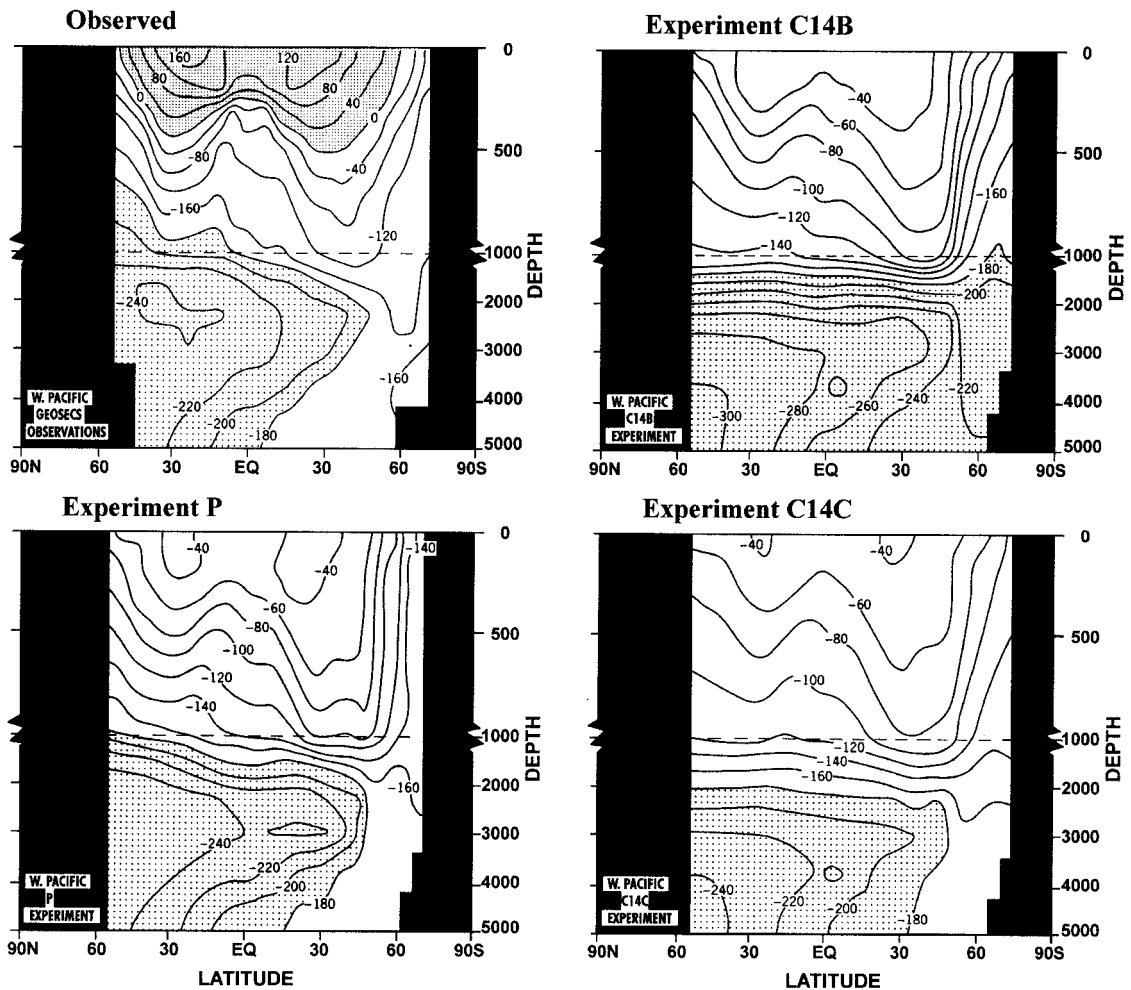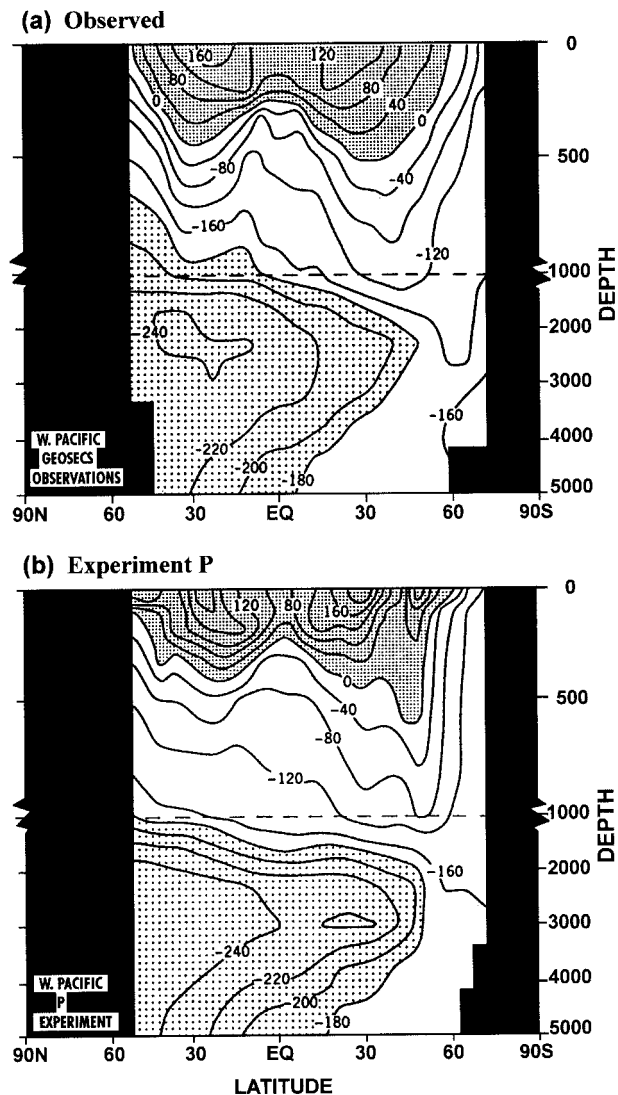
Figure 2. Western Pacific sections of Δ^{14}C (per mil) in observations (top left) and in the natural radiocarbon experiments P, C14B, and C14C of *Toggweiler et al.* [1989a]. Experiments C14B and C14C are from two robust-diagnostic experiments (Cl4B treats vertical diffusion rates with a depth-dependent profile, whereas C14C adopts a constant vertical diffusivity). Experiment P is identical to experiment C14B, only there is no interior robust-diagnostic restoring of temperature-salinity (T-S).

by the interior restoring of T-S to observations; they need not be formed at the sea surface. Indeed, surface water overturn is largely suppressed by the stable stratification that is artificially maintained through the internal restoring terms. With reduced convection and vertical motion, realistic quantities of ^{14}C do not get injected into the deep ocean, exposing a problem with the robust-diagnostic technique. One of the key conclusions of the TDB studies is therefore that a robust diagnostic simulation, in spite of a more realistic model T-S, is inferior to a prognostic run in representing important ocean ventilation processes. This result shows that geochemical tracers are an important adjunct to T-S in ocean model validation efforts, since a "correct" T-S field can theoretically support spurious circulation patterns.

Another study employing natural radiocarbon to assess model circulation and water mass formation is that of *England and Rahmstorf* [1999], who analyze idealized age and Δ^{14}C in a series of experiments with different tracer mixing parameterizations. Like TDBa, their

model is run at coarse model *resolution*, thereby requiring a *mixing* scheme to approximate the effects of *oceanic eddies* and other subgrid-scale processes. Figure 4 shows mean profiles of radiocarbon simulated in the North Atlantic Ocean (0°–70°N), the Indian Ocean north of the equator, the North Pacific Ocean (0°–70°N), and the Southern Ocean at the latitude band 55°–70°S. Scatterplots of basin-wide GEOSECS observations are also included for comparison. The model experiments are run with either Cartesian (HOR), isopycnal (ISO), or *Gent and McWilliams* [1990] (GM) mixing parameterization. The details of diffusion coefficients used in each model run are given in Table 2. The goal of the *England and Rahmstorf* [1999] study is to assess which mixing scheme, if any, results in a realistic simulation of deep-ocean ventilation.

Observations of Δ^{14}C suggest that the North Atlantic Ocean is relatively well ventilated to great depth (Figure 4a). In contrast, no model experiments run by *England and Rahmstorf* [1999] capture the depth of North Atlan-

(a) Observed

(b) Experiment P

Figure 3. Western Pacific section of $\Delta^{14}C$ (per mil) in (a) observations and (b) the bomb-produced $\Delta^{14}C$ simulation P of *Toggweiler et al.* [1989b] during 1974. A clear anthropogenic signal of $\Delta^{14}C$ is seen in this experiment compared with *Toggweiler et al.* [1989a] (Figure 2).

tic Deep Water (NADW) penetration. Instead, there is a clear delineation between upper well-ventilated NADW and lower $\Delta^{14}C$-depleted waters (particularly under *Gent and McWilliams* [1990] (hereinafter referred to as GM)). Additional GM experiments with an enhanced seasonal cycle of T-S and/or inclusion of the topographic stress parameterization of *Holloway* [1992] do not rectify this problem. In the North Pacific Ocean, simulated ventilation timescales vary greatly between the GM and non-GM runs; typical middepth NPDW radiocarbon is about $-180‰$ in ISO and $-260‰$ to $-280‰$ in the GM runs (compared with $-230‰$ to $-250‰$ in observations). Similar trends can be seen in the Indian Ocean (Figure 4b). Overall, the HOR and ISO runs significantly underestimate the ventilation timescales for deep-water renewal in the Pacific and

Indian Oceans, whereas the GM runs significantly overestimate them. This is largely due to model behavior in the Southern Ocean. There, the model equivalent of CDW is too young in the HOR and ISO cases. The GEOSECS measurements of $\Delta^{14}C$ indicate a near-uniform Southern Ocean value of $-160‰$, whereas the HOR and ISO cases simulate radiocarbon to be only depleted to about $-120‰$. This is due to rapid overturn of $\Delta^{14}C$-rich surface waters at this latitude band (a result of excessive diapycnal mixing; see also *England and Hirst* [1997]). In contrast, all GM cases overestimate the $\Delta^{14}C$ depletion of CDW, indicating that this water mass is erroneously old under that scheme. Slow downslope flows and weak interior currents under GM explain these spuriously depleted levels of $\Delta^{14}C$ (for further details, see *England and Rahmstorf* [1999]). Overall, no model case considered by *England and Rahmstorf* [1999] captures global ocean renewal rates to acceptable levels of accuracy.

Simulations of bomb-produced $\Delta^{14}C$ can be used to assess shorter-timescale circulation and water mass ventilation than that discernible from prebomb simulations. This is achieved by monitoring the transient uptake of bomb-produced ^{14}C in the model [e.g., TDBb; *Follows and Marshall*, 1996; *Rogers et al.*, 1997] (see also Figure 1). For example, TDBb assessed the model representation of Subantarctic Mode Water (SAMW) renewal by plotting $\Delta^{14}C$ at 755-m depth during 1972, 1981, and 1990 (Figure 5). High concentrations of ^{14}C reveal ventilation by water that was in recent contact with the postbomb atmosphere. TDBb find a clear analogy between their model renewal of SAMW and that obtained in a detailed water mass analysis by *McCartney* [1977]. They note that the northward Ekman-driven flow of cold Subantarctic surface waters creates dynamically unstable stratification, forcing surface waters to be overturned to depth. They find particularly strong convection in the southeast Indian Ocean, revealed by clear ^{14}C ventilation at that location (Figure 5). SAMW then spreads northwestward under the subtropical gyre. A similar though somewhat weaker signal can be seen in the southeastern Pacific Ocean, which dominates in the mechanism for AAIW renewal in a similar model [*England et al.*, 1993]. At the time of the TDBb study, ^{14}C measurements were too sparse to assess their model representation of SAMW formation. Since the completion of the World Ocean Circulation Experiment (WOCE) observational program, a greater number of ^{14}C observations are available [e.g., *Key*, 1996] and should be used to reassess water mass formation processes in commonly used ocean models.

3. TRITIUM

Tritium (^3H) is a radioactive isotope (or radionuclide) of hydrogen that was produced by atmospheric nuclear bomb testing in the 1950s and 1960s in an
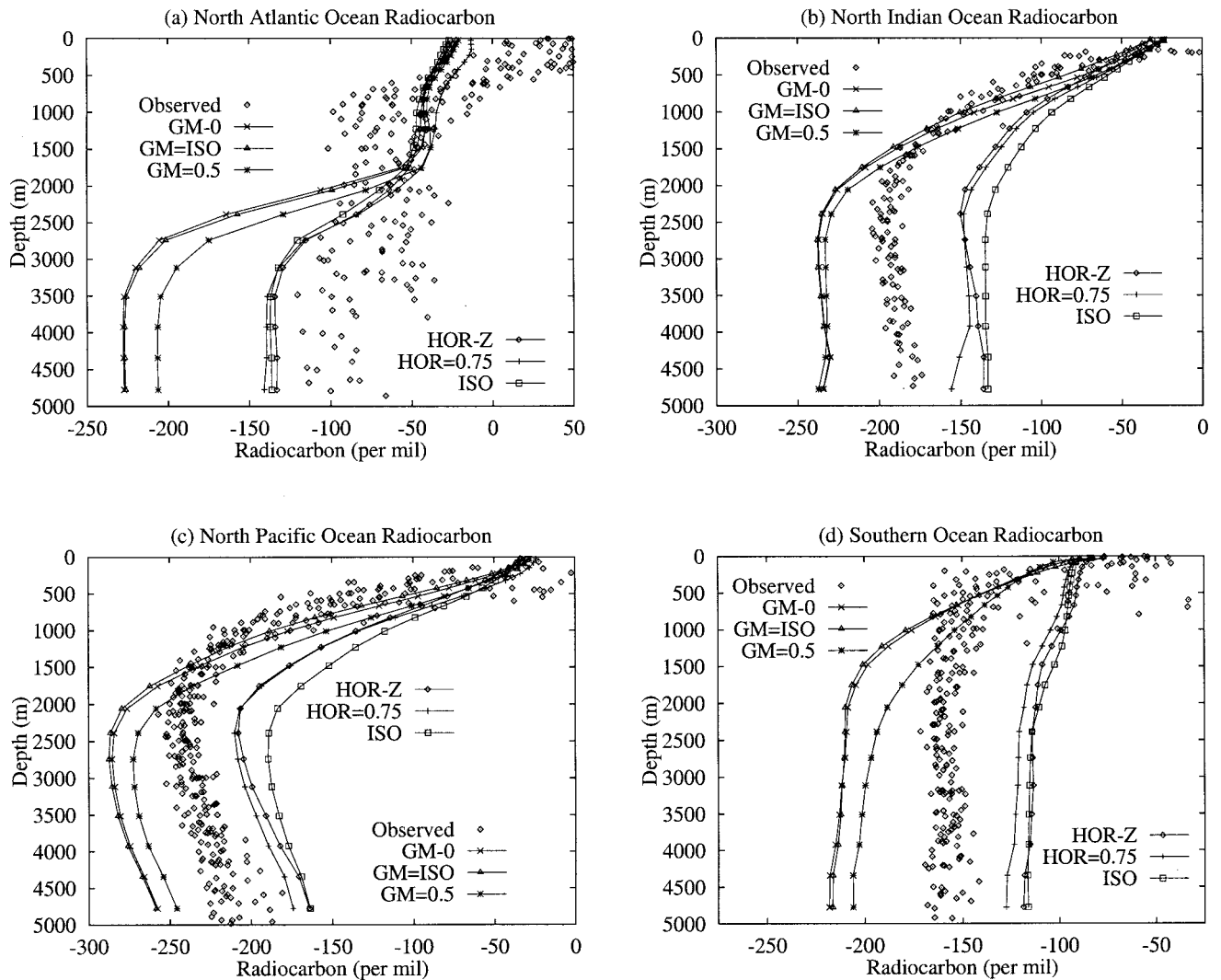
Figure 4. Mean model profiles of radiocarbon in (a) the North Atlantic Ocean (0°–70°N), (b) the Indian Ocean north of the equator, (c) the North Pacific Ocean (0°–70°N), and (d) the Southern Ocean at the latitude band 55°–70°S from *England and Rahmstorf* [1999]. The model cases include runs with either Cartesian (HOR), isopycnal (ISO), or *Gent and McWilliams* [1990] (GM) mixing parameterization (Table 2). Scatterplots of basin-wide Geochemical Ocean Sections Study (GEOSECS) observations are overlain for comparison. Reprinted with permission from the American Meteorological Society.

amount greatly exceeding its natural abundance. Because of its time-dependent atmospheric history (Figure 6), it is classed as a transient tracer. It decays into ^{3}He with a half-life of 12.43 years [*Taylor and Roether*, 1982]. Its input function into the world oceans is rather complex, depending on rainfall, air moisture, geographic location, and river input [*Weiss and Roether*, 1980; *Doney et al.*, 1992, 1993]. Input from marine air masses depends on latitude and rainfall/water vapor, the latitude dependence being weighted heavily toward those regions where nuclear bomb testing occurred (40°–50°N; see also Figure 7). This geographic inhomogeneity can be exploited when tracing ventilation pathways of subducted waters. Air masses that move out over the sea from land have higher inputs for a given latitude than do marine air masses, because gas exchange over land is not

as effective in removing tritium as it is over the ocean. Tritium concentrations are about 4 times higher in continental air as compared with marine air. This must be factored into ocean simulations of tritium uptake. Finally, river input of tritium is significant, because catchment areas over land can concentrate tritium-borne rainfall into single entry points into the ocean. Tritium has been measured and analyzed in several studies of oceanic circulation, particularly in the North Atlantic [e.g., *Jenkins and Rhines*, 1980; *Jenkins*, 1988; *Schlosser et al.*, 1995]

The first use of tritium as a tracer in a general circulation model was documented by *Sarmiento* [1983]. He included bomb-produced tritium uptake in a model of the Atlantic Ocean north of 20°S. To minimize computational cost, the ^{3}H tracer simulation was run off-line

TABLE 2. Model Experimental Design of *England and Rahmstorf* [1999]

Experiment	Subgrid-Scale Eddy Parameterization
HOR-Z	horizontal mixing profile, $A_{HH} = 1.0$ (surface) to 0.5 (bottom) $\times 10^3$ m^2 s^{-1}
HOR = 0.75	horizontal mixing (constant $A_{HH} = 0.75 \times 10^3$ m^2 s^{-1})
ISO	isopycnal mixing profile $A_\rho(z)$, background $A_{HH} = 0.75 \times 10^3$ m^2 s^{-1}
GM-0	GM, $\kappa = 1 \times 10^3$ m^2 s^{-1}, isopycnal mixing profile $A_\rho(z)$; zero A_{HH}
GM-H	same as in GM-0, only A_{HH} is nonzero (0.75 $\times 10^3$ m^2 s^{-1})
GM = ISO	same as in GM-0, only $A_\rho = \kappa = 1 \times 10^3$ m^2 s^{-1}
GM = 0.5	same as in GM-0, only $\kappa = 0.5 \times 10^3$ m^2 s^{-1}

The seven cases listed include Cartesian-mixing experiments (HOR-Z and HOR = 0.75), an isopycnal mixing experiment (ISO), and four *Gent and McWilliams* [1990] (GM) experiments. A_{HH} refers to the horizontal diffusivity, $A_\rho(z)$ refers to a depth-dependent profile for isopycnal diffusion, and κ refers to the GM isopycnal thickness diffusivity.

using the circulation fields derived from an annual-mean forced ocean model. This avoids the need to recalculate T-S, the horizontal components of velocity, and the barotropic stream function at each time step (see also section 7). Instead, only ^{3}H is predicted according to the tracer equation

$$d(^3H)/dt = L(^3H) - \lambda^3H + \text{sources}, \qquad (1)$$

where $L(^3H)$ refers to the model parameterized diffusion and λ is the decay constant for tritium. In some preliminary experiments with no model convection and internal restoring of T-S below 1000 m, *Sarmiento* [1983] found that the uptake of tritium was on the whole too

weak in the ocean model. To correct this problem, the model was forced to artificially convect tritium in regions where deep mixed layers are observed (following the *Levitus* [1982] March mixed-layer depth climatology). In its original state, the off-line model carried no convection to inject sufficient quantities of tritium into the ocean. Another approach to this problem is to use the model's convective overturn fields to force tracer uptake (see, e.g., *Ribbe and Tomczak* [1997] and section 7).

Some results from the *Sarmiento* [1983] model run are included in Figures 8 and 9. The total content of tritium in the North Atlantic model is shown in Figure 8, revealing a very rapid oceanic uptake in the early 1960s,
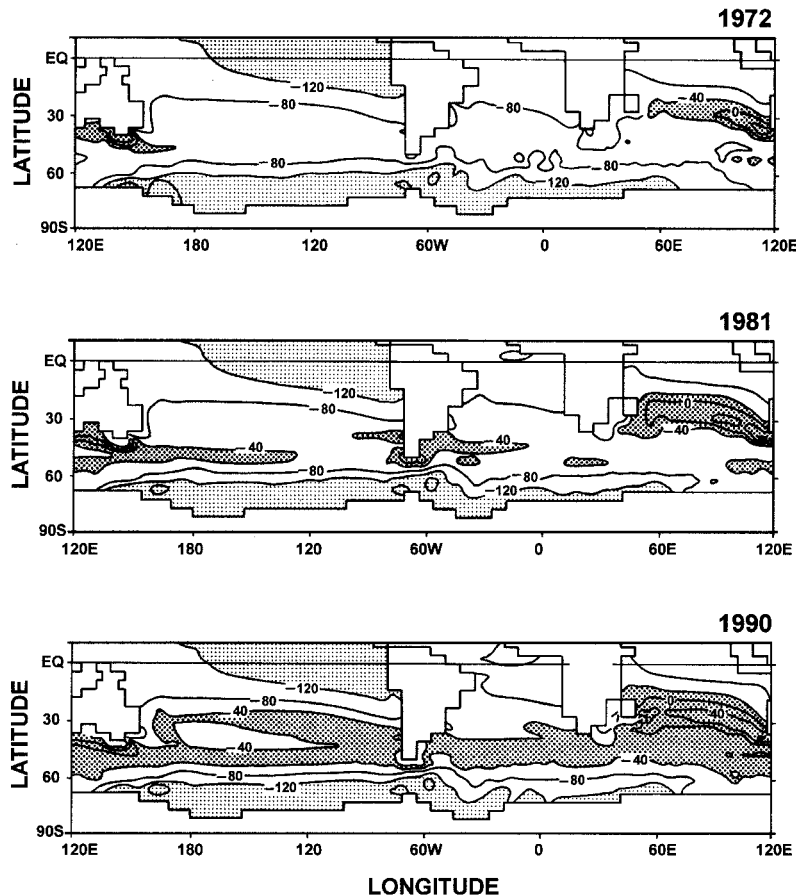

Figure 5. Maps of predicted Δ^{14}C (per mil) at 755-m depth during 1972, 1981, and 1990 in the bomb-produced Δ^{14}C simulation of *Toggweiler et al.* [1989b]. Carbon 14 values in excess of $-40‰$ indicate the presence of bomb-produced ^{14}C.

a peak content during 1966, followed by a very gradual decrease for the remainder of the model run. This loss of oceanic tritium during the latter stages of the model run is due mostly to the natural radioactive decay of tritium (which has a mean life of just less than 18 years). *Sarmiento* [1983] finds that the total tritium predicted for 1972 in the model is about 16% more than the observations suggest. Because of possible errors in the *Weiss and Roether* [1980] input functions, *Sarmiento* [1983] subtracted 16% from all model-predicted ^{3}H fields before comparing with observations, which is reasonable since the tracer equation is linear. However, it could also be spurious model behavior that resulted in unrealistic uptake of ^{3}H, compromising the validity of the model-data comparison. Further sensitivity tests of the technique of surface tritium forcing should probably have been performed.

A model-observation comparison of tritium along the GEOSECS western Atlantic section is shown in Figure 9 from the *Sarmiento* [1983] model. Simulations of tritium uptake have also been performed by *Maier-Reimer and Hasselmann* [1987] and *Heinze et al.* [1998]; results from these models are included in Figure 10. *Sarmiento* [1983] only shows the model tritium in the upper 1000 m, whereas *Maier-Reimer and Hasselmann* [1987] and *Heinze et al.* [1998] show their Atlantic GEOSECS simulations to the bottom of the ocean. Apparent in the earlier two simulations is weaker than observed tritium concentrations in outflowing upper NADW. A signal of southward penetrating tritium at around 1200-m depth is missing in the *Maier-Reimer and Hasselmann* [1987] model run, indicating an unrealistically weak outflow rate of NADW. In addition, only a mild signal of deeper tritium is seen south of the Greenland-Iceland-Scotland Ridge, suggesting their model is not capturing the denser variety of NADW associated with deep wintertime convection in the Greenland Sea. This situation is apparently remedied in the more recent *Heinze et al.* [1998] model: A tritium signature of 0.2 TU (tritium unit) reaches 4500 m and 40°N by 1972, in agreement with the GEOSECS data. However, to achieve this, *Heinze et al.* [1998] appear to have spuriously deep convective mixed layers, with near-uniform tritium concentrations of 4.0 TU reaching 3000 m at 60°N. In the GEOSECS section, notable vertical gradients of tritium are seen in this region, which may be a result of interannual variability in NADW not resolved by the model.

Since the *Sarmiento* [1983] and *Maier-Reimer and Hasselmann* [1987] studies, relatively few global models of tritium uptake have been analyzed, apart from the recent simulation by *Heinze et al.* [1998]. On a regional scale, *Jia and Richards* [1996] have assessed tritium uptake in an isopycnic model of the North Atlantic Ocean. Simpler conceptual modeling studies have also been made, such as using tritium and ^{3}He concentrations for determining the age and ventilation rates of seawater in the North Atlantic [e.g., *Doney and Jenkins*, 1994]. Part of the reason for this apparent reluctance to study tri-
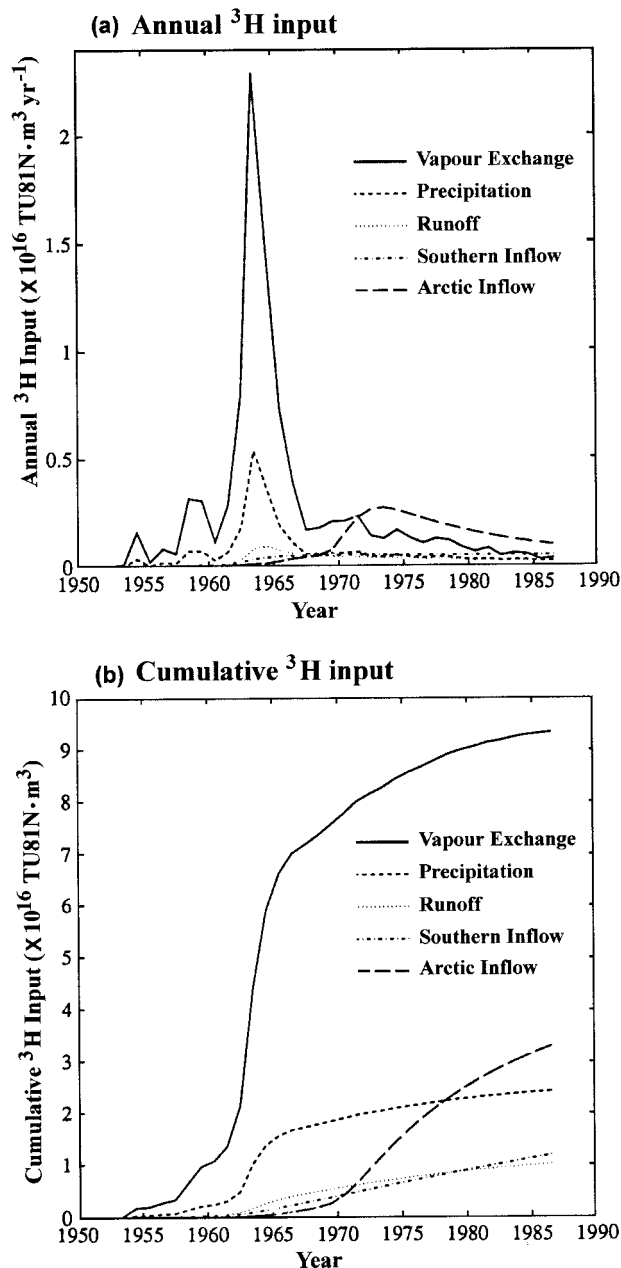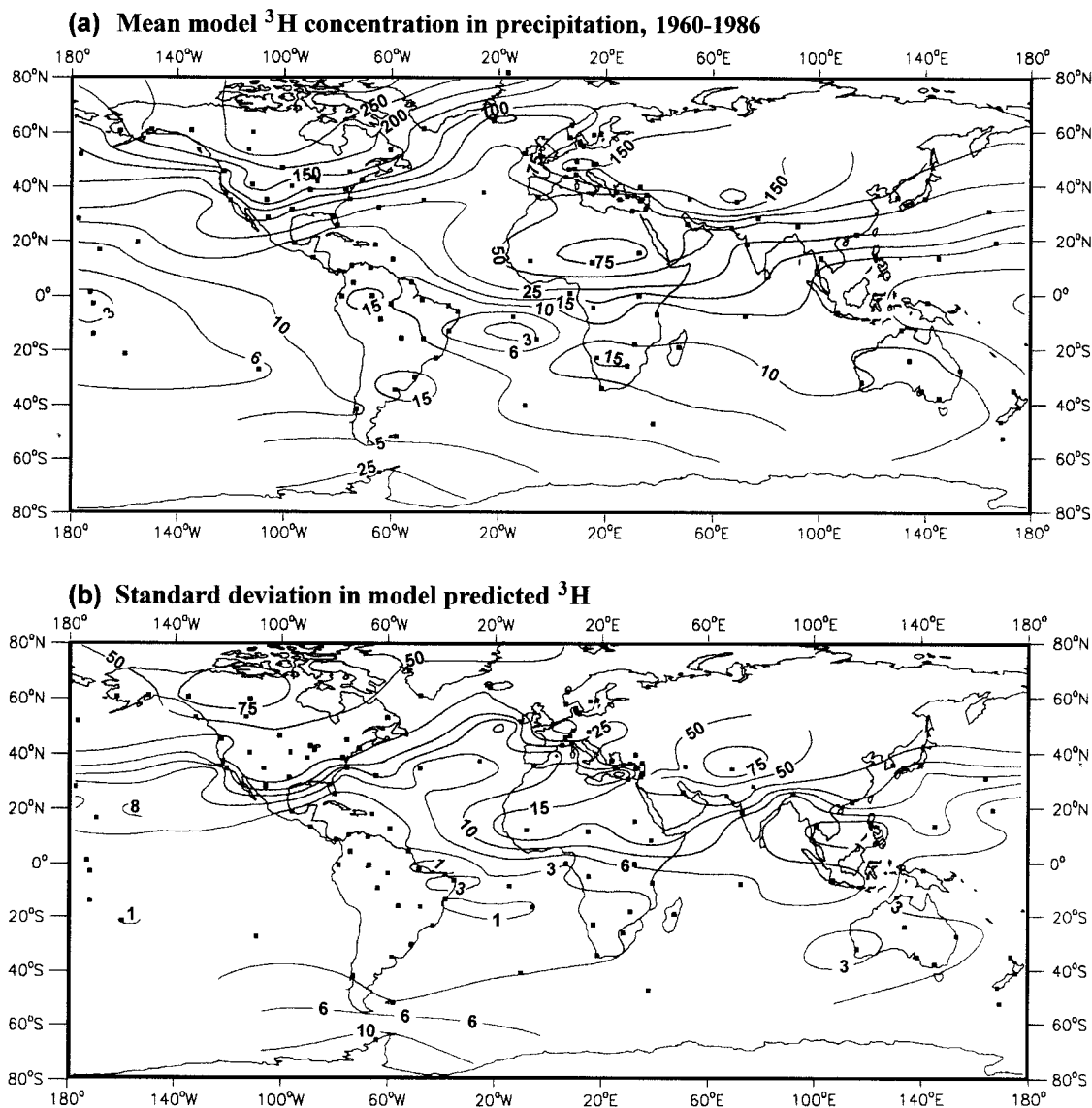

Figure 6. Time histories and sources of the (a) annual ^{3}H delivery and (b) cumulative input for the North Atlantic Ocean [after *Doney et al.*, 1993].

tium uptake in global models could be the significant uncertainties associated with specifying its input function. Another might be that chlorofluorocarbons have now been measured globally as part of WOCE, whereas they were not sampled during the GEOSECS program. In addition, CFCs are inert transient tracers whose solubility properties, atmospheric history, and air-sea exchange are for the most part well understood.

4. CHLOROFLUOROCARBONS

The industrial release of chlorofluorocarbons (CFCs) began in the early 1930s and accelerated greatly during

(a) Mean model ^{3}H concentration in precipitation, 1960-1986

**(b) Standard deviation in model predicted ^{3}H**

Figure 7. (a) Mean and (b) standard deviation of the tritium concentration in precipitation estimated by *Doney et al.* [1992] for the period 1960–1986.

the subsequent 3 decades (Figure 11). Despite the discovery that CFCs destroy stratospheric ozone [*Molina and Rowland*, 1974], the atmospheric concentration of these gases has continued to rise until very recently [*Elkins et al.*, 1993]. Even though virtually all production and release occurs in the Northern Hemisphere, rapid mixing rates in the lower atmosphere and the chemical stability of CFCs ensure relatively uniform distributions of these gases over the troposphere. Thus their input functions are significant over the entire ocean, unlike a number of bomb-produced tracers (e.g., tritium), whose atmospheric concentrations favor the Northern Hemisphere. This gives CFCs an advantage over tritium in model analyses of Southern Ocean water masses, though it may be noted that the CFC/tritium ratio is useful for determining ventilation timescales for certain processes [e.g., *Schlosser et al.*, 1991].

Because CFCs are weakly soluble in seawater, they are dissolved at the sea surface like most other atmospheric gases. However, relatively low solubility and negligible biological interactions ensure that the ocean uptake of CFC is only a small component of the global cycling of these gases (unlike, say, CO_2). Recent developments in ocean technology have enabled the seawater concentrations of CFC-11 and CFC-12 to be measured with relative ease [*Bullister and Weiss*, 1988]. Even in small-volume (30 cm^3) water samples, CFC concentrations are detectable down to 0.005×10^{-12} mol kg^{-1} (0.005 pmol kg^{-1}), 3 orders of magnitude smaller than the typical near-surface concentrations of today. Upper level traces of CFC get redistributed vertically by convection and subduction and then horizontally by interior ocean currents and mixing. Recently ventilated waters are therefore characterized by comparatively high concentrations of these anthropogenic gases.

Unlike the majority of ocean tracers (e.g., nitrates,
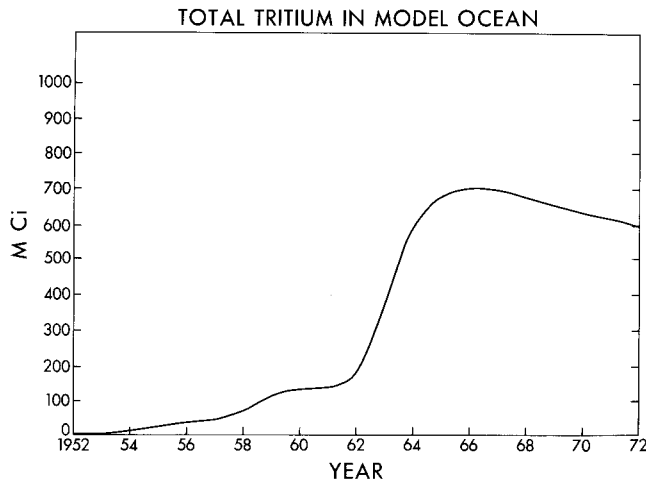
Figure 8. Integrated total tritium content in the North Atlantic model of *Sarmiento* [1983]. Reprinted with permission from the American Meteorological Society.

silicates, oxygen, and ^{14}C), CFCs are not known to be influenced by biological processes and are very stable compounds; they therefore serve as relatively unambiguous tracers of the present-day ocean circulation over decadal to interdecadal timescales. Direct measurements of the concentration of CFCs in the ocean are now routinely used to add information to conventional hydrographic surveys [e.g., *Weiss et al.*, 1985; *Wallace and Lazier*, 1988; *Bullister*, 1989; *Rhein*, 1991; *Trumbore et al.*, 1991; *Schlosser et al.*, 1991; *Doney and Bullister*, 1992; *Gordon et al.*, 1992; *Warner and Weiss*, 1992; *Fine*, 1993; *Smethie*, 1993; *Roether et al.*, 1993]. With relatively well known atmospheric histories [*Bullister*, 1989; *Walker et al.*, 2000] and solubility properties in seawater [*Warner and Weiss*, 1985], CFCs can be readily incorporated into ocean models [e.g., *England et al.*, 1994; *England*, 1995; *Haine and Richards*, 1995; *Robitaille and Weaver*, 1995; *Dixon et al.*, 1996; *England and Hirst*, 1997; *Caldeira and Duffy*, 1998; *Craig et al.*, 1998; *Goosse et al.*, 1999]. The goal of such studies is principally to test the model water mass ventilation characteristics and to validate their associated renewal schemes against observations.

One of the key CFC-11 sections used to assess Southern Ocean circulation and water mass formation in ocean models is the Ajax section reported by *Warner and Weiss* [1992]. This section was taken north-south along the Greenwich meridian in the South Atlantic during October 1983 to January 1984. It is reproduced in Plate 1 along with simulated CFC-11 in a number of model experiments, including cases from *England* [1995], *Robitaille and Weaver* [1995], *Dixon et al.* [1996], *Caldeira and Duffy* [1998], *Craig et al.* [1998], and *England and Hirst* [1997]. The observed section of *Warner and Weiss* [1992] reveals a number of features of Southern Ocean water mass circulation, namely, penetration of AAIW to around 1000-m depth near 40°S, upwelling of older CFC-depleted CDW at 50°–60°S, and ventilation by Antarctic Bottom Water (AABW) below 4000-m depth near 70°S. The models have varying degrees of success at reproducing these aspects of observed CFC in the Southern Ocean. *England* [1995], *Robitaille and Weaver* [1995], *Caldeira and Duffy* [1998], and *England and Hirst* [1997] all find excessive downward penetration of CFC-11 over much of the Ajax section, particularly near 55°–70°S, in control runs with either Cartesian (HOR) or isopycnal (ISO) mixing. They relate this to excessive vertical convection at these latitudes, which is due to erroneously low densities in the model equivalent of CDW. Some improvement in the model simulations is noted when the *Gent and McWilliams* [1990] (GM) mixing parameterization is adopted [*England*, 1995; *Robitaille and Weaver*, 1995] or when higher Antarctic salinities are specified [*Caldeira and Duffy*, 1998; *England and Hirst*, 1997]. The GM terms in the tracer advection equations enable the model runs to be integrated with zero horizontal diffusion. They also assist downslope flows of dense water types, thereby enabling denser deep waters to ventilate the model ocean. This in turn suppresses unrealistic vertical convection in the Southern Ocean by increasing stratification near 50°–70°S [see *Danabasoglu and McWilliams*, 1995; *Hirst and McDougall*, 1996; *England and Hirst*, 1997]. The cases with enhanced near-surface Antarctic salinities also act to inhibit Southern Ocean convection away from the polar waters by densification of CDW (excessively so in the *Caldeira and Duffy* [1998] run).

Craig et al. [1998] obtain Southern Ocean CFC penetration that is reasonable, though notably too weak in AAIW and AABW (see Plate 1b). Compared with the other models, the *Craig et. al.* [1998] case is run at
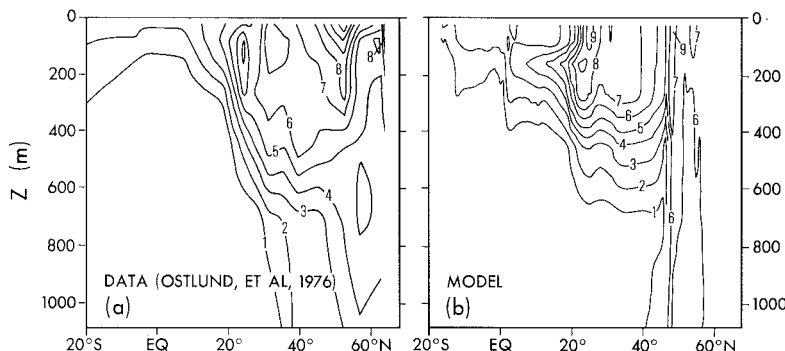
Figure 9. Tritium concentrations along the north-south GEOSECS section in the western Atlantic. (a) Measurements made in 1972. (b) The model of *Sarmiento* [1983]. Reprinted with permission from the American Meteorological Society.
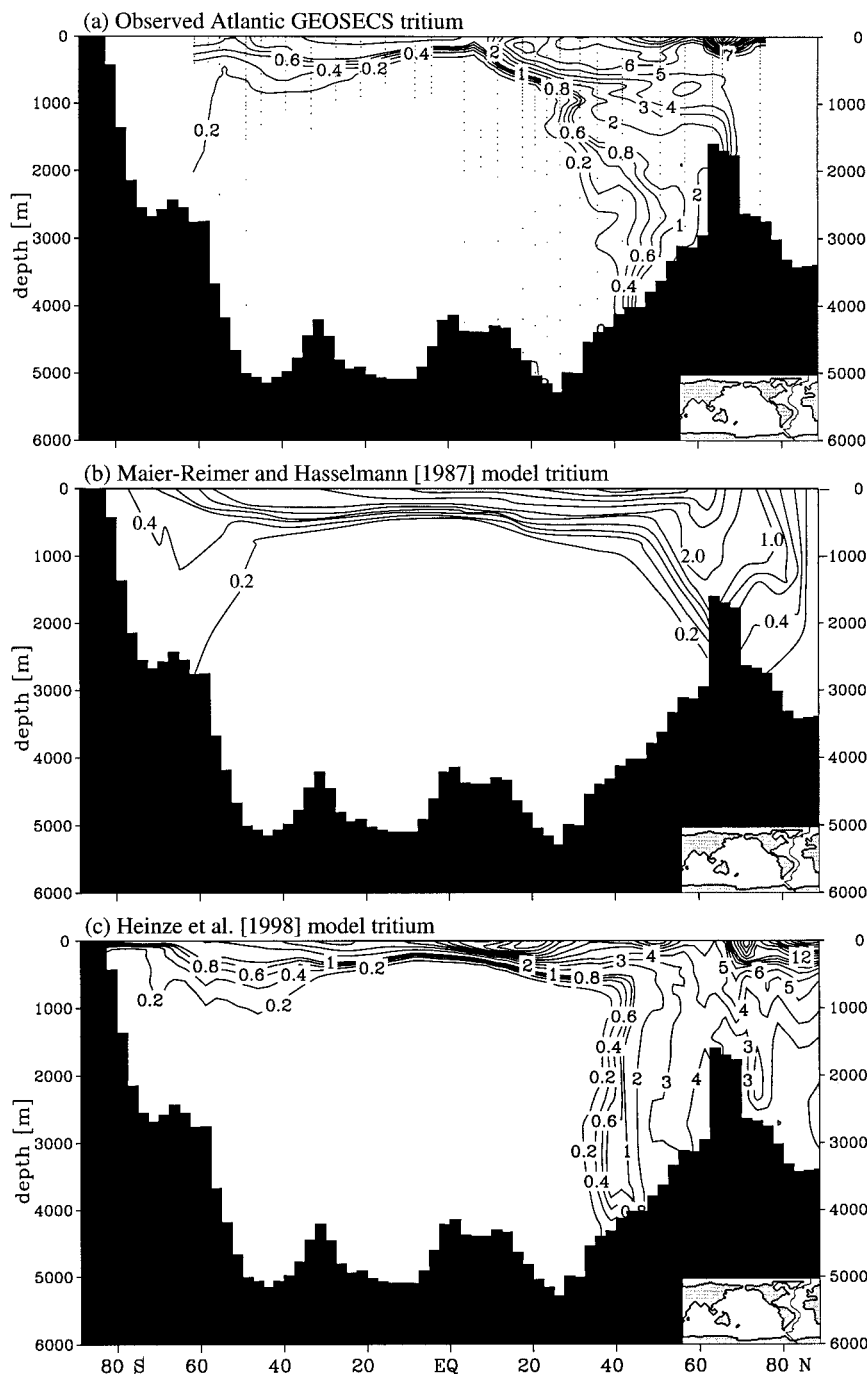
Figure 10. Tritium concentrations along the north-south GEOSECS section in the western Atlantic. (a) Measurements made in 1972. (b) The model of *Maier-Reimer and Hasselmann* [1987]. (c) The model of *Heinze et al.* [1998].

somewhat higher horizontal resolution (~1°) and uses an interior T-S restoring south of 67°S (the robust-diagnostic technique described by TDBa). In addition, the model is not in an equilibrated state when CFCs are included: it is only integrated for 22 years from its initial conditions (namely, climatological T-S). As such, deep T-S properties will not have changed much from their initial values during the short spin-up time, so that the CFC uptake experiment is effectively run in robust-diagnostic mode below about 800 m. The weak CFC penetration in AAIW and AABW is likely due to this, and for bottom waters, to the interior T-S restoring

south of 67°S. Both of these factors will tend to reduce convection and vertical motions in the water mass formation regions.

Dixon et al. [1996] have been perhaps the most successful at reproducing observed CFC along the Ajax section (Plate 1f). However, unlike the studies discussed above, they use coupled model-generated wind speeds and sea ice to calculate CFC fluxes. The climate model they use is known to have spuriously weak winds over the Southern Ocean (systematically weaker by around 25–30%) and a sea ice coverage that is too extensive around Antarctica [e.g., *Manabe et al.*, 1991, 1992]. Because

CFC forcing is determined by a wind speed–dependent gas piston velocity (that of *Wanninkhof* [1992]) and set to zero in the presence of model sea ice, both of these factors contribute to weaker than observed CFC fluxes over the Southern Ocean near 55°–70°S. This is consistent with the *Dixon et al.* [1996] finding that they simulate lower than observed CFC-11 in the upper Southern Ocean and excessive CFC at depth (compare Plates 1f and 1a). It would appear they are capturing reasonable CFC by inadvertently underestimating the air-sea flux of CFC under the subpolar westerlies. This is discussed further in section 7.

CFCs have also been widely used to assess model circulation and water mass formation in the North Atlantic [e.g., *England et al.*, 1994; *England*, 1995; *Robitaille and Weaver*, 1995; *Caldeira and Duffy*, 1998; *Craig et al.*, 1998; *England and Hirst*, 1997; *England and Holloway*, 1998; *Redler et al.*, 1998]. Typically, these studies identify deficient model outflow transport of CFC-burdened NADW, and most only capture a single CFC core (corresponding to upper NADW). Outflowing CFC content is generally too weak due to sluggish interior model currents, particularly at coarse resolution. The lack of a deeper core of CFC is due to poor model representation of dense water overflowing the Greenland-Iceland-Scotland Ridge, analogous to poor tritium [*Maier-Reimer and Hasselmann*, 1987] and radiocarbon (TDBa) simulations in the deep North Atlantic.

Examples of CFC observations and coarse-resolution simulations in outflowing NADW are included in Figures 12–14. The observed CFC data help reveal the exact pathway of transport of NADW in the Deep Western Boundary Current (DWBC) [e.g., *Weiss et al.*, 1985; *Pickart et al.*, 1989; *Smethie*, 1993; *Rhein*, 1994]. *Weiss et al.* [1985] identify a well-defined core of relatively high CFC concentration water near 1600-m depth at the equator in upper NADW during early 1983 (see Figures 12 and 13). A corresponding set of model simulations of CFC in outflowing upper NADW is included for comparison (model details are given by *England and Holloway* [1998]). Farther upstream in the outflowing NADW (32°–45°N), *Smethie* [1993] finds two distinct layers of CFC near the continental slope (Figure 14a). Simulations of CFC at the *Smethie* [1993] Western Boundary Exchange Experiment (WBEX) section are included in Figure 14.

Except for a model case including the topographic stress parameterization of *Eby and Holloway* [1994] (TOPO) and an experiment with enhanced North Atlantic wintertime forcing (NAW), the model runs exhibit much weaker CFC-11 concentrations in the western boundary outflow compared with observations (Figures 12 and 13). The model DWBC is deficient in CFC-11 because the timescale for NADW outflow is too slow. The long timescale is primarily due to unrealistically sluggish deep currents, particularly in the case with GM tracer diffusion. In addition, in all model runs, part of the path of NADW outflow includes a questionable loop
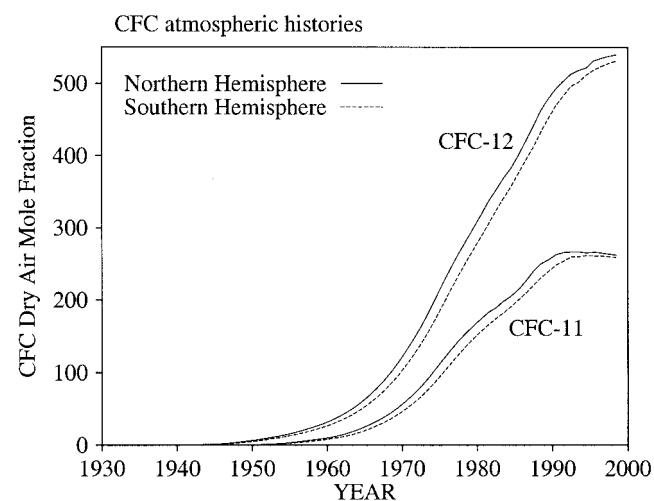

Figure 11. Reconstructed history of the atmospheric dry air mole fractions of CFC-11 and CFC-12 in the Northern and Southern Hemispheres. In effect, the Southern Hemisphere concentrations lag the Northern Hemisphere values by just over 1 year [from *England*, 1995].

eastward from the Labrador Sea into the northeastern Atlantic Basin, effectively increasing the required outflow journey by around 4000 km [*England et al.*, 1994]. The additional circulation eastward ages the water mass by at least 8 years (depending on the speed of the model currents), thereby yielding much lower CFC concentrations in the NADW extension.

Farther upstream in the outflowing NADW (Figure 14a), the two distinct layers of CFC near the continental slope correspond to upper NADW (800- to 1500-m depth) and lower NADW (at about 3500-m depth). The upper maximum feeds the CFC core detected in the *Weiss et al.* [1985] $\sigma_{1.5} = 34.63$ kg m^{-3} density surface of Figure 12a. The deeper core originates from dense water with classical NADW properties overflowing the Greenland-Iceland-Scotland Ridge [*Smethie*, 1993], a feature not typically resolved by coarse-resolution ocean models [e.g., TDBa; *England*, 1993; *Hirst and Cai*, 1994]. Figure 14 includes the corresponding coarse-resolution simulations of CFC-11 at WBEX stations 22–38 during April–May 1986. Clearly apparent in the model-observation comparison is the absence of any deeper CFC burdened NADW. The absence of any CFC in lower NADW is related to the shallow meridional overturning cells simulated in the model [*England and Holloway*, 1998], with little contribution of dense water overflowing the Greenland-Iceland-Scotland Ridge. Some experiments were rerun with a deepened ridge topography; little change in meridional overturning of CFC was noted. It would appear that at coarse climate model resolutions, there are chronic problems in capturing NADW production and outflow, with slow boundary currents and no lower NADW signal.

Only a handful of high-resolution simulations have been made of CFC uptake in the North Atlantic Ocean.
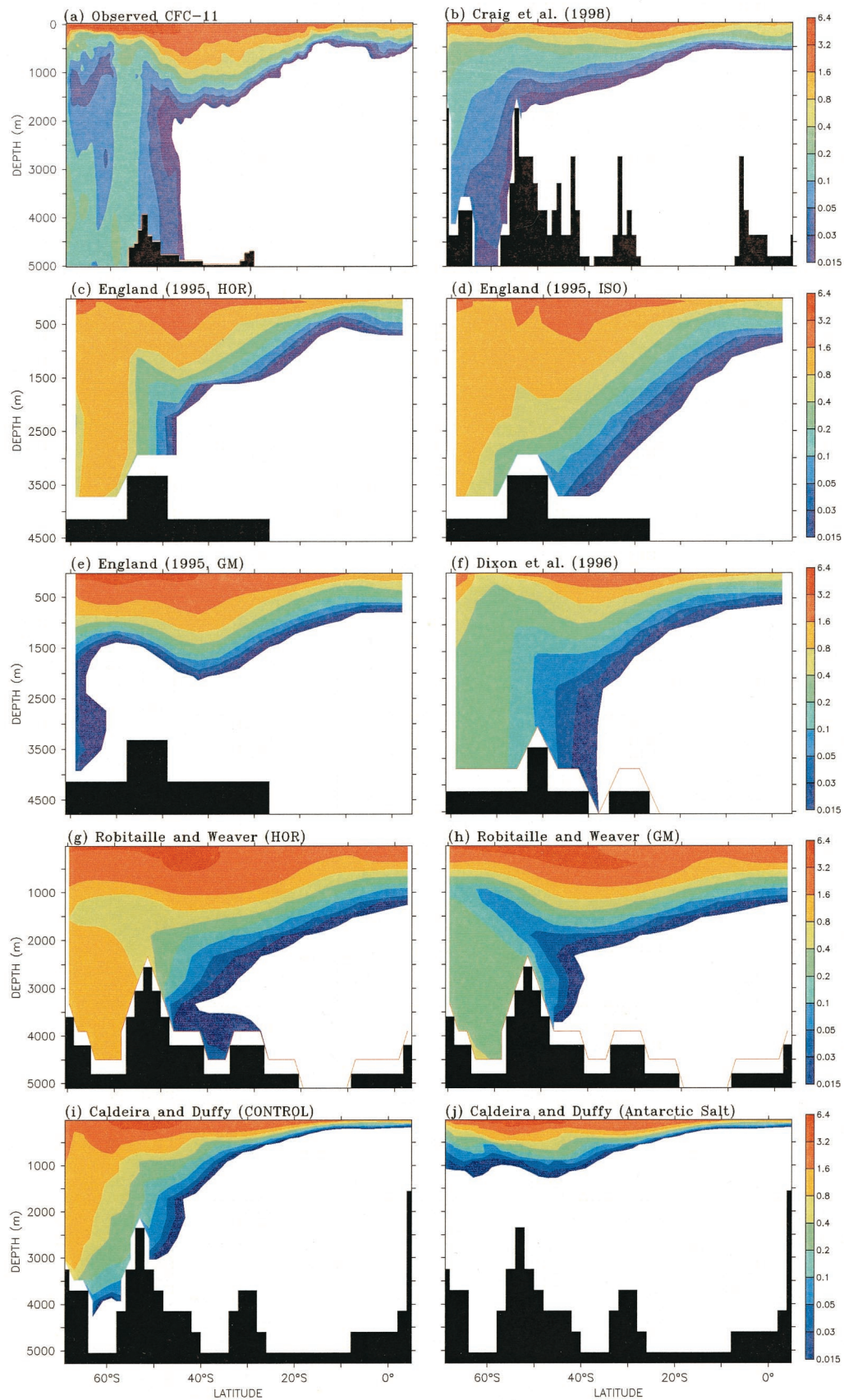
Plate 1. Latitude-depth sections of dissolved CFC-11 along the Greenwich meridian during late 1983 in observations and several ocean models. (a) Observed (redrafted from *Warner and Weiss* [1992]). (b) *Craig et al.* [1998]. (c–e) *England* [1995]. (f) *Dixon et al.* [1996]. (g and h) *Robitaille and Weaver* [1995]. (i and j) *Caldeira and Duffy* [1998].
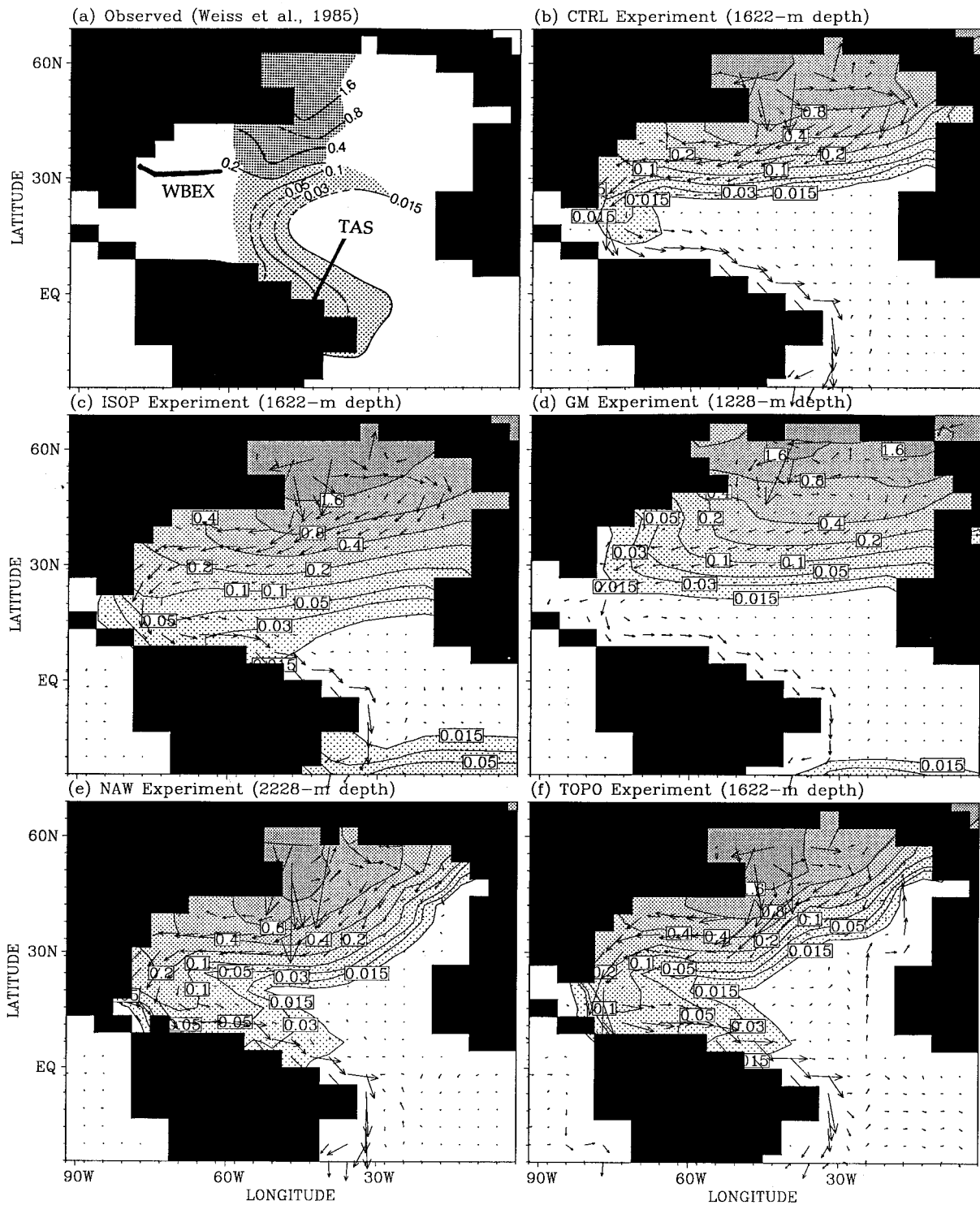
Figure 12. (a) Observed CFC-11 on the $\sigma_{1.5} = 34.63$ kg m^{-3} density surface measured during December 1982 to February 1983 as part of the Transient Tracers in the Ocean (TTO) program (redrafted from *Weiss et al.* [1985]). The density surface was selected by *Weiss et al.* [1985] to cut through the maximum southward extension of the CFC signal in the Deep Western Boundary Current (DWBC). (b–f) Simulated model currents and CFC-11 at the depth of maximum CFC content in the DWBC during February 1983 from *England and Holloway* [1998]. The model cases include versions with Cartesian mixing (CTRL), isopycnal mixing (ISOP), the eddy advection scheme of *Gent et al.* [1995] (GM), a version with enhanced surface thermohaline forcing (NAW), and finally a case that incorporates the effects of topographic stress as in the work of *Eby and Holloway* [1994]. In Figure 12a, the location of the Tropical Atlantic Study (TAS) and Western Boundary Exchange Experiment (WBEX) depth sections plotted in Figures 13 and 14 are shown.
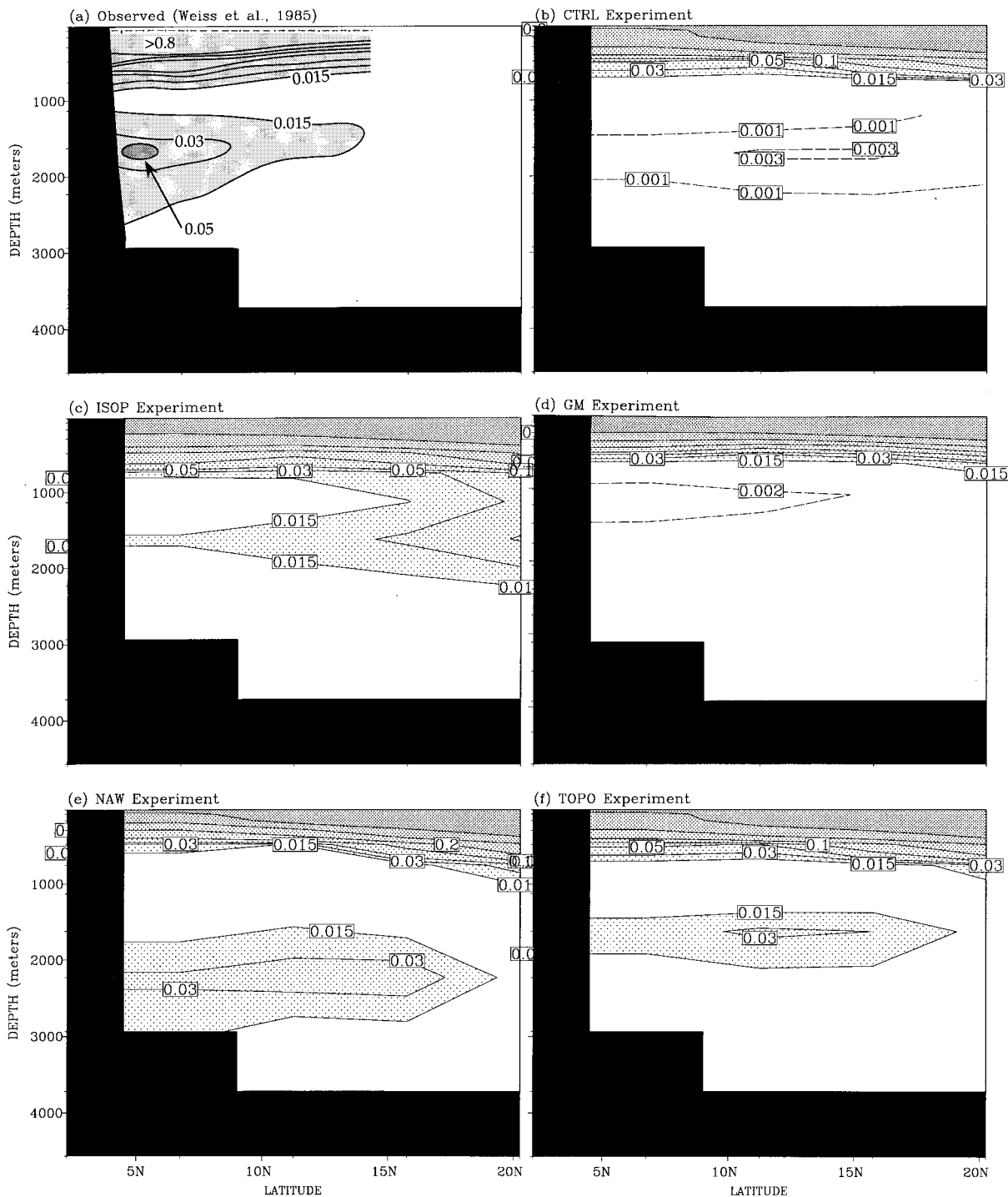
Figure 13. (a) Observed CFC-11 on the TAS section extending from near the South American continent at the equator northeastward toward the Mid-Atlantic Ridge, as shown in Figure 12a (redrafted from *Weiss et al.* [1985]). (b–f) Corresponding sections of simulated CFC-11 in each model case during February 1983. Contour levels are drawn at the standard values, with an additional set of weaker CFC-11 concentrations shown in the DWBC in experiments CTRL and GM.

The results of one such simulation, that of *Redler and Dengg* [1999], are included in Plate 2. This diagram compares CFC-12 in outflowing NADW in two model runs, one coarse (4/3°) and the other eddy-permitting (1/3°). Both cases employ a bottom boundary layer scheme to maintain a signal of dense water overflowing the Greenland-Iceland-Scotland Ridge. *Redler and Dengg* [1999] find that at fine resolution there is a distinct CFC signal in the DWBC, in qualitative agreement with observations. In contrast, a diffuse pattern is simu-

lated at coarse resolution, with CFC spreading southeastward from the northern formation regions, at odds with observations. Thus even at ~1° resolution and using a bottom boundary layer scheme, ocean climate models may not capture realistic CFC signals in the North Atlantic.

5. BIOGEOCHEMICAL TRACER MODELING

In order to understand and quantify the ocean carbon cycle, a number of prognostic three-dimensional biogeochemical tracer models have been developed in recent years [e.g., *Bacastow and Maier-Reimer*, 1990; *Maier-Reimer and Bacastow*, 1990; *Maier-Reimer*, 1993a, 1993b; *Sarmiento et al.*, 1993]. While the principal motivation behind these studies is to gain an understanding of the processes that control the uptake of carbon dioxide, in doing so they simulate other chemical components of seawater such as phosphate, silicate, and oxygen, as well as organic and inorganic carbon compounds. These can be used to assess the circulation and water mass formation in ocean models.

Three-dimensional models of ocean carbon uptake range in complexity from a simple nonbiological CO_2 perturbation assumption [e.g., *Sarmiento et al.*, 1992; *Taylor*, 1995] through to more complex biogeochemical tracer cycles [e.g., *Maier-Reimer and Bacastow*, 1990; *Najjar et al.*, 1992; *Sarmiento et al.*, 1993, 1995]. The simpler model assumes a "perturbation" approach, namely, that the preindustrial ocean carbon cycle continues without being affected by anthropogenic influences, such as increasing atmospheric CO_2 or the resulting changes in ocean circulation [see, e.g., *Sarmiento et al.*, 1992]. This enables the model to ignore biological processes, thereby greatly simplifying the seawater chemistry. Such simulations typically rely on other tracers (e.g., tritium and radiocarbon) to validate the circulation fields before including anthropogenic CO_2 uptake.

More complex models incorporating biological processes normally include the production of biogenic organic matter and nutrients at the surface, transport of biogenic material to the deep waters, and remineralization. This requires the ocean model to carry a number of chemical tracers as prognostic variables, including carbon compounds (such as total dissolved inorganic carbon (DIC) and calcium carbonate ($CaCO_3$), often defined for the different carbon isotopic species ^{12}C, $\delta^{13}C$, and $\Delta^{14}C$), as well as phosphate, dissolved oxygen, particulate organic matter, and silicate. Often radiocarbon is included for model validation purposes. For a more complete review of the seawater chemistry included in models of the oceanic carbon cycle, the reader is referred to *Maier-Reimer and Bacastow* [1990], *Maier-Reimer* [1993a, 1993b], and *Sarmiento et al.* [1993, 1995]. For the purpose of the present paper, we focus on the possibility of assessment of circulation and water mass
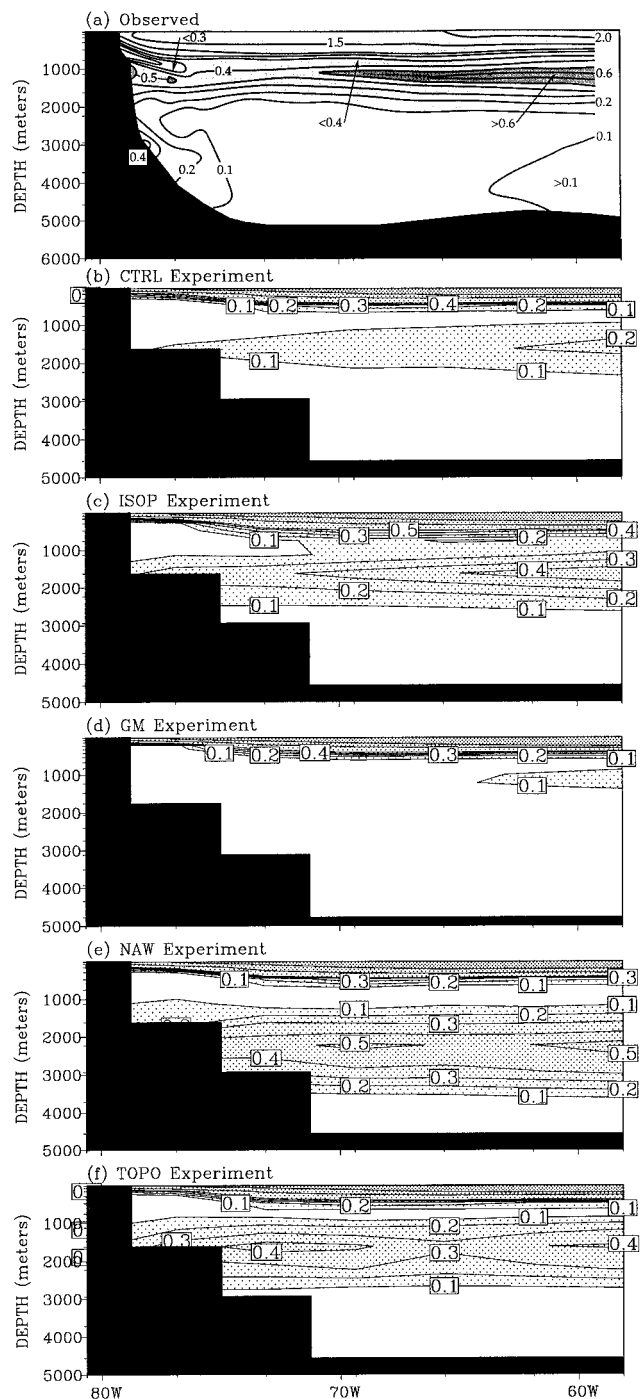
Figure 14. (a) Vertical section of observed CFC-11 along WBEX stations 22–38 near 32°–34°N (redrafted from *Smethie* [1993]). The WBEX section location is indicated in Figure 12a. CFC-11 concentrations greater than 0.1 pmol kg^{-1} are shaded. (b–f) Corresponding sections of simulated CFC-11 in each model case during April–May 1986 from *England and Holloway* [1998]. Contour levels are drawn at 0.1, 0.2, 0.3, 0.4, 0.5, 0.6, 1.0, 1.5, and 2.0 pmol kg^{-1}.

formation using tracers that are a component of ocean carbon cycle models.

Figure 15 shows simulated and observed estimates of the uptake of anthropogenic DIC along the GEOSECS
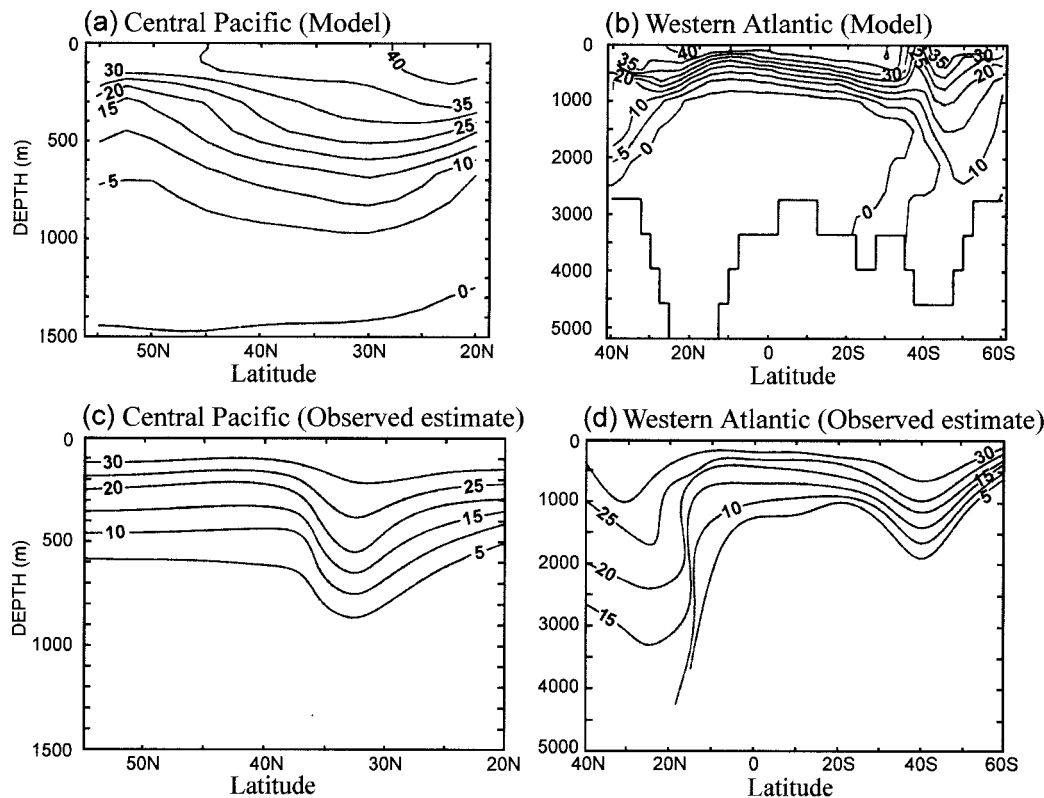
Figure 15. Simulated and observed estimates of the distribution of anthropogenic dissolved inorganic carbon (DIC) along the GEOSECS central Pacific and western Atlantic sections [from *Taylor*, 1995; and *Chen*, 1982a, 1982b]. Contour interval is 5 μmol kg^{-1}. It should be noted that considerable uncertainty remains in the observed estimates.

central Pacific and western Atlantic section [from *Chen*, 1982a, 1982b; *Taylor*, 1995]. It should be noted that there remains considerable uncertainty in the *Chen* [1982a, 1982b] estimates (more recent attempts to quantify anthropogenic DIC are given by *Gruber et al.* [1996], *Gruber* [1998], and *Sabine et al.* [1999]). The *Taylor* [1995] simulations were performed using an inorganic carbon cycle model embedded in a global ocean model with no inclusion of biological processes. Taylor's model partly agrees with the *Chen* [1982a, 1982b] estimates, though notably the Southern Ocean uptake of DIC is too strong and the North Atlantic drawdown is somewhat too weak. This could be because (1) the model has excessive deep ventilation of Southern Ocean waters, (2) the simplified perturbation approach is inadequate, or (3) there are errors in the observed estimates. Without additional simple tracers such as radiocarbon, *Taylor* [1995] could not have separated the effects of circulation from those linked with observational errors or biological processes. His model's representation of ^{14}C indicates weak and shallow NADW ventilation and a spuriously strong Southern Ocean influence on deep North Atlantic waters. It therefore suggests that the simulation of anthropogenic CO$_2$ uptake is compromised by a poor representation of global water mass formation. Clearly, though, anthropogenic DIC cannot serve as an unambiguous test of ocean model performance.

This example of carbon cycle modeling highlights the advantage of including additional nonbiological tracers for assessing the models' circulation and water mass formation. Another approach at separating biological and circulation effects is to study the model tracer field in two carbon cycle simulations; one with biota and one without. An example of this can be seen in Figure 16, which shows western Pacific GEOSECS sections of total dissolved inorganic carbon (DIC) in a model without biota, with biota, and as measured by *Craig et al.* [1981]. A validation of the ocean model against observations is difficult because both biology and circulation influence the DIC distribution. However, we can separate these effects by using two model experiments as shown in Figure 16. The case without biota reveals the role played by solubility and ocean circulation, namely, the greater dissolution of CO$_2$ at high latitudes, its participation in the large-scale thermohaline overturning circulation, and its subsequent outgassing in upwelled tropical waters. The biological pump enhances this effect in upwelling regions and generates a downward flux of carbon due to remineralization of particulate carbon at depth. This separation of biological effects from circulation processes facilitates the diagnosis of the role water mass formation plays in the oceanic carbon cycle.

The simulation of deep phosphate and silicate in ocean carbon cycle models primarily reveals the ocean's
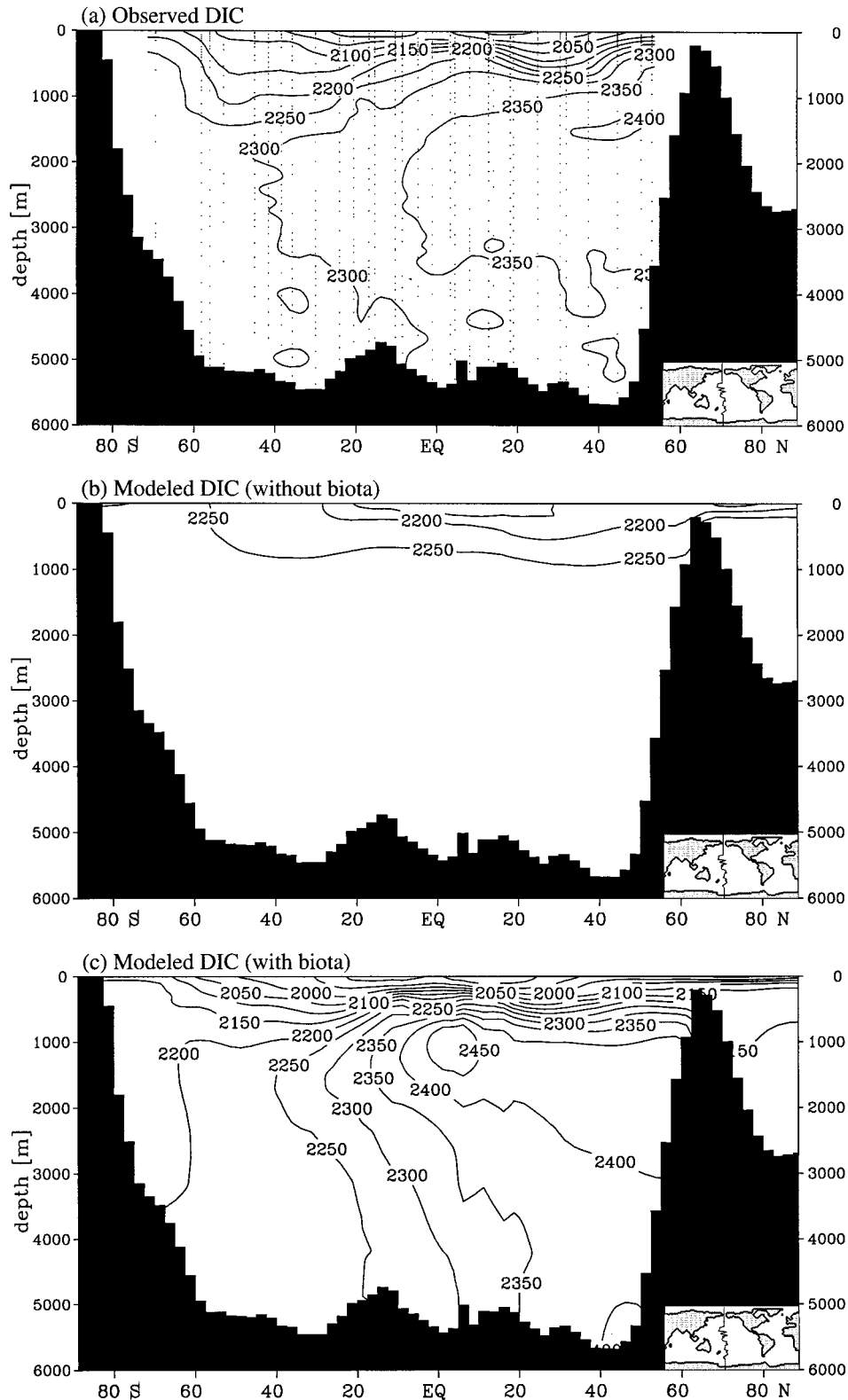
Figure 16. Western Pacific GEOSECS section of total dissolved inorganic carbon (DIC) (a) as measured by *Craig et al.* [1981] compared with a carbon uptake model (b) without biota and (c) with biota.

conveyor belt at depth (e.g., Figure 17). Younger waters have low concentrations of phosphate and silicate, and are enriched in oxygen and ^{14}C, whereas older waters show higher concentrations in phosphate and silicate and are oxygen-depleted. This can be used to assess model water masses in much the same way as in observational oceanography. For example, Figure 18 shows a scatterplot of oxygen versus phosphate in the model of
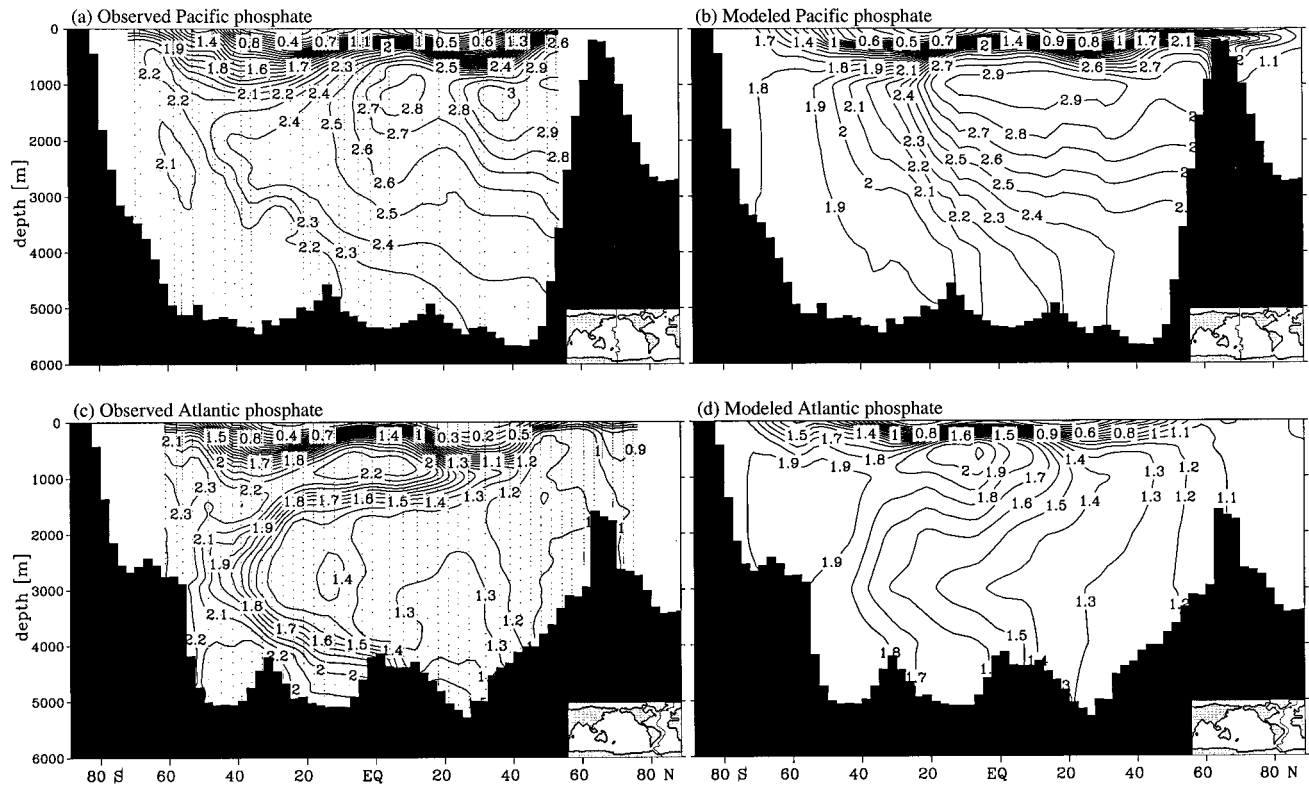
Figure 17. GEOSECS sections of phosphate. (a) Observed western Pacific and (b) predicted western Pacific in the *Maier-Reimer* [1993b] model. (c) Observed western Atlantic and (d) predicted western Atlantic in the *Maier-Reimer* [1993b] model.

Maier-Reimer [1993b] as well as the global model distribution of $PO_4^* = PO_4 + O_2/177 - 1.95$ at 3000-m depth. *Broecker et al.* [1991] have shown that PO_4^* can be regarded as a physical tracer at depth because the effects of remineralization have been canceled out. The value 1.95 is arbitrarily subtracted in order to obtain numbers similar to those for phosphate. The oxygen-phosphate scatterplot reveals mixing between the two end members NADW and Weddell Sea Bottom Water (WSBW) in the Atlantic. In contrast, there is a linear relationship between PO_4 and O_2 over much of the Pacific and Indian Oceans, with a line slope matching the assumed constant Redfield ratio. This suggests a nearly constant value of PO_4^* in these regions, as seen in Figure 18b. The distribution of PO_4^* at 3000-m depth reveals the mixing effects between the end members NADW ($PO_4^* = 0.7$) and WSBW ($PO_4^* = 1.8$); in much of the Pacific Ocean for example, PO_4^* is almost uniform at values between 1.35 and 1.4, indicating a model mixing ratio of 30:70 between NADW and WSBW [*Maier-Reimer*, 1993b].

Mean depth profiles of ^{14}C, phosphate, oxygen, DIC, and alkalinity in the Antarctic and North Pacific regions are shown for observations (GEOSECS) and the global carbon cycle model of *Maier-Reimer* [1993b] in Figure 19. The measured properties are from a limited region, whereas the mean model values are taken basinwide, and so a standard deviation is indicated at each model level to reveal horizontal variations. Apparent in the

North Pacific profiles is the relative success of the model in capturing deep phosphate, alkalinity, and DIC, whereas oxygen and ^{14}C show notable model-observation discrepancies. This difference partly reflects the insensitivity of properties such as PO_4 and DIC to different circulation fields, whereas O_2 and ^{14}C can vary greatly depending on the simulated water mass overturning rates. Near Antarctica, model deep waters are too oxygenated and high in ^{14}C content, revealing overly rapid AABW ventilation. This results in North Pacific deep waters that are also too young (i.e., too high in oxygen and ^{14}C content). In spite of these errors in simulated water mass formation, the natural carbon cycle tracers are reasonably well captured by the model.

6. EXOTIC TRACERS

Thus far we have examined the use of radiocarbon, tritium, chlorofluorocarbons, and standard biogeochemical tracers in analyzing the circulation and water mass formation in ocean models. There are generally enough direct measurements of these tracers to enable meaningful comparisons with model simulations, at least along specific cruise transects. There is a suite of other chemical tracers that are present in seawater and have the potential for use in ocean modeling studies. Examples include argon, helium, and cesium, as well as radio-
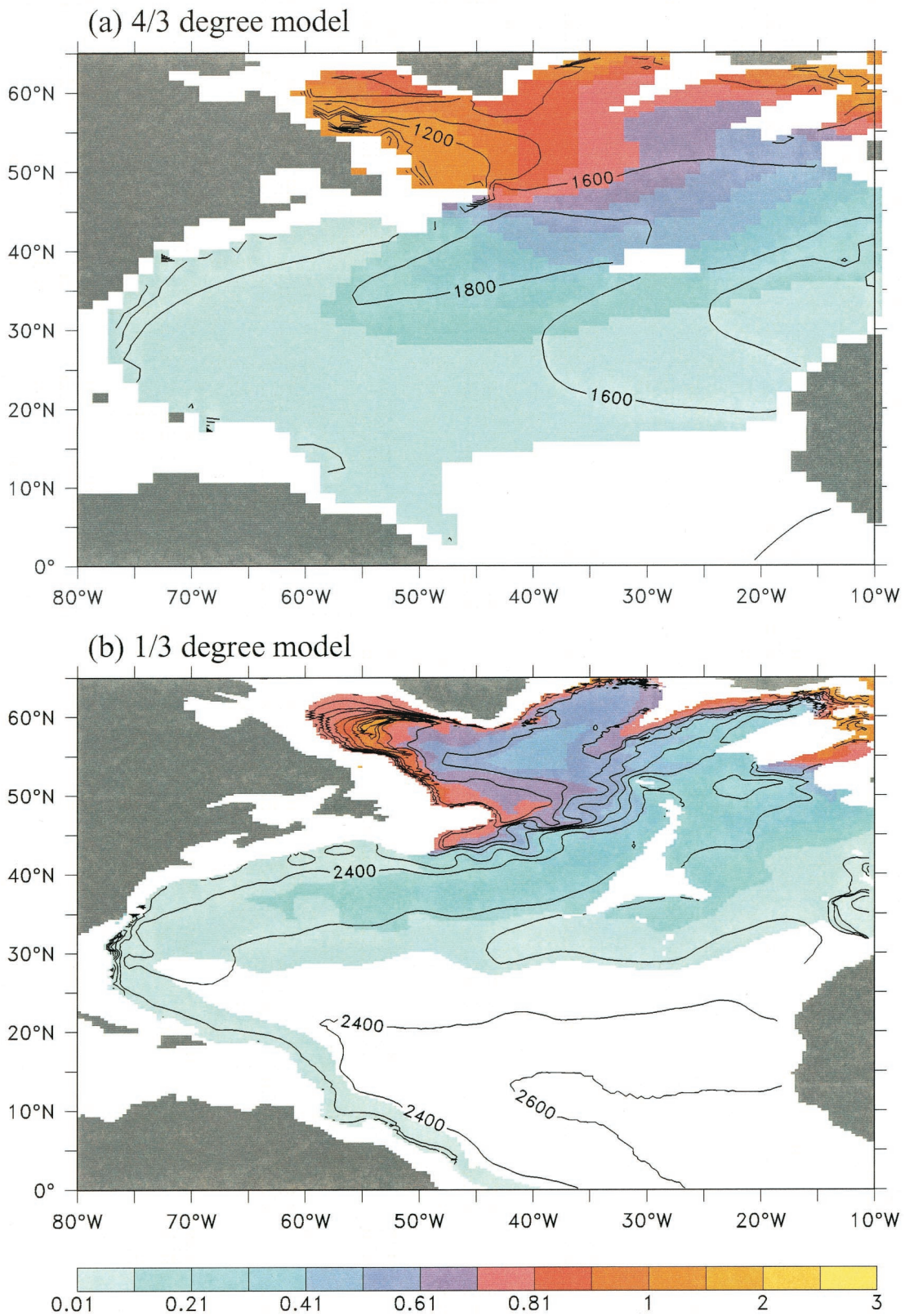
Plate 2. Distribution of CFC-12 on isopycnal surfaces corresponding to maximum North Atlantic Deep Water (NADW) outflow in 1988 in the *Redler and Dengg* [1999] simulations: (a) the 4/3° model and (b) the 1/3° model. The color bar indicates CFC concentrations in pmol kg^{-1}, with isopycnal layer depths contoured (meters). Reprinted with permission from the World Ocean Circulation Experiment.
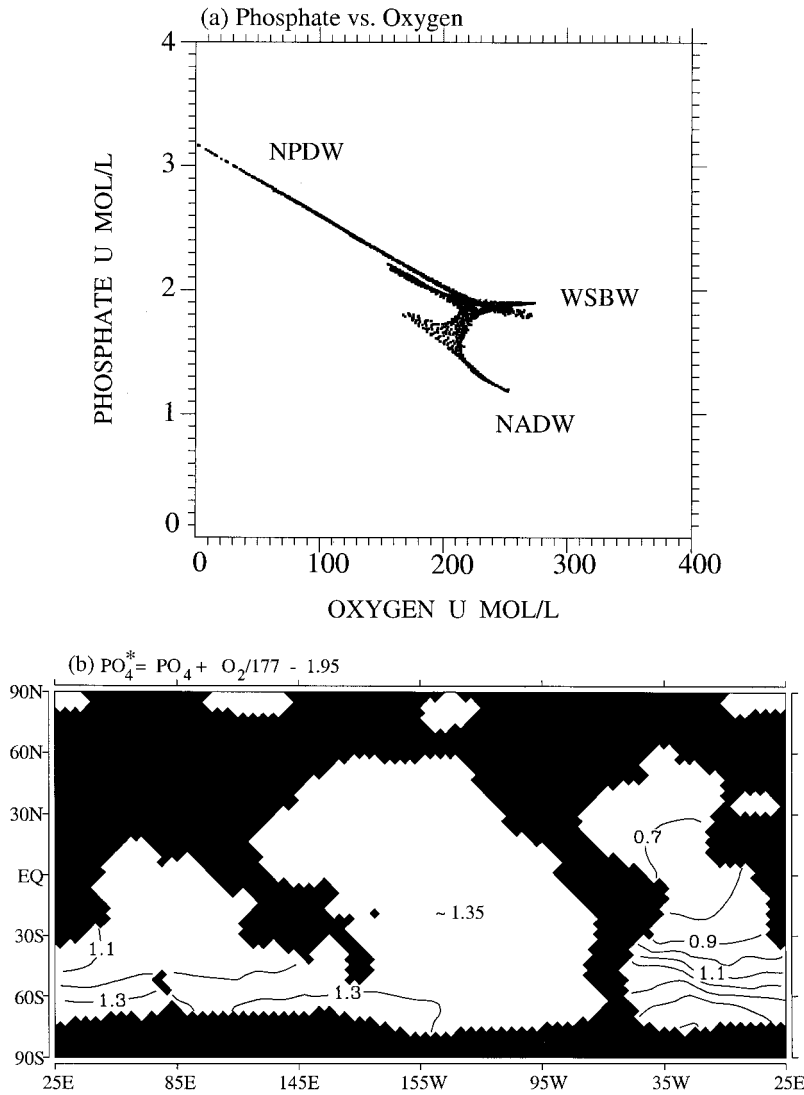
Figure 18. (a) Scatterplot of oxygen versus phosphate in the model of *Maier-Reimer* [1993b]. Water mass signatures indicated are Weddell Sea Bottom Water (WSBW), North Atlantic Deep Water (NADW), and North Pacific Deep Water (NPDW). (b) Global model distribution of $PO_4^* = PO_4 + O_2/177 - 1.95$ at 3000-m depth.

active isotopes of common tracers such as silicon and oxygen. There are generally not many observations of these tracers in the ocean because of measurement difficulty, sometimes requiring large-volume sampling of seawater and subsequent complex chemical analyses. Mantle helium is perhaps an exception in this context, with several transects made during WOCE. For those tracers that have been only sparsely measured over the ocean, some have properties that can be used to diagnose water masses and their ventilation mechanisms in ocean models. Also, if sufficient samples exist in a certain region, then limited-area model assessment can be performed.

6.1. Argon-39

Argon-39 is produced in the atmosphere by cosmic rays like radiocarbon, and being a noble gas, its distribution in seawater is not affected by any biogeochemical processes. It can therefore be included in a model in much the same way as radiocarbon, being carried as a mixing ratio $^{39}Ar/^{40}Ar$. Because of its much shorter

lifetime compared with radiocarbon (400 years as opposed to 8267 years), the structure of $^{39}Ar/^{40}Ar$ in the deep ocean is quite different from $\Delta^{14}C$. *Maier-Reimer* [1993b] and *Orr et al.* [1998] have included $^{39}Ar/^{40}Ar$ as a prognostic tracer in global ocean models. *Orr et al.* [1998] study Atlantic Ocean behavior in two simulations, reporting some success at model assessment using ^{39}Ar. Because of only very sparse measurements in the ocean [*Loosli*, 1989], however, argon is not ideal as a validation tool. To date, only around 100 measurements of ^{39}Ar have been made, although most of these are in the Atlantic Ocean.

Noting the different radioactive lifetimes for ^{39}Ar and ^{14}C, *Maier-Reimer* [1993b] used these tracers to diagnose the models' dominant water mass transformation processes. A scatter diagram of ^{39}Ar against ^{14}C below 1000-m depth in his ocean model is shown in Figure 20. The structure of the scatter reveals the relative importance of diffusion and advection in the model. For a decaying tracer B with lifetime λ the one-dimensional advection equation is solved by $B \approx \exp(-\lambda x/u)$,
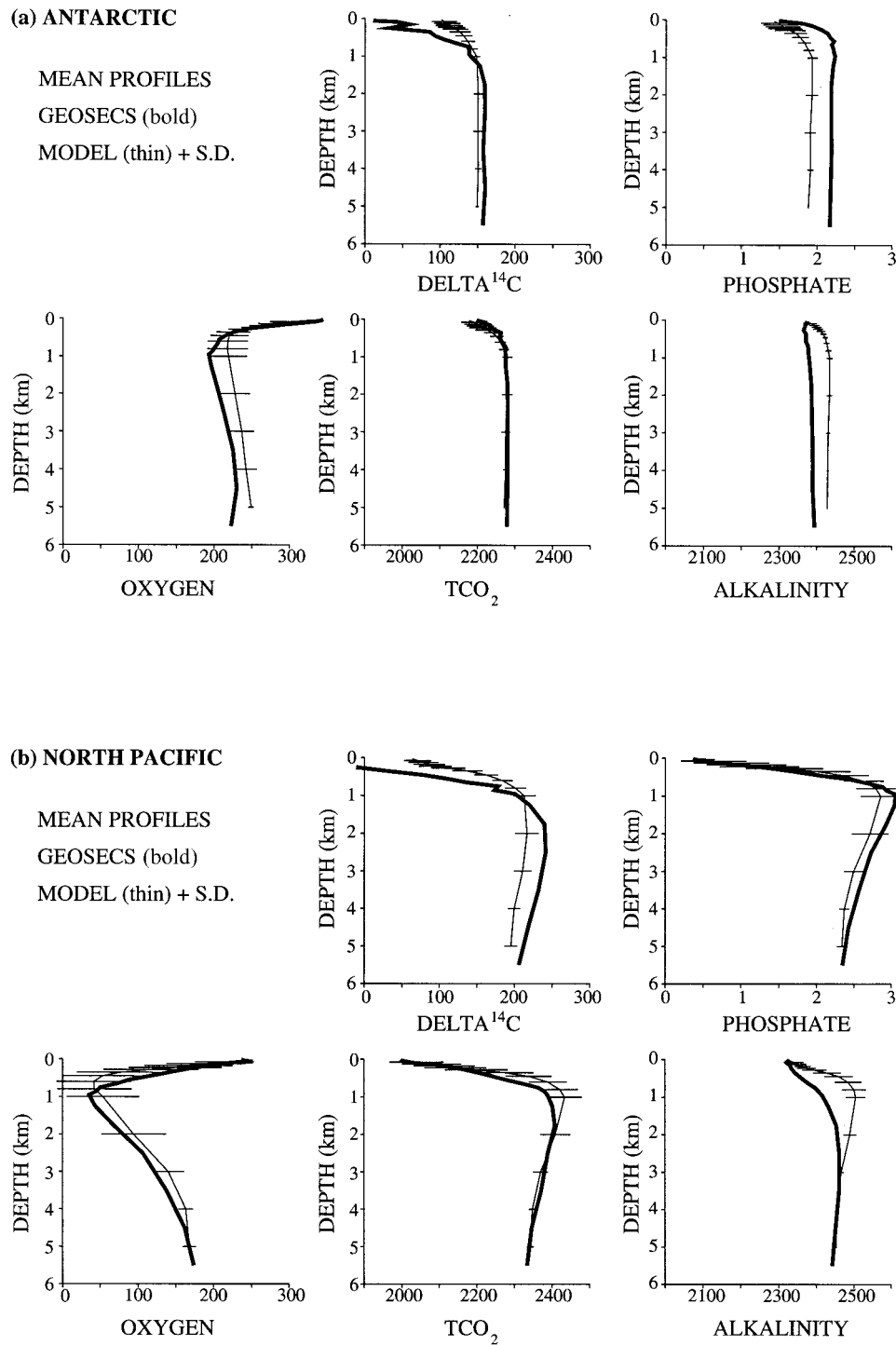
Figure 19. Mean depth profiles of ^{14}C, phosphate, oxygen, DIC, and alkalinity in the (a) Antarctic and (b) North Pacific regions for observations (GEOSECS, bold curves) and the global carbon cycle model of *Maier-Reimer* [1993b] (thin curves). The model profiles also include standard deviation bars at each horizontal level.

whereas the diffusion equation is solved by $B \approx \exp(-x(\lambda/D)^{1/2})$, where u is the advection speed and D is the diffusivity. The theoretical covariation between ^{39}Ar and ^{14}C with decay constants λ_a and λ_c would then be $^{39}Ar = (^{14}C)^{\lambda_a/\lambda_c}$ for pure advection and $^{39}Ar = (^{14}C)^{(\lambda_a/\lambda_c)^{1/2}}$ for pure diffusion [*Maier-Reimer*, 1993b].

Figure 20 includes curves of these two covariance relationships, showing water mass transformation to be predominantly advective in the North Pacific and Indian Oceans, as well as near the formation regions of AABW and NADW. Diffusive mixing dominates the tracer balance in the Antarctic Circumpolar Current (ACC), con-
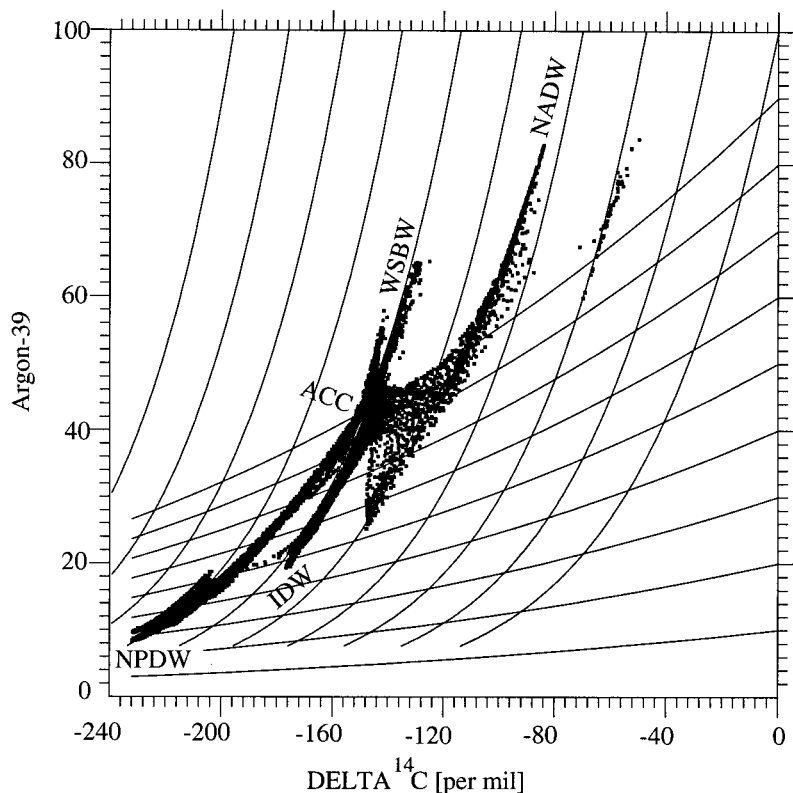
Figure 20. A scatter diagram of ^{39}Ar against ^{14}C below 1000-m depth in the *Maier-Reimer* [1993b] ocean model. The curves with steep slopes indicate the theoretical advective aging for source waters with different radiocarbon content. The curves with flatter slopes indicate the same for exclusive diffusion. Water masses indicated are Weddell Sea Bottom Water (WSBW), North Atlantic Deep Water (NADW), North Pacific Deep Water (NPDW), and Indian Deep Water (IDW). Waters in the Antarctic Circumpolar Current (ACC) are also labeled.

sistent with findings that horizontal diffusion dominates water mass transformation in the ACC in models of coarse resolution and with simple lateral mixing parameterization [e.g., *England*, 1993]. This ^{39}Ar/^{14}C analysis demonstrates the utility of chemical tracers in the diagnosis of water mass transformation in ocean models.
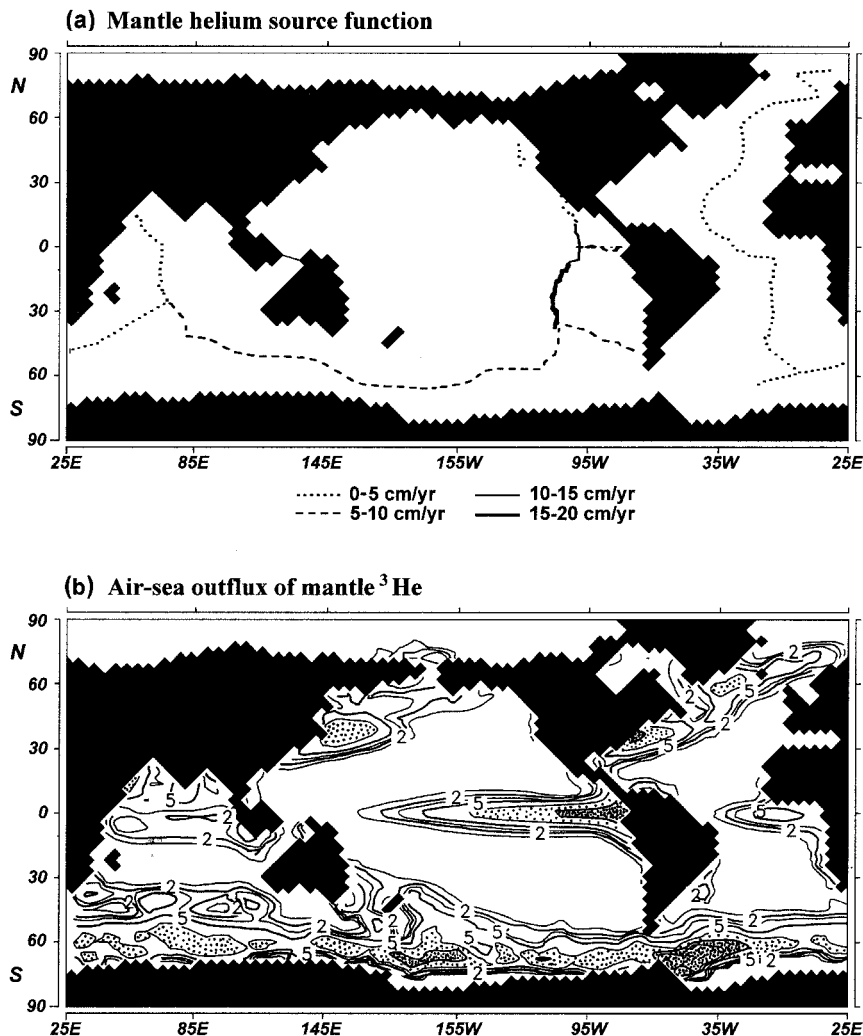
6.2. Mantle Helium

The injection of mantle helium into the deep sea can be used to trace abyssal ocean circulation [e.g., *Lupton and Craig*, 1981]. It can also be simulated within ocean general circulation models [e.g., *Farley et al.*, 1995]. Helium produced in hydrothermal fluids in seafloor volcanism has a distinctive isotopic signature: It is highly enriched in ^{3}He relative to ^{4}He compared with atmospheric helium. Including mantle helium in an ocean model can therefore provide information complementary to that provided by atmospheric tracers such as CFCs or ^{14}C, because mantle helium can trace middepth to abyssal flows in regions not ventilated by anthropogenic tracers. However, source functions of mantle helium are still under investigation, so the tracer is not ideal for direct validation studies. Models of mantle ^{3}He uptake assume injection along the mid-ocean ridge axes with different local spreading rates (e.g., see Figure 21a). *Farley et al*. [1995] assume that the hydrothermal effluents achieve neutral buoyancy 300 m above the ridge axis and estimate a spatial structure for the ^{3}He plume. The forcing assumptions are based on observational studies of helium sources in mantle volcanism. Generally, mod-

elers neglect the atmospheric source of ^{3}He as a radioactive by-product of bomb-produced tritium, so simulations are only valid away from recently ventilated North Atlantic and Antarctic waters.

Results from a simulation of mantle helium uptake are shown in Figures 21 and 22. The model data are taken from a more recent integration of the *Farley et al.* [1995] experiment with increased vertical resolution. The outflux of oceanic mantle ^{3}He is indicative of deepwater upwelling (e.g., in the equatorial Pacific and western boundary currents) or convective overturn (in the North Atlantic and Southern Oceans), both processes bringing deeper ^{3}He-enriched waters to the surface. In comparison with GEOSECS sections, the model exhibits excessive loss of ^{3}He through abyssal to surface upwelling in the Pacific Ocean, whereas the simulation in the Indian Ocean retains too much mantle helium. The model results in the Atlantic Ocean (not shown) are more ambiguous because of uncertainties in the mantle helium input rates. The lack of model ^{3}He in the middepth Pacific Ocean led *Farley et al*. [1995] to speculate that their model removes Pacific Deep Water too rapidly through equatorial upwelling. However, uncertainties in the input source function for mantle helium remain. *Farley et al*. [1995] attempt to use their study to constrain both mantle fluxes of ^{3}He and deep-sea circulation in the ocean model. This can only be achieved by first using a less ambiguous tracer, such as natural radiocarbon, to calibrate the model circulation fields.

(a) Mantle helium source function

(b) Air-sea outflux of mantle ^{3}He

Figure 21. (a) Source function of mantle helium in the model of *Farley et al.* [1995]. Mantle ^{3}He is injected along the mid-ocean ridge axes with different local spreading rates. (b) Air-sea outflux of oceanic mantle ^{3}He simulated by *Farley et al.* [1995]. Units are pmol m^{-2}. Contours are drawn at 1, 2, 3, 5, 10, and 20 pmol m^{-2}. Regions >10 pmol m^{-2} are shaded.

## 6.3. Other Radioisotopes: ^{32}Si, ^{85}Kr, ^{90}Sr, ^{137}Cs

Ocean model simulations have been carried out using a number of other natural and artificial radioisotopic tracers. For example, the distribution of silicon-32, a natural cosmogenic isotope like ^{14}C or ^{39}Ar, was studied in a global ocean model by *Peng et al.* [1993]. They conclude that ^{32}Si, with a half-life of 120 years, is most interesting as a monitor of oceanic upwelling in models. However, they note that observations of ^{32}Si are both sparse and difficult to make, and they in fact speculate that those made as part of GEOSECS could be erroneous, as they show little surface-to-bottom or ocean-to-ocean variations. They also caution that the oceanic input of ^{32}Si is stochastic, limiting its usefulness in ocean model assessment.

Other studies of tracer uptake in global ocean models include particle reactive radionuclides such as Th-230 and Pa-231 [e.g., *Henderson et al.*, 1999]. Krypton-85 has the potential for use in model assessment, although apart from some regional measurements (e.g., ^{85}Kr in the Greenland and Norwegian Seas [*Smethie et al.*, 1986; *Smethie and Swift*, 1989]), there are presently too few observations to allow meaningful model validation over

large scales. Strontium-90 was also thought to be a potentially useful oceanic tracer during the 1980s, with a bomb-produced input function quite similar to tritium and a half-life of 28.0 years. However, it turns out that oceanic ^{90}Sr is more difficult to measure accurately than ^{3}H, and its database remains quite sparse. As far as we know, it has not yet been incorporated into a global ocean circulation model (for a regional simulation, see *Stanev et al.* [1999]).

Artificial radiotracers leaked from nuclear reactors, such as ^{137}Cs from the Chernobyl power station accident [*Buesseler et al.*, 1990], can be used to assess circulation models of nearby regional seas. For example, *Staneva et al.* [1999] study Black Sea circulation and water mass formation in a model calibrated by ^{137}Cs produced in nuclear weapons testing and Chernobyl fallout. Their model can reproduce the observed vertical structure of ^{137}Cs rather well, indicating that they have captured the major ventilation processes driving Black Sea circulation. *Harms* [1997] undertakes a similar study in the Kara Sea, modeling the dispersion of ^{137}Cs and ^{239}Pu hypothetically released from dumped waste sites used by the former Soviet Union.
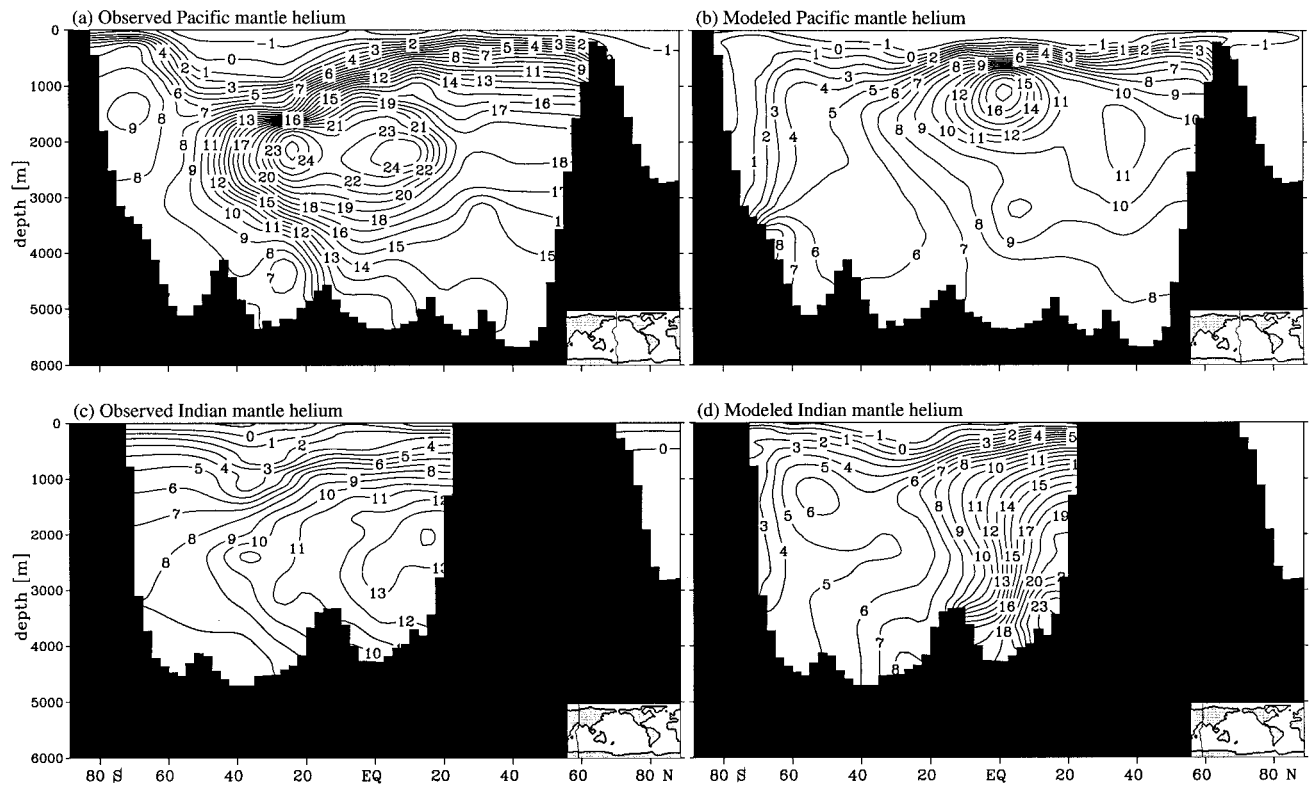
Figure 22. GEOSECS sections of helium: (a) observed Pacific Ocean ³He, (b) modeled Pacific mantle helium, (c) observed Indian Ocean ³He, and (d) modeled Indian Ocean mantle helium. Model results are from a more recent version of the *Farley et al*. [1995] simulation with increased vertical resolution.

6.4. Stable Isotopes: $\delta^{18}O$ and $\delta^{13}C$

Certain stable isotopes, such as $\delta^{18}O$ and $\delta^{13}C$, have been incorporated into ocean circulation models for paleoceanographic applications [e.g., *Heinze et al*., 1991; *Mikolajewicz*, 1996; *Schmidt*, 1998]. Direct oceanic measurements of these tracers are quite sparse and their concentrations are complicated by fractionation, so they are generally not used solely for ocean model assessment. For example, $\delta^{18}O$ concentrations are determined by fractionation during evaporation and sea-ice formation as well as by the isotopic content of rainfall and runoff entering the oceans ($\delta^{18}O$ is therefore thought to be closely related to salinity). Distributions of $\delta^{13}C$ are controlled by the opposing effects of temperature and productivity on the fractionation of isotopes. As such, modelers tend to incorporate these tracers with the multipurpose of model assessment and investigation of fractionation effects. In addition, these tracers are important in the context of paleoceanographic studies: They are measured in deep-sea cores and coral debris and used to infer paleoclimatic conditions, including oceanic T-S [e.g., *Shackleton*, 1977; *Duplessy et al*., 1991].

Schmidt [1998] has studied the distribution of $\delta^{18}O$ in a global ocean circulation model. Part of the goal of his study was to assess the relationship between surface $\delta^{18}O$ and salinity, because paleosalinity reconstructions generally assume a simple linear relationship [e.g., *Duplessy et al*., 1991]. *Schmidt* [1998] is largely able to

capture observed surface GEOSECS gradients of $\delta^{18}O$ (e.g., Figure 23a), though he notes that $\delta^{18}O$ and salinity are only regionally linearly related in his model, with a clear distinction between the tropical oceans and the subtropics (Figure 23b). This suggests that care needs to be taken when reconstructing past salinity values from deep-sea cores. Simple linear $\delta^{18}O$-S relationships need to be assessed using denser sampling than that obtained during the GEOSECS program.

Maier-Reimer [1993b] simulated $\delta^{13}C$ in a coupled ocean-biogeochemical model. Part of the reason for doing this was to determine fractionation effects for isotopes of carbon, including $\delta^{14}C$. Figure 24 shows a comparison between model and observed $\delta^{13}C$ in the western Atlantic Ocean. The model assumes simple constant fractionation and performs reasonably well, particularly in bottom waters and to some extent in NADW. However, there are overly depleted concentrations of $\delta^{13}C$ in the equatorial intermediate waters, with levels less than half those observed. This indicates a problem either with the parameterization of isotope fractionation or with the model circulation in this region. Some questions also remain as to the accuracy of the reported GEOSECS $\delta^{13}C$ estimates of *Kroopnick* [1985].

6.5. Purposeful Release Tracers: SF_6

Deliberate tracer release experiments have been undertaken to study the circulation and mixing in certain
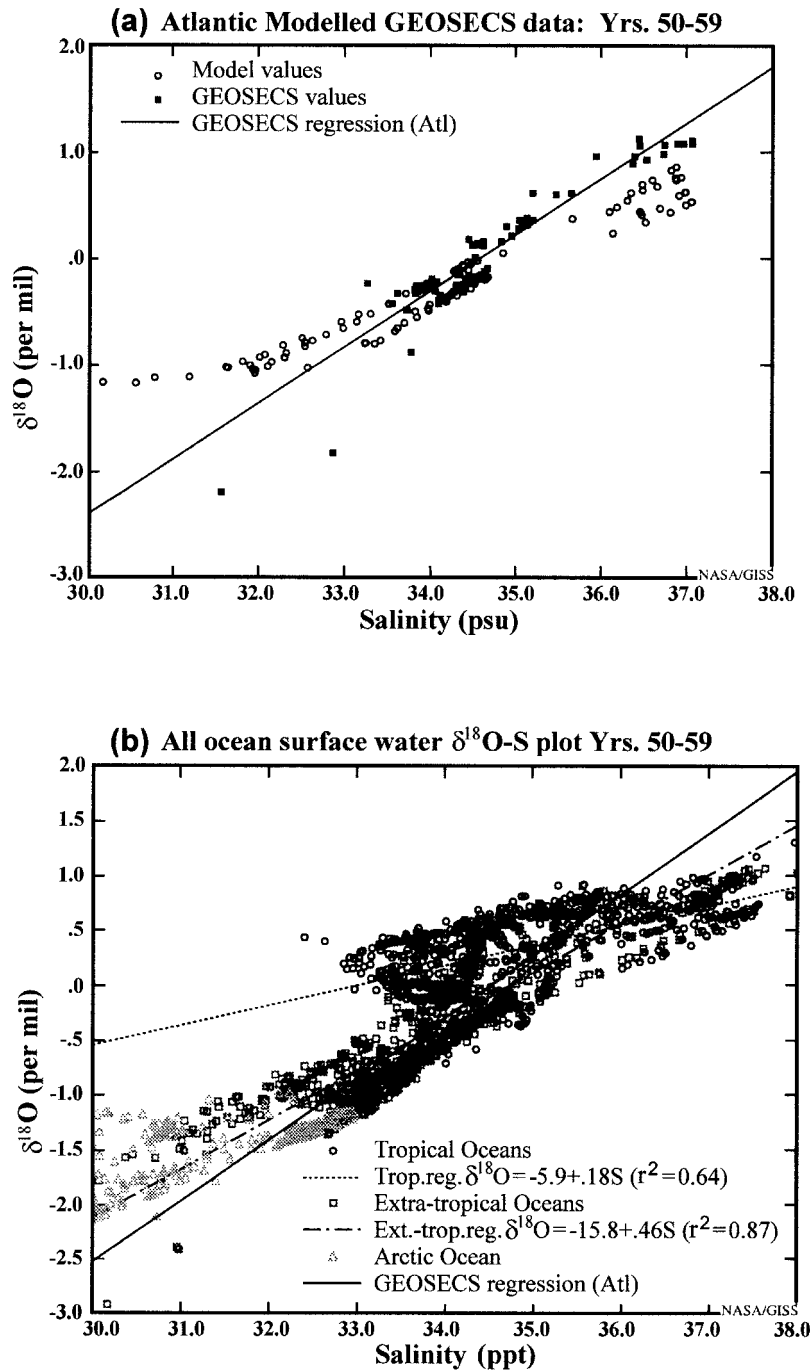
Figure 23. (a) Relationship between surface $\delta^{18}O$ and salinity for GEOSECS data and the global model of *Schmidt* [1998]. (b) Relationship between $\delta^{18}O$ and salinity for surface data points in the global model of *Schmidt* [1998]. Values are split into the tropical, extratropical and Arctic Oceans. Regression lines are fitted separately for each subregion. Also shown is the regression line for the GEOSECS Atlantic data.

locations of the ocean. For example, fluorescent dyes have been used to study diapycnal mixing [e.g., *Woods*, 1968]. Detection levels of these dyes are insufficient to study isopycnal mixing over spatial scales much longer than 1 km. More recently, sulfur hexafluoride (SF_6) has been used to study diapycnal/isopycnal mixing over much larger scales [e.g., *Watson et al.*, 1991; *Ledwell et al.*, 1993; *Ledwell et al.*, 1998], since SF_6 can be measured down to levels as weak as 10^{-17} mol [*Lovelock and Ferber*, 1982]. Typically, the tracer is released within a limited domain (e.g., 20 × 20 km in the North Atlantic Tracer Release Experiment, or NATRE), and subsequent surveys of SF_6 are made at regular intervals over a region covering the dispersion of the tracer. In NATRE, surveys were conducted just after the initial tracer release and subsequently every 6 months for $2\frac{1}{2}$ years.

A map of the initial (May 1992) NATRE SF_6 tracer patch and that measured during April–May 1993 is shown in Figure 25 [from *Ledwell et al.*, 1998]. Note the different spatial scales on the map; the SF_6 tracer patch has spread from a 30- × 20-km zone in May 1992 to about a 1000- × 1000-km region 1 year later. Isopycnal mixing rates can be inferred from the dispersed SF_6 field. In addition, the tracer spreading can be incorporated into an ocean circulation model. For example,
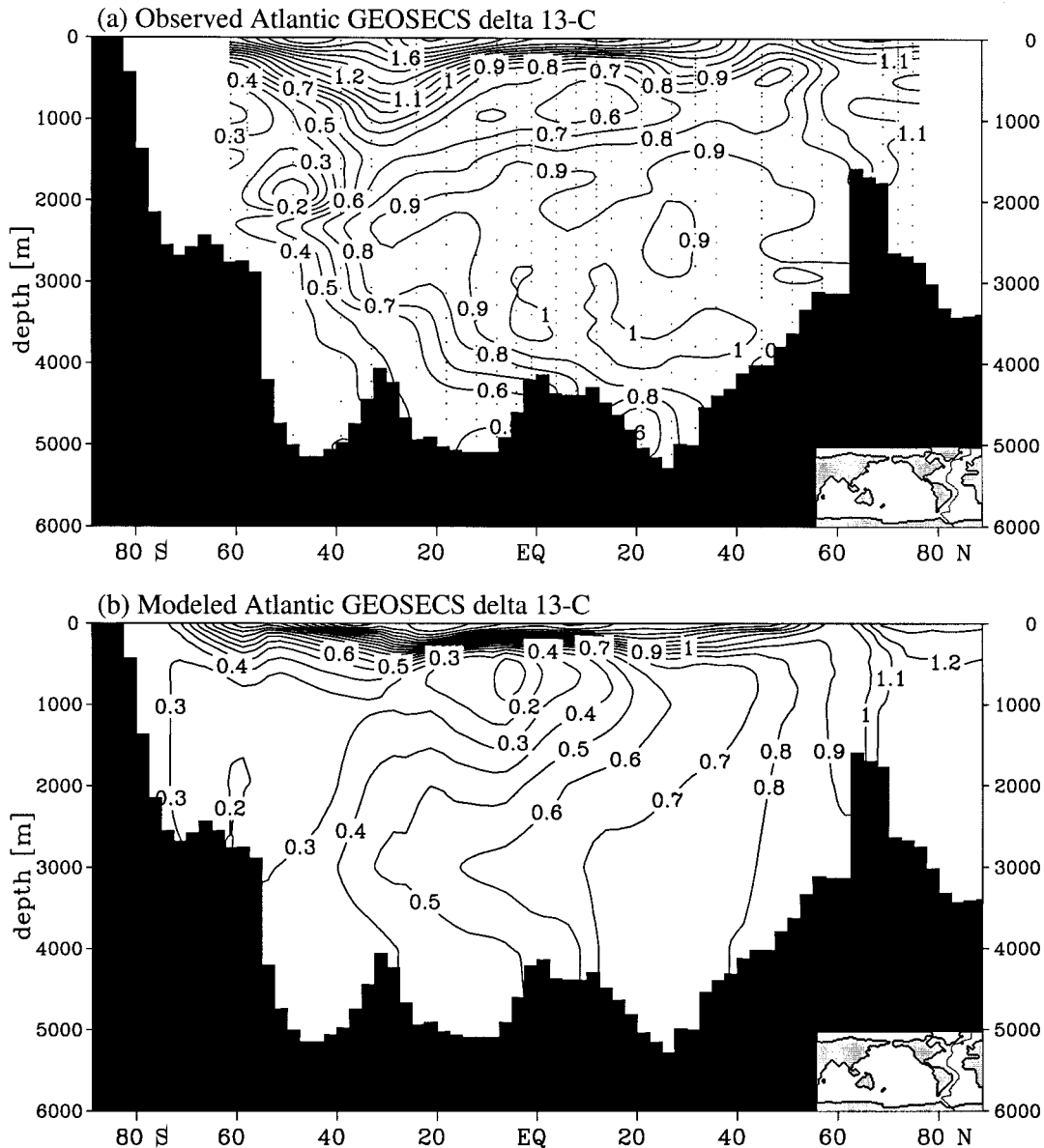
Figure 24. A comparison between model [*Maier-Reimer*, 1993b] and observed [*Kroopnick*, 1985] δ^{13}C in the western Atlantic Ocean GEOSECS section. In the observations, sample locations are indicated. Contour interval is 0.1‰.

Sundermeyer and Price [1998] study the stirring of the NATRE SF_6 tracer patch in a quasi-geostrophic model of the region. Clearly, the spatial scales of the SF_6 patch limit the application of this tracer to regional scales. Nevertheless, SF_6 is inert and its source function is well known, so it is an unambiguous tracer of ocean circulation near the injection region.

7. INCLUDING TRACERS IN MODELS: UNCERTAINTIES AND LIMITATIONS

Using a chemical tracer to assess circulation and water masses in ocean models requires knowledge of the tracer's source function and a faithful representation of its seawater chemistry. Some of these issues have been discussed above for the range of geochemical tracers that have been used in ocean modeling studies. In certain instances, the seawater chemistry is well known, whereas the input function is a source of uncertainty (e.g., tritium, mantle ^{3}He). For others, complex seawater chemistry necessitates inclusion of other chemical tracers and parameterization of biological effects (e.g., CO_2, O_2, PO_4). In this section we focus on some of the uncertainties and limitations in simulating chemical tracer uptake in ocean models. For a detailed review of these issues for tracers involved in the oceanic carbon cycle (section 5) and the so-called exotic tracers (section 6), the reader is referred to the relevant literature given above and in Table 1. Likewise, uncertainties in the

source function for tritium (section 3) will not be discussed here; they are explored in detail by *Weiss and Roether* [1980], *Doney et al.* [1992, 1993], and others. Topics to be covered in this section include the role of the parameterized gas piston velocity for tracers that enter the ocean via an air-sea gas flux (e.g., CFCs, CO_2), uncertainties due to ocean variability, and limitations in regional tracer modeling. We also examine how tracers should be included in ocean and climate models, such as what surface gas forcing should be adopted and whether an off-line model of the tracer suffices.

7.1. Importance of the Air-Sea Gas Piston Velocity

The physical law governing air-sea gas exchange can be written as $Q = k(\alpha C_{atm} - C_w)$, where Q is the gas flux across the air-sea interface (fluxes from the atmosphere into the ocean are positive), k is the gas piston velocity, α is the solubility coefficient, C_{atm} is the atmospheric concentration of the gas over the sea surface, and C_w is the concentration of the tracer in the near-surface seawater. This is the relation that is adopted for forcing air-sea fluxes of gaseous tracer substances in ocean models [e.g., *Maier-Reimer*, 1993b; *England et al.*, 1994]. For a gas whose near-surface seawater and atmospheric concentrations are known, and whose solubility properties are well defined, estimating the air-sea gas flux simply requires a parameterization of the gas piston velocity k. Normally, the model-predicted surface level concentrations define C_w, an atmospheric inventory defines C_{atm}, and α is obtained from studies of solubility properties such as those by *Weiss* [1970], *Weiss* [1974], and *Warner and Weiss* [1985].

Several researchers have suggested bulk wind speed-dependent parameterizations for the gas transfer velocities of certain gases [e.g., *Smethie et al.*, 1985; *Liss and Merlivat*, 1986; *Wanninkhof*, 1992]. (Liss and Merlivat and Wanninkhof are hereinafter referred to as LM86 and W92, respectively.) An excellent review of these studies is given by W92. Figure 26 shows the estimated dependence of k on wind speed after *Smethie et al.* [1985], LM86, and W92. Substantial variation (up to a factor of 2) can be seen between the three gas exchange studies, with the W92 quadratic dependencies and the *Smethie et al.* [1985] Transient Tracers in the Oceans (TTO) values greatly exceeding the parameterization of LM86. In the case of W92, this is because he takes into account possible chemical enhancement effects at low wind speed (such as turbulence at the air-sea interface) and the time variability of surface winds. There remains some debate as to which parameterization of k should be adopted in ocean models. Several researchers have explored air-sea tracer flux sensitivity to changes in k (e.g., [14]C [*Toggweiler et al.*, 1989a], anthropogenic CO_2 [*Sarmiento et al.*, 1992], and CFCs [*England et al.*, 1994]). In a model run with a 100% increase in k, *Sarmiento et al.* [1992] report significant sensitivity in localized regions of convective overturn but only a ~10% increase in global anthropogenic CO_2 uptake by 1986. It should be noted

(a) Initial (May, 1992)
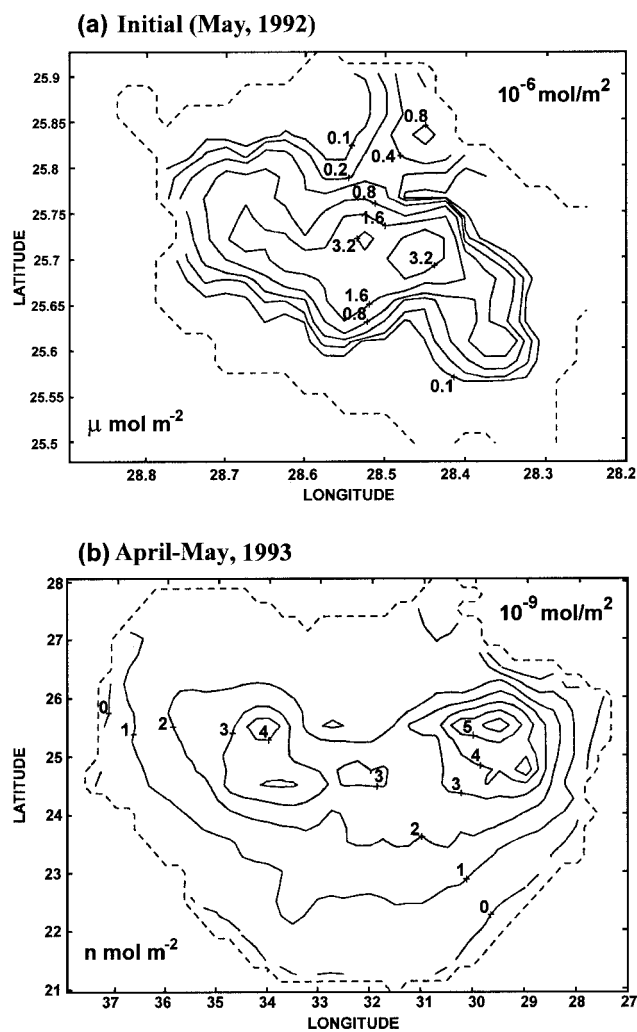
(b) April-May, 1993

Figure 25. Map of the initial (May 1992) North Atlantic Tracer Release Experiment (NATRE) SF_6 tracer patch and that measured during April–May 1993 [from *Ledwell et al.*, 1998]. Note the different concentration and spatial scales in the two panels; the SF_6 tracer patch has spread from a highly concentrated 30- $\times$ 20-km zone in May 1992 to a more diluted 1000- $\times$ 1000-km region 1 year later.

that for model validation studies, where regional model-observation comparisons are made, uncertainties in convection regions are problematic.

Here we examine the effects of k in determining model uptake of CFC, a gas that attains saturated equilibrium relatively quickly in the ocean [e.g., *Broecker and Peng*, 1982]. For more slowly equilibrating gases, such as CO_2, we would expect a higher degree of sensitivity. Two uptake experiments are run within the global model of *England* [1995]; one following the W92 parameterization of k, the other adopting the LM86 relationship. This will give us some idea as to how sensitive CFC uptake can be to the choice of k. The ocean model employs seasonal surface forcing and adopts simple Cartesian mixing of tracers. The CFC flux is limited in regions of observed sea-ice cover, and climatological wind speeds [*Esbenson*
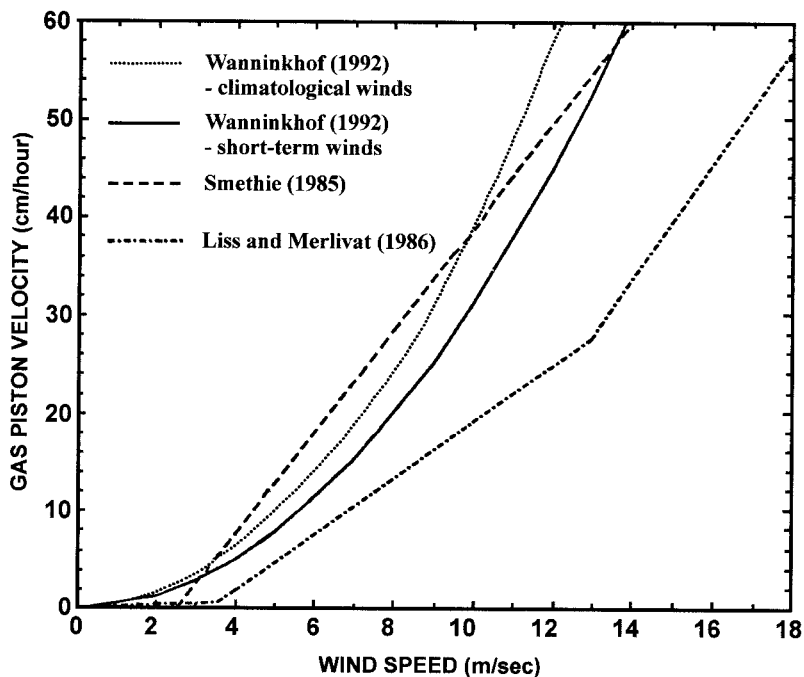
Figure 26. Estimated dependence of the gas piston velocity (k, cm h^{-1}) on wind speed (m s^{-1}) after *Smethie et al.* [1985] (long-dashed curve), *Liss and Merlivat* [1986] (dash-dotted curve), and *Wanninkhof* [1992] (solid curve for short-term winds, dotted curve for long-term mean winds).

and Kushnir, 1981] are used to compute k. Plate 3 shows zonal-mean CFC-11 in the South Atlantic Ocean in 1995 using the W92 parameterization of k, as well as the percentage reduction in CFC-11 when the ocean model is rerun using LM86 k. The LM86 parameterization leads to significantly weaker CFC-11 uptake, particularly in regions of water mass formation. Maximum differences in simulated CFC occur in AAIW and AABW (~16–20% reduction), with significant interior differences also seen in NADW outflow (~10–12% reduction). Overall, errors associated with uncertainties in k appear to be of the order of 5–15% for CFC uptake.

For typical wind speeds in the Southern Ocean (8–10 m s^{-1}), adopting LM86 yields a 35–40% decrease in k (Figure 27). At higher and lower wind speeds this difference is even greater. This can lead to significantly decreased CFC uptake in certain water masses, as shown above. Further studies in air-sea gas flux parameterization will lead to greater certainty in the form of k most suitable for ocean tracer models. Present uncertainties in k can lead to nontrivial and systematic errors in gas exchange in ocean model simulations.

7.2. Off-Line Tracer Modeling

Tracer simulations are sometimes calculated in an "off-line model," in which the steady state fields of T-S and u-v from a full general circulation model are used to advect and mix the tracer. This is potentially useful in models of high resolution where the computational cost of an "on-line" tracer model can be prohibitive. Examples of this can be found in the off-line tracer models of *Sarmiento* [1983], *Ribbe* [1996], and *Ribbe and Tomczak* [1997] (Ribbe and Tomczak are hereinafter referred to as RT97). Although computational savings are made

with such an approach, there are important factors that must be considered. For example, *Sarmiento* [1983] did not use the model-predicted convection to drive tritium overturn in the North Atlantic. Instead, he artificially imposed convective mixing to the depth of the winter-time mixed layer estimated by *Levitus* [1982]. This means the simulation is not a true validation test of the North Atlantic model, because tritium is fluxed into the interior without regard to the model-predicted convection.

RT97 examine tracer uptake using the annual-mean advection (u, v) and convection fields from the Fine Resolution Antarctic Model (FRAM). However, FRAM was run using a seasonal cycle of surface forcing, so this technique could alias important seasonal effects. For example, the annual-mean convection depth is probably around 30% of the maximum wintertime mixed layer depth, so penetration of tracer in their off-line model will not be as deep as it should be. Their model will simulate year-round convection of tracer in a shallow convective layer, rather than intermittent deeper convection. This compromises the RT97 findings for water masses such as Subantarctic Mode Water.

In fine-resolution models, transient eddies can have a significant impact on the tracer distribution, although this is impractical to incorporate explicitly in an off-line model. It would require saving a vast amount of model data, to the extent that the off-line model would be more computationally intensive than a full on-line version. A possible compromise is to include eddy mixing and advection effects derived from integral statistics of the full on-line model. Thus far, no such tracer simulations have been performed using global eddy-resolving models. RT97 approximate diffusion rates by simple Cartesian mixing, that is, $A_{\mathrm{H}}(\partial^2 C/\partial x^2 + \partial^2 C/\partial y^2) + A_{\mathrm{V}}\partial^2 C/\partial z^2$,
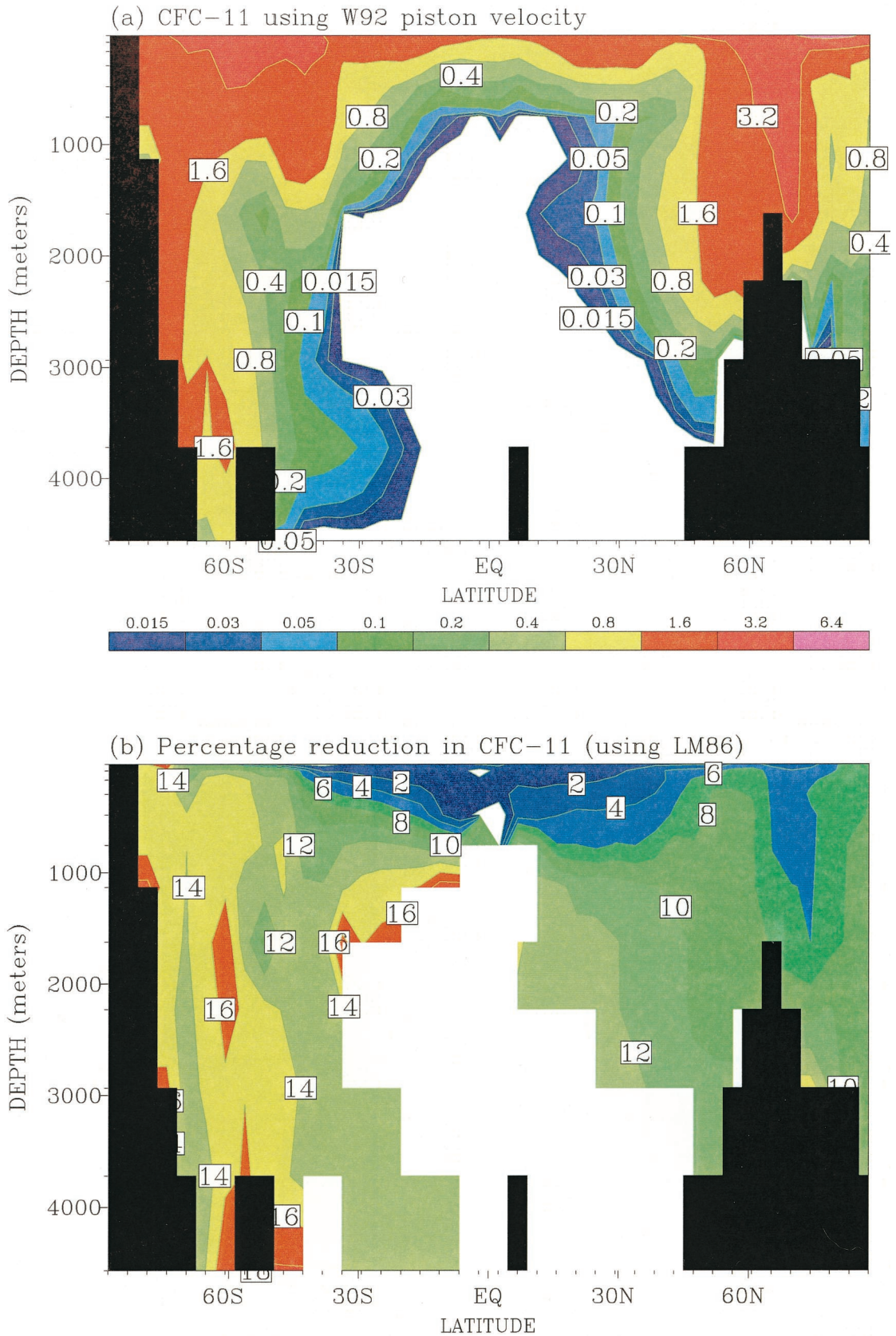
Plate 3. (a) Basin-averaged CFC-11 simulated in 1995 in the Atlantic Ocean using the *Wanninkhof* [1992] formulation of piston velocity k. (b) Percentage reduction in CFC-11 content when the same ocean model is rerun using the *Liss and Merlivat* [1986] parameterization for k.

where A_H and A_V are the horizontal and vertical diffusion coefficients and C is tracer content. This is unrealistic, as the FRAM model uses biharmonic mixing and also partially resolves eddies, which mix and advect tracers. The annual mean u-v field employed by RT97 cannot take account of transient eddy advection effects. Thus, for a number of reasons, the *Ribbe and Tomczak* [1997] off-line tracer model misrepresents the physics of the on-line FRAM system.

A clever innovation of the off-line tracer model approach has been developed by *Aumont et al.* [1998] for nontransient tracers such as natural radiocarbon. The technique is to minimize computational costs by seeking initial conditions that should be close to the final solution. *Aumont et al.* [1998] initialize their ^{14}C run with an off-line equilibrated simulation using four-grid cell-averaged velocity fields from the full model. That is, the output from the physical ocean model of higher resolution is used to spin up a lower-resolution initial ^{14}C field without a full numerical integration of the momentum and tracer equations. Only ^{14}C is computed over a grid 4 times coarser than the full model. In turn, the coarser-grid off-line model can be initialized using a similar degradation approach. *Aumont et al.* [1998] employ two such degradations in their study and note that more could be employed for fine-resolution models. The resulting radiocarbon fields then require substantially less time to attain equilibration in the full on-line version, because they are already close to the final equilibrated ^{14}C. This results in substantial computational savings (a factor of 17 is noted for the double degradation case) and negligible loss of accuracy so long as the full on-line version is run for several hundred years. This technique is, however, only appropriate for "steady state" chemical tracers such as natural ^{14}C, where long integration times are required for full equilibration. The method cannot easily be applied, for example, in studies of transient tracer uptake (e.g., CFCs or bomb ^{14}C).

7.3. Ocean Model Equilibration

When including transient tracers in simulations, the physical ocean model should be fully equilibrated prior to incorporation of the tracer. Coarse-resolution models are inexpensive enough to ensure a steady state ocean circulation before chemical tracer uptake is simulated [e.g., TDBa, TDBb; *England and Hirst*, 1997]. Studies of tracers in higher-resolution global models [e.g., *Craig et al.*, 1998; *Ribbe and Tomczak*, 1997] normally include tracer uptake well before the model is equilibrated with respect to interior water T-S. This means that processes such as deep convection and ocean currents will still be adjusting to the surface forcing when the tracers are included. The results from such studies should therefore be viewed with caution for water masses that are not equilibrated in the physical ocean model. This includes outflowing NADW and AABW, and even possibly AAIW, for models integrated for only about 20 years prior to tracer inclusion. Off-line model techniques such
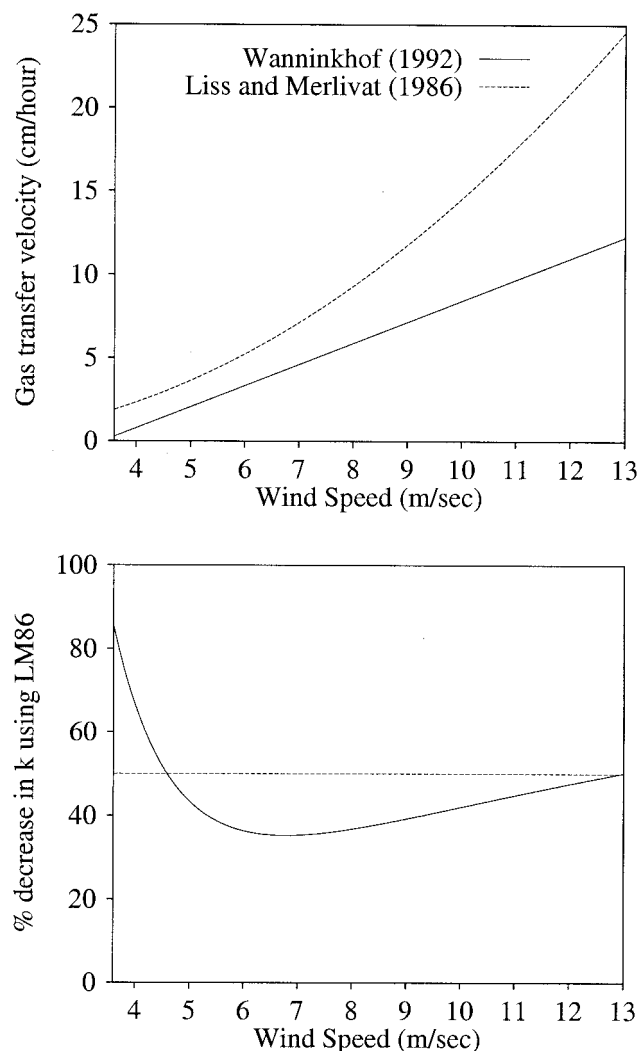
Figure 27. Comparison of the *Wanninkhof* [1992] and *Liss and Merlivat* [1986] parameterizations of gas piston velocity for typical wind speeds over the open ocean. In the Southern Ocean (wind speeds of the order of 8–10 m s^{-1}), adopting Liss and Merlivat yields a 35–40% decrease in k.

as those described above (e.g., the degradation approach of *Aumont et al.* [1998]) cannot remedy this problem because they are only appropriate for equilibrium tracers such as natural radiocarbon.

7.4. Tracers in Coupled Climate Models

It is of interest to consider how tracer simulations should be performed within coupled climate models. If the focus of the study is to simulate, for example, the oceanic carbon cycle during anthropogenic climate change, the air-sea flux of carbon should be simulated using the model-derived fields of wind speed, sea ice, T-S, and so on [*Sarmiento and Le Quéré*, 1996]. This is because these variables are likely to change during the climate change run, affecting the simulated carbon uptake by the ocean. Indeed, the very goal of such studies is to examine how changed climatic conditions will alter

the oceanic uptake of CO_2. If, however, the goal of the study is to validate the ocean model used within the climate system [e.g., *Dixon et al.*, 1996], we recommend that two techniques be used to check the oceanic uptake of the tracer. The first simply uses model fields to derive the surface tracer flux (as was done by *Dixon et al.* [1996]). The second adopts observed wind speed, sea ice, and T-S to estimate the gas flux. This is because coupled models can simulate erroneous wind speeds and sea ice, which renders the gas fluxes biased in some way during the tracer uptake run.

This point is demonstrated in Figures 28 and 29, which show two different scenarios in which a "good" CFC simulation can be achieved in a climate model in spite of spurious oceanic circulation. In the first case the ocean model has spurious convection in polar waters, resulting in erroneously warm near-surface water and a melt back of sea ice, forming an open ocean polynya in conflict with observations (Figure 28). Using observed sea ice to estimate the air-sea CFC exchange would mean zero gas flux over the spurious polynya, leading to no CFC loading of the convected waters. If, however, the model sea ice were used to force the CFC flux, the convected waters would be CFC-laden and the spurious oceanic circulation would be exposed. In the second scenario the climate model simulates too much Antarctic sea ice and its subpolar wind belt is too weak (Figure 29). This is the case in certain coupled models, such as that of *Dixon et al.* [1996]. In the example shown, spurious ocean overturn and vertical mixing occur in the subpolar waters. Using model sea ice and winds to force CFC uptake leads to a weak gas flux over the spurious overturning region, resulting in weak CFC loading in the overturned waters. As such, the coupled climate model can have an apparently good simulation of CFC in spite of spurious overturn in subpolar waters. This is likely to be the case in the *Dixon et al.* [1996] study, as discussed below.

To examine this, we have run the *England* [1995] isopycnal mixing case using two gas-forcing techniques. This model case was set up to have the same geometry, resolution, and mixing parameterization as the *Manabe et al.* [1991] coupled model, which *Dixon et al.* [1996] analyzed for CFC uptake. In the first experiment the W92 gas flux parameterization uses observed climatological wind speeds to compute k [*Esbenson and Kushnir*, 1981]. It also uses observed T-S to compute CFC solubilities and Schmidt numbers and observed sea ice to limit air-sea gas fluxes in regions of ice coverage. In the second experiment, exactly the same forcing technique is employed, only the *Manabe et al.* [1991] coupled model wind speed, sea-ice coverage, and ocean T-S are used to compute k, solubilities, Schmidt numbers, and ice-reduced gas exchange. The *Dixon et al.* [1996] runs were made on-line within the coupled model, so their simulations will still differ from our second model experiment because the climate model has day-to-day variability. However, this is substantially less than the month-to-month variability for wind speed, sea surface temperature, sea surface salinity, and ice coverage. As such, the second experiment approximates the tracer uptake forcing employed by *Dixon et al.* [1996].

Results for both model experiments and their difference are included in Plate 4 along the Ajax section. Whereas the standard *England* [1995] case shows quite erroneous CFC uptake (Plate 4b), we get substantially reduced and reasonably realistic CFC using the same circulation model only with *Dixon et al.* [1996] gas forcing (Plate 4c). The CFC inventories are only fractionally stronger than the actual *Dixon et al.* [1996] simulation, which suggests that our uncoupled ocean model and gas uptake approximate their run reasonably well. This apparently good CFC simulation is due to (1) the coupled model simulating weak Southern Ocean winds (about 20–30% weaker than observed, resulting in a slower gas piston velocity k), and (2) the coupled model simulating an excessive coverage of sea ice around Antarctica. Both these factors play an approximately equal role in reducing Southern Ocean CFC uptake in the model.

More careful examination of Plate 4 reveals that the observation-derived fluxes yield realistic surface level CFC-11, whereas the *Dixon et al.* [1996] forcing systematically underestimates surface content, particularly at 70°–50°S. This is also the case in the original *Dixon et al.* [1996] coupled model run (see Plate 1f). The *Dixon et al.* [1996] case is approximately 20–90% undersaturated in surface-layer CFC over the Southern Ocean, which is much higher than observed. It is suggested therefore that their model CFC forcing leads to artificially weak CFC fluxes over the subpolar Southern Ocean, leading to a weak loading of CFC over the convective overturn region. This compromises their validation study.

7.5. Chemical Tracers in Regional Models

Specifying boundary conditions for chemical tracers in regional ocean models can be problematic, especially for transient tracers. Even if a model domain is selected to have open boundaries that coincide with a WOCE hydrographic section, it is necessary to extrapolate the time-dependent tracer content at the open boundary, which requires assumptions about the long-term ocean circulation in particular regions. Examples of regional transient tracer modeling include those by *Redler et al.* [1998] and *Redler and Dengg* [1999].

The problem of regional transient tracer modeling is demonstrated in the North Atlantic model of *Redler et al.* [1998], wherein an open boundary exists at 18°S. While the high-resolution model is able to reproduce observed CFC patterns in the DWBC quite well (Plate 2), it fails to show up features in the equatorial current regime like the eastward flow of CFC-enriched water at depths near 2000 m. In the model, advection of water with low CFC concentration from the south dilutes the near-equatorial waters, and this is entirely a boundary condition effect. *Redler et al.* [1998] did not have ade-
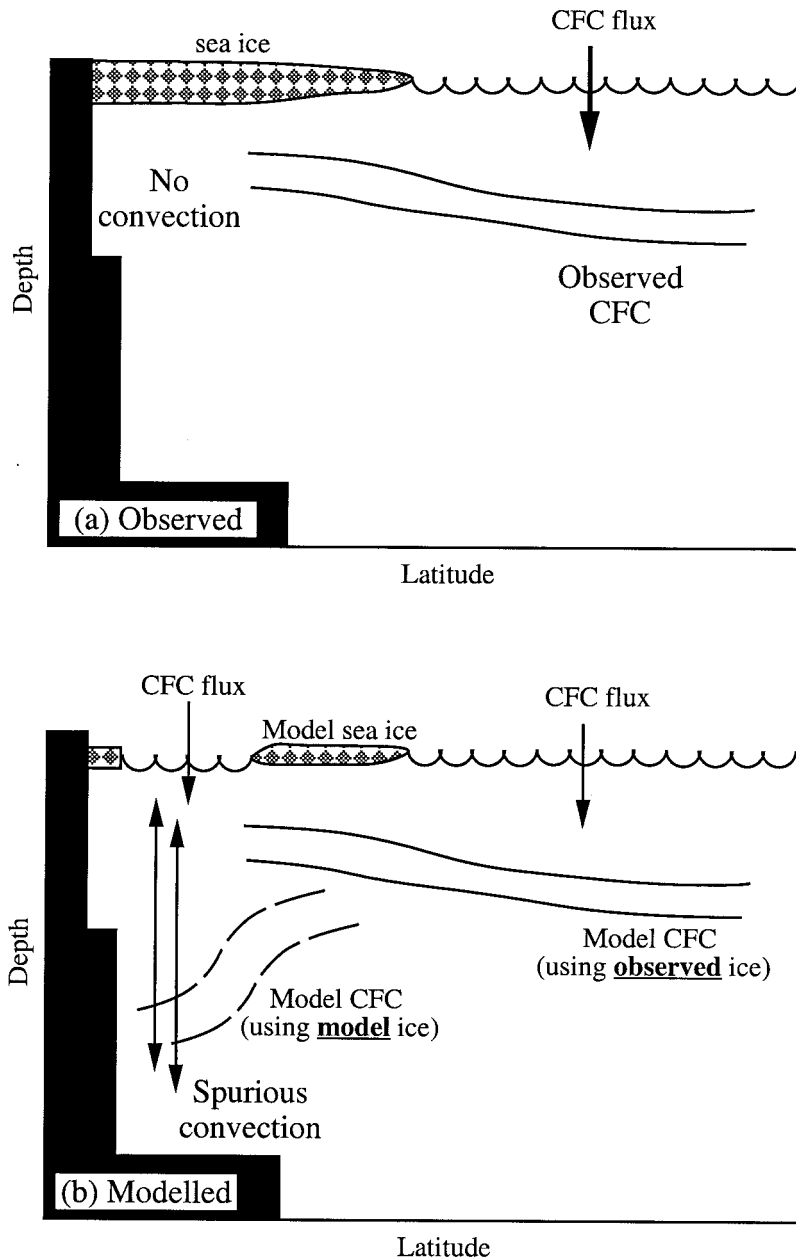
Figure 28. Scenario in which using observed sea ice in a coupled model tracer validation study can lead to an apparently good simulation in spite of spurious convection in polar waters. Using observed sea ice to force CFC uptake would mean no gas flux in the spurious polynya created by the unrealistic convection, leading to no CFC loading in the convected waters.

quate estimates of CFC content at the southern open boundary to properly address this question.

7.6. Ocean Variability and Tracer Modeling

The ocean's thermohaline circulation exhibits substantial variability on interannual, decadal, centennial, and longer timescales [see, e.g., *Roemmich and Wunsch*, 1984; *Dickson et al.*, 1996; *Rintoul and England*, 2000; *Weaver et al.*, 2000]. As such, chemical tracer uptake by the ocean changes with time, being absorbed in varying quantities depending on water mass formation rates. For example, natural ^{14}C and PO_4^* suggest that AABW formation rates were on average 15 Sv (1 sverdrup (Sv) equals 10^6 m^3 s^{-1}) over the past 800 years, whereas CFC inventories (tracking the last few decades) suggest

AABW production has slowed to <5 Sv in recent times [*Broecker et al.*, 1999]. This is a source of uncertainty in ocean model assessment, as invariably an assumption of annual-cycle steady state circulation is made. For example, present-day deep Pacific Ocean radiocarbon content is determined by past ventilation rates (from as long as 1000 years ago). So model assessment using natural ^{14}C implicitly assumes that the climate conditions of today (as used to force the model) have more or less persisted for hundreds of years. This is very unlikely to be the case. As yet, no attempt has been made to estimate the magnitude of this type of uncertainty in tracer model assessment.

Mesoscale oceanic variability can introduce a sampling error into measured transient tracer fields [*Haine*
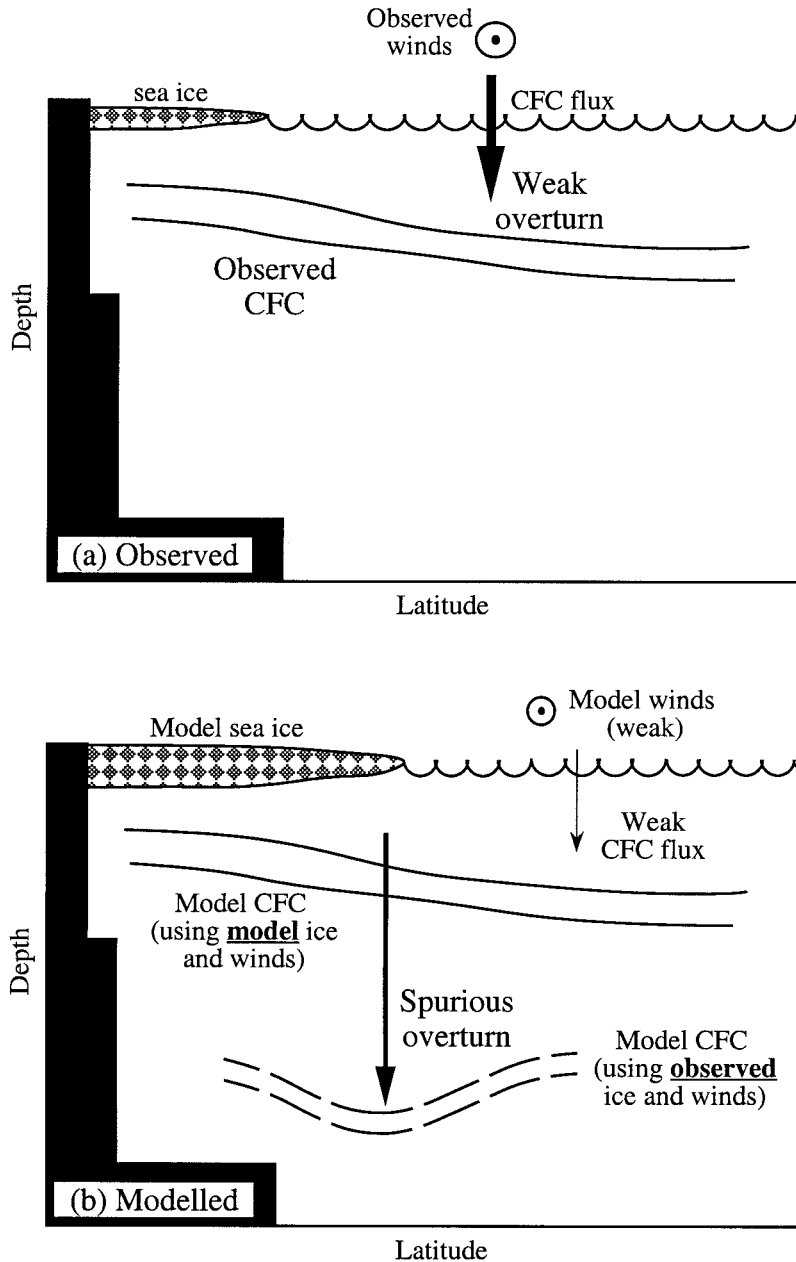
Figure 29. Scenario in which using model sea ice and winds in a coupled climate tracer validation study can lead to an apparently good simulation in spite of spurious overturn in subpolar waters. Using model sea ice and winds to force CFC uptake would lead to a weak gas flux over the spurious overturning region, leading to weak CFC loading in the overturned waters. This is a schematic of what is likely to have occurred in the *Dixon et al.* [1996] study.

and Gray, 2001]. For example, a one-time basin-wide hydrographic section can take several months to complete, which means small-scale spatial and temporal variability is aliased, and seasonal cycles and interannual variability are not resolved. Oceanic variability is ubiquitous and evident at many scales, so we can expect a degree of aliasing in tracer data products. Direct model validation can therefore be limited, as a model might resolve a spectral range different from what is present in a measured data set. To assess model skill directly, we need to quantify the sampling error, including that due to mesoscale variability [see *Haine and Gray*, 2001] and to seasonal and interannual cycles.

8. SUMMARY AND CONCLUSIONS

We have reviewed the use of a range of chemical tracers in ocean models, particularly with regard to their application in assessing circulation and water mass formation. Tracers that have been used in this context include tritium, chlorofluorocarbons, natural and bomb-produced radiocarbon, and to a lesser extent, oxygen, silicate, phosphate, isotopes of organic and inorganic carbon compounds, and some noble gases (e.g., helium and argon). It was seen that substantially more information could be derived from tracer experiments than from using T-S alone. Natural chemical tracers such as iso-

topes of carbon and argon are particularly useful for examining model processes associated with older water masses, such as North Pacific and Circumpolar Deep Water. For example, *Maier-Reimer* [1993b] complements a simulation of ^{14}C with ^{39}Ar to elucidate the relative roles of advection and diffusion in water mass spreading in the deep ocean. However, ^{39}Ar measurements in the ocean are very sparse, limiting this tracer in validation efforts. As such, we primarily advocate radiocarbon ($\Delta^{14}C$) in attempts to assess ocean models with regard to long-timescale circulation processes.

Complications with seawater chemical and biological cycles fundamentally limit tracers such as oxygen and phosphate in the context of ocean model validation. Radiocarbon can be simulated as a ratio of $^{14}C/^{12}C$, thereby mostly avoiding complications associated with the biological consumption and remineralization of this isotope. Anthropogenic tracers such as tritium, chlorofluorocarbons, and bomb-produced ^{14}C are well suited for analyzing model ventilation over decadal timescales, such as the renewal of AAIW and ventilation pathways of NADW and AABW. Bomb tritium favors a Northern Hemisphere uptake, so interhemispheric input differences can be exploited to distinguish thermocline ventilation pathways in models and observations. It should be noted, however, that the source function of tritium is less accurately known compared with that of CFCs. In addition, the ^{3}H half-life of ~12 years limits its penetration into the ocean interior subsequent to subduction. In view of this and present uncertainties in the tritium input function, CFCs and bomb-produced ^{14}C appear to be the best chemical tracers for decadal to interdecadal ocean model assessment.

Using model simulations of radiocarbon, TDBa and TDBb showed that restoring the interior water mass field to observed T-S actually degrades the model's representation of observed ventilation processes. This is because the model water mass formation mechanisms, such as convection and subduction, are largely suppressed by the stable-stratified density field that is artificially maintained by the internal T-S restoring terms. This finding directly points to geochemical tracers as an important adjunct to T-S in ocean model validation efforts, since a "correct" T-S field can theoretically support spurious circulation patterns.

Other chemical tracer studies have helped to reveal inadequacies in coarse resolution model representation of key water mass formation processes, in particular convection, downslope flows, and deep-ocean currents. These models can chronically exaggerate the spatial scales of open-ocean convection and boundary currents, while underestimating deep flow speeds and diffusing downslope flows with excessive lateral mixing. Higher-resolution models alleviate many of these problems [e.g., *Semtner and Chervin*, 1992; *Böning et al.*, 1996], though in global mode they typically only resolve thermocline ventilation due to shorter integration times. In addition, most resort to high-latitude T-S restoration to simulate

reasonable interior water mass characteristics. This can result in spuriously weak chemical tracer uptake at high latitudes, for reasons similar to those detailed by TDBa.

There are some remaining limitations and uncertainties in using chemical tracers to assess ocean models. For example, input functions and surface boundary conditions need to be well known. Uncertainties remain in the gas piston velocity k, and in tritium and mantle helium source functions. In coupled climate models, validation requires separate model runs to isolate errors in surface tracer uptake from errors in the simulated circulation. Oceanic variability also confounds model assessment by introducing an unknown sampling error distribution, both spatial and temporal, into measured data. In off-line tracer models, uncertainties exist in the degree to which mean circulation fields alias internal model variability. Specifying lateral boundary conditions in regional models can be problematic, especially for transient tracers.

Future work in chemical tracer modeling includes ongoing improvement in assessment techniques, minimization of uncertainties in boundary conditions and chemical/biological cycles, and more formal quantification of model skill. Though beyond the scope of this paper, it is worth noting that chemical tracer measurements have been assimilated into ocean models, with researchers reporting model improvement in tracer-constrained simulations [see, e.g., *Meméry and Wunsch*, 1990; *Schlitzer*, 1996; *Follows et al.*, 1999; *Gray and Haine*, 2000]. As such, tracers can be used to assess and directly constrain ocean model simulations. Coordinated model intercomparison projects are also being actively pursued [e.g., *Orr*, 1999; *Orr et al.*, 2001]. Other future directions include the incorporation of tracers into high-resolution models (including data assimilation), assessment using multitracer and multivariable approaches (e.g., property-property analyses), and the use of models to extrapolate tracer data and estimate sampling error fields. Many of these activities rely on the implementation of a long-term global measurement program for ocean chemical tracers.

Chemical tracers are incorporated into ocean models for a variety of applications. These include ocean model validation efforts (e.g., CFCs, tritium, radiocarbon), studies of the oceanic carbon cycle (e.g., oxygen, carbonates, phosphates, nitrates), the diagnosis of model circulation mechanisms (e.g., argon, helium), data assimilation studies (e.g., CFCs, tritium), and the investigation of paleoceanographic circulation (carbon-13, oxygen-18). We have reviewed the use of chemical tracers in the context of assessing ocean circulation models. We highly recommend the simulation of chemical tracers in climate model assessment and validation studies and as a tool for analyzing water mass mixing and transformation in ocean models. A cost-effective approach is to simulate natural ^{14}C to assess long-timescale processes and CFCs for decadal to interdecadal ocean ventilation.
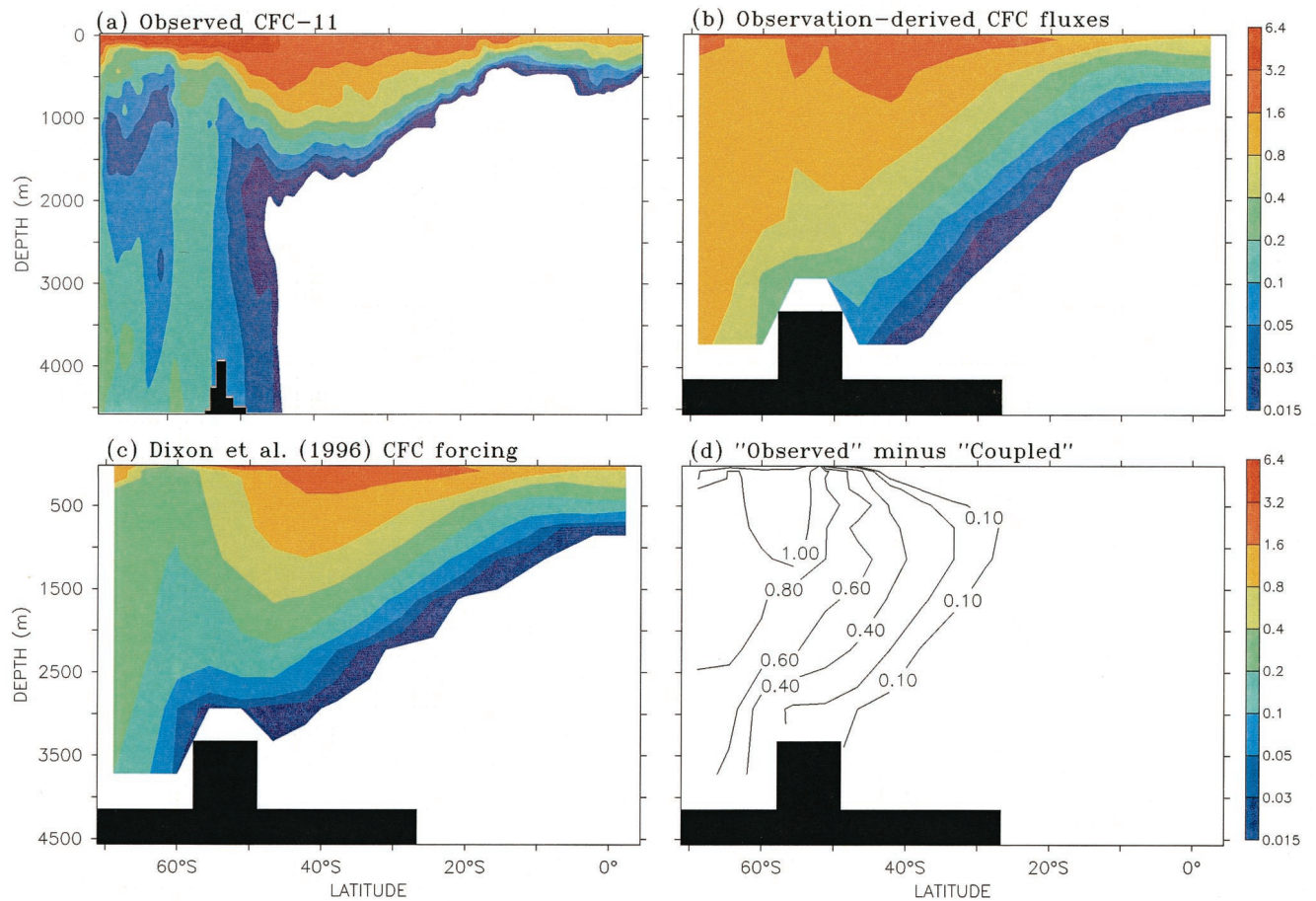
Plate 4. CFC-11 along the Ajax section in the South Atlantic (a) as observed; (b) in the *England* [1995] isopycnal run (ISO, using observation-derived CFC fluxes); (c) when ISO is rerun using *Dixon et al.* [1996] coupled model wind speed, sea-ice coverage and ocean T-S to compute k, solubilities, Schmidt numbers, and ice-reduced gas exchange; and (d) the difference between the two model runs. In Plate 4d, contours are drawn every 0.2 pmol kg^{-1}, with an additional curve at 0.1 pmol kg^{-1}. In the "observation-derived CFC flux" experiment, the *Wanninkhof* [1992] gas flux parameterization uses observed climatological winds to compute k and observed sea ice to limit air-sea gas fluxes in regions of ice coverage.

GLOSSARY

Chemical tracer: In the oceanographic context, any chemical compound, element, or isotope that is dissolved in seawater. These include naturally occurring compounds such as phosphates, silicates, nitrates, and carbonates as well as anthropogenic or man-made compounds (e.g., chlorofluorocarbons). Table 1 summarizes the main chemical tracers used to assess ocean circulation models and/or those included in biogeochemical models. Some naturally occurring tracers (e.g., radiocarbon, tritium, and carbon dioxide) have been dramatically increased in abundance due to human activities such as nuclear bomb testing and fossil fuel use. These tracers have a transient or time-dependent history and so can be useful in tracking ventilation processes in the ocean.

Ocean circulation model: A numerical computer simulation of flow patterns in the sea. These are analogous to atmospheric models that are used to predict weather patterns and climate, using known conservation equations over a discrete grid. Ocean models can be set up to study a range of phenomena: from the currents and water mass formation in the global ocean down to regional-scale flows (e.g., El Niño events) and circulation regimes in harbors and bays. They can require intensive computational calculations to resolve important oceanic processes such as eddies. Normally, they are forced by winds and air-sea fluxes of heat and fresh water. The tidal cycle is only considered in coastal-zone modeling. The models then predict ocean currents, temperature, salinity, and sometimes sea level.

Model resolution, oceanic eddies, and mixing: The "resolution" of an ocean model is the horizontal and/or vertical distance between adjacent grid boxes. Horizontal resolution is particularly important, as oceanic eddies have a relatively small spatial scale (~10–100 km, depending on latitude). Because eddies are energetic and have the capacity to mix and advect water properties, their effects must be parameterized in models of "coarse" resolution (>1/2°). A number of different mix-

ing schemes are presently used, from simple Cartesian mixing (wherein diffusion rates are aligned along the model grid) to more sophisticated schemes that orient mixing along isopycnal surfaces or take account of the effects of eddy-induced advection. It should be noted that all present-day global climate models are run at non-eddy-resolving resolution.

Ocean carbon cycle: The uptake and redistribution of carbon compounds (such as CO_2) by the oceans [see, e.g., *Heimann*, 1993]. Carbon compounds, both organic and inorganic, are exchanged between the ocean and atmosphere. In addition, a range of chemical, physical, and biological processes influence the distribution of carbon compounds in seawater and transformations between organic and inorganic species. These include biological consumption, chemical reactions in seawater, remineralization, upwelling, horizontal transport, mixing, and air-sea gas exchange. For example, because the oceans absorb, consume, and redistribute a component of anthropogenic CO_2, the recent rise in this atmospheric gas is substantially less than that expected from fossil fuel burning and deforestation.

Water mass: A body of ocean water with a common formation history, having its origin in a particular region of the ocean [*Tomczak*, 1999]. Typically, this implies a certain T-S and dissolved gas tracer signature. Some of the main large-scale water masses in the ocean include North Atlantic Deep Water (NADW), Antarctic Bottom Water (AABW), Antarctic Intermediate Water (AAIW), and Circumpolar Deep Water (CDW). Water masses are formed at the sea surface and ventilate the interior by subduction, convection, direct advection (ocean currents), and mixing. The "age" of a water mass is the time elapsed since the water was last at the sea surface. Some water masses (e.g., CDW) are formed primarily by a mixing product of other water masses (in the case of CDW, a product of NADW, AABW, and AAIW).

Ocean ventilation: The renewal of interior waters by seawater that has been in contact with the atmosphere. This occurs via any vertical transport mechanism, including subduction (direct advection of surface waters downward), convection (dense water overturn due to cold or saline surface conditions), and mixing (such as that generated by wind-driven turbulence). Deep-ocean currents then spread these waters into the ocean interior. In surface waters the atmosphere imprints a temperature-salinity (T-S) and chemical tracer signature via air-sea exchanges of heat, freshwater, and gases. This creates a certain surface water mass characteristic. Subsequent to the subduction or convective overturn of the surface water mass, it is only interior mixing and biogeochemical cycles (and for radionuclides, the natural decay of chemical isotopes) that modify the original atmospheric imprint.

Radioisotope (or radionuclide):   Atoms, such as radiocarbon (^{14}C) and tritium (^{3}H), that spontaneously undergo nuclear transformations at a fixed decay rate

and in doing so attain greater stability. The decay timescale varies greatly between isotopes (e.g., ^{14}C has a half-life of 5730 years compared with 12.4 years for ^{3}H and 269 years for ^{39}Ar). Naturally occurring radioisotopes are normally cosmogenic; that is, they are created in the atmosphere by cosmic rays. Artificial radioisotopes, such as ^{85}Kr and ^{137}Cs, are usually a result of nuclear bomb testing or nuclear reactor leakage.

REFERENCES

Aumont, O., J. C. Orr, D. Jamous, P. Monfray, O. Marti, and G. Madec, A degradation approach to accelerate simulations to steady-state in a 3-D tracer transport model of the global ocean, *Clim. Dyn.*, *14*, 101–116, 1998.

Bacastow, R., and E. Maier-Reimer, Ocean circulation model of the carbon cycle, *Clim. Dyn.*, *4*, 95–125, 1990.

Böning, C. W., F. O. Bryan, W. R. Holland, and R. Döscher, Deep water formation and meridional overturning in a high-resolution model of the North Atlantic, *J. Phys. Oceanogr.*, *26*, 1142–1164, 1996.

Broecker, W. S., and T. H. Peng, *Tracers in the Sea*, 690 pp., Lamont-Doherty Earth Obs., Palisades, N. Y., 1982.

Broecker, W. S., S. Blanton, W. M. Smethie, and G. Ostlund, Radiocarbon decay and oxygen utilization in the deep Atlantic Ocean, *Global Biogeochem. Cycles*, *5*, 87–117, 1991.

Broecker, W. S., S. Sutherland, and T. H. Peng, A possible 20th-century slowdown of Southern Ocean deep water formation, *Science*, *286*, 1132–1135, 1999.

Bryan, K., Models of the world ocean, *Dyn. Atmos. Oceans*, *3*, 327–338, 1979.

Bryan, K., and L. J. Lewis, A water mass model of the world ocean, *J. Geophys. Res.*, *84*, 2503–2517, 1979.

Buesseler, K. O., S. A. Casso, M. C. Hartman, and H. D. Livingston, Determination of fission products and activities in the Black Sea following the Chernobyl accident, *J. Radioanal. Nucl. Chem.*, *138*, 33–47, 1990.

Bullister, J. L., Chlorofluorocarbons as time-dependent tracers in the ocean, *Oceanography*, , 12–17, 1989.

Bullister, J. L., and R. F. Weiss, Anthropogenic chlorofluorocarbons in the Greenland and Norwegian Seas, *Science*, *221*, 265–268, 1983.

Bullister, J. L., and R. F. Weiss, Determination of the CCl_3F

and CCl_2F_2 in seawater and air, *Deep Sea Res.*, *35*, 839–853, 1988.

Caldeira, K., and P. B. Duffy, Sensitivity of simulated CFC-11 distributions in a global ocean model to the treatment of salt rejected during sea-ice formation, *Geophys, Res. Lett.*, *25*, 1003–1006, 1998.

Chen, C.-T. A., On the distribution of anthropogenic CO_2 in the Atlantic and Southern Oceans, *Deep Sea Res.*, *5*, 563–580, 1982a.

Chen, C.-T. A., Oceanic penetration of excess CO_2 in a cross section between Alaska and Hawaii, *Geophys. Res. Lett.*, *9*, 117–119, 1982b.

Craig, H., W. S. Broecker, and D. Spencer, *GEOSECS Pacific Expedition: Sections and Profiles*, U.S. Govt. Print. Off., Washington, D. C., 1981.

Craig, A. P., J. L. Bullister, D. E. Harrison, R. M. Chervin, and A. J. Semtner, A comparison of temperature, salinity, and chlorofluorocarbon observations with results from a 1° resolution three-dimensional global ocean model, *J. Geophys. Res.*, *103*, 1099–1119, 1998.

Danabasoglu, G., and J. C. McWilliams, Sensitivity of the global ocean circulation to parameterizations of mesoscale tracer transports, *J. Clim.*, *8*, 2967–2987, 1995.

Dickson, R. R., J. R. N. Lazier. J. Meincke, P.B. Rhines, and J. Swift, Long-term coordinated changes in the convective activity of the North Atlantic, *Prog. Oceanogr.*, *38*, 241–295, 1996.

Dixon, K. W., J. L. Bullister, I. H. Gammon, and R. J. Stouffer, Examining a coupled climate model using CFC-11 as an ocean tracer, *Geophys. Res. Lett.*, *23*, 1957–1960, 1996.

Doney, S. C., and J. L. Bullister, A chlorofluorocarbon section in the eastern North Atlantic, *Deep Sea Res.*, *39*, 1857–1883, 1992.

Doney, S. C., and W. J. Jenkins, Ventilation of the Deep Western Boundary Current and Abyssal Western North Atlantic: Estimates from tritium and He distributions, *J. Phys. Oceanogr.*, *24*, 638–659, 1994.

Doney, S. C., D. M. Glover, and W. J. Jenkins, A model function of the global bomb tritium distribution in precipitation, 1960–1986, *J. Geophys. Res.*, *97*, 5481–5492, 1992.

Doney, S. C., W. J. Jenkins, and H. G. Östlund, A tritium budget for the North Atlantic, *J. Geophys. Res.*, *98*, 18,069–18,081, 1993.

Duffy, P. B., D. Eliason, A. J. Bourgeois, and C. Covey, Simulation of bomb radiocarbon in two ocean general circulation models, *J. Geophys. Res.*, *100*, 22,545–22,563, 1995a.

Duffy, P. B., P. Eltgroth, A. J. Bourgeois, and K. Caldeira, Effect of improved subgrid-scale transport of tracers on uptake of bomb radiocarbon in the GFDL ocean general circulation model, *Geophys. Res. Lett.*, *22*, 1065–1068, 1995b.

Duffy, P. B., K. Caldeira, J. P. Selvaggi, and M. I. Hoffert, Effect of subgrid-scale mixing parameterizations on simulated distributions of natural ^{14}C, temperature, and salinity in a three-dimensional ocean general circulation model, *J. Phys. Oceanogr.*, *27*, 498–523, 1997.

Duplessy, J.-C., L. Labeyrie, A. Julliet-Leclerc, F. Maitre, J. Duprat, and M. Sarnthein, Surface salinity reconstruction of the North Atlantic Ocean during the last glacial maximum, *Oceanol. Acta*, *14*, 311–324, 1991.

Eby, M., and G. Holloway, Sensitivity of a large-scale ocean model to a parameterization of topographic stress, *J. Phys. Oceanogr.*, *24*, 2577–2588, 1994.

Elkins, J. W., T. M. Thompson, T. H. Swanson, J. H. Butler, B. D. Hall, S. O. Cummings, D. A. Fisher, and A. G. Raffo, Decrease in the growth rates of atmospheric chlorofluorocarbons 11 and 12, *Nature*, *364*, 780–783, 1993.

England, M. H., Representing the global-scale water masses in ocean general circulation models, *J. Phys. Oceanogr.*, *23*, 1523–1552, 1993.

England, M. H., Using chlorofluorocarbons to assess ocean climate models, *Geophys. Res. Lett.*, *22*, 3051–3054, 1995.

England, M. H., and A. C. Hirst, Chlorofluorocarbon uptake in a world ocean model, 2, Sensitivity to surface thermohaline forcing and subsurface mixing parameterization, *J. Geophys. Res.*, *102*, 15,709–15,731, 1997.

England, M. H., and G. Holloway, Simulations of CFC content and water mass age in the deep North Atlantic, *J. Geophys. Res.*, *103*, 15,885–15,901, 1998.

England, M. H., and S. Rahmstorf, Sensitivity of ventilation rates and radiocarbon uptake to subgrid-scale mixing in ocean models, *J. Phys. Oceanogr.*, *29*, 2802–2827, 1999.

England, M. H., J. S. Godfrey, A. C. Hirst, and M. Tomczak, The mechanism for Antarctic Intermediate Water renewal in a world ocean model, *J. Phys. Oceanogr.*, *23*, 1553–1560, 1993.

England, M. H., V. C. Garçon, and J.-F. Minster, Chlorofluorocarbon uptake in a world ocean model, 1, Sensitivity to the surface gas forcing, *J. Geophys. Res.*, *99*, 25,215–25,233, 1994.

Esbenson, S. K., and Y. Kushnir, The heat budget of the global ocean: An atlas based on estimates from surface marine observations, *Rep. 29*, Clim. Res. Inst., Oreg. State Univ., Corvallis, 1981.

Farley, K. A., E. Maier-Reimer, P. Schlosser, and W. S. Broecker, Constraints on mantle ^3He fluxes and deep-sea circulation from an ocean general circulation model, *J. Geophys. Res.*, *100*, 3829–3839, 1995.

Fiadiero, M. E., Three-dimensional modeling of tracers in the deep Pacific Ocean, 2, Radiocarbon and the circulation, *J. Mar. Res.*, *40*, 537–550, 1982.

Fine, R. A., Circulation of Antarctic Intermediate Water in the South Indian Ocean, *Deep Sea Res.*, *40*, 2021–2042, 1993.

Follows, M. J., and J. C. Marshall, On models of bomb ^{14}C in the North Atlantic, *J. Geophys. Res.*, *101*, 22,577–22,582, 1996.

Follows, M., D. Stammer, and C. Wunsch, Ventilation of CFC-11 in a global ocean circulation model constrained by WOCE data, *Int. WOCE Newsl.*, *35*, 3–5, 1999.

Gent, P. R., and J. C. McWilliams, Isopycnal mixing in ocean circulation models, *J. Phys. Oceanogr.*, *20*, 150–155, 1990.

Gent, P. R., J. Willebrand, T. J. McDougall, and J. C. McWilliams, Parameterizing eddy-induced tracer transports in ocean circulation models, *J. Phys. Oceanogr.*, *25*, 463–474, 1995.

Goosse, H., E. Deleersnijder, T. Fichefet, and M. H. England, Sensitivity of a global coupled ocean sea-ice model to the parameterization of vertical mixing, *J. Geophys. Res.*, *104*, 13,681–13,695, 1999.

Gordon, A. L., R. F. Weiss, W. M. Smethie, and M. J. Warner, Thermocline and intermediate water communication between the South Atlantic and Indian Oceans, *J. Geophys. Res.*, *97*, 7223–7240, 1992.

Gordon, H. B., and S. P. O'Farrell, Transient climate change in the CSIRO coupled model with dynamic sea ice, *Mon. Weather Rev.*, *125*, 875–907, 1997.

Gray, S. L., and T. W. N. Haine, Constraining a North Atlantic Ocean general circulation model with chlorofluorocarbon observations, *J. Phys. Oceanogr.*, in press, 2000.

Gruber, N., Anthropogenic CO_2 in the Atlantic Ocean, *Global Biogeochem. Cycles*, *12*, 165–191, 1998.

Gruber, N., J. L. Sarmiento and T. F. Stocker, An improved method for detecting anthropogenic CO_2 in the oceans, *Global Biogeochem. Cycles*, *10*, 809–837, 1996.

Guilyardi, E., and G. Madec, Performance of the OPA/ARPEGE-T21 global ocean-atmosphere coupled model, *Clim. Dyn.*, *13*, 149–165, 1997.

Haine, T. W. N., and S. L. Gray, Quantifying mesoscale variability in ocean transient tracer fields, *J. Geophys. Res*., in press, 2001.

Haine, T. W. N., and K. J. Richards, The influence of the seasonal mixed layer on oceanic uptake of CFCs, *J. Geophys. Res., 100*, 10,727–10,744, 1995.

Harms, I. H., Modelling the dispersion of ^{137}Cs and ^{239}Pu released from dumped waste in the Kara Sea, *J. Mar. Syst*., *13*, 1–20, 1997.

Heimann, M., The global carbon cycle in the climate system, in *Modelling Oceanic Climate Interactions*, edited by D. Anderson and J. Willebrand, *NATO ASI Ser., 111*, 299–336, 1993.

Heinze, C., E. Maier-Reimer, and K. Winn, Glacial pCO$_2$ reduction by the world ocean: Experiments with the Hamburg carbon cycle model, *Paleoceanography*, *6*, 395–430, 1991.

Heinze, C., E. Maier-Reimer, and P. Schlosser, Transient tracers in a global OGCM: Source functions and simulated distributions, *J. Geophys. Res*., *103*, 15,903–15,922, 1998.

Henderson, G. M., C. Heinze, R. F. Anderson, and A. M. E. Winguth, Global distribution of the ^{230}Th flux to ocean sediments constrained by GCM modeling, *Deep Sea Res*., *46*, 1861–1893, 1999.

Hirst, A. C., and W. Cai, Sensitivity of a world ocean GCM to changes in subsurface mixing parameterization, *J. Phys. Oceanogr*., *24*, 1256–1279, 1994.

Hirst, A. C., and T. J. McDougall, Deep water properties and surface buoyancy flux as simulated by a Cartesian model including eddy-induced advection, *J. Phys. Oceanogr*., *26*, 1320–1343, 1996.

Holloway, G., Representing topographic stress for large-scale ocean models, *J. Phys. Oceanogr*., *22*, 1033–1046, 1992.

Jia, Y., and K. J. Richards, Tritium distributions in an isopycnic model of the North Atlantic, *J. Geophys. Res*., *101*, 11,883–11,901, 1996.

Jenkins, W. J., Using anthropogenic tritium and ^{3}He to study subtropical gyre ventilation and circulation, *Philos. Trans. R. Soc. London, Ser. A*, *325*, 43–61, 1988.

Jenkins, W. J., and P. Rhines, Tritium in the deep North Atlantic Ocean, *Nature*, *286*, 877–880, 1980.

Jenkins, W. J., and W. M. Smethie, Transient tracers track ocean climate signals, *Oceanus*, *29*, 29–32, 1996.

Johns, T. C., R. E. Carnell, J. F. Crossley, J. M. Gregory, J. F. B. Mitchell, C. A. Senior, S. F. B. Tett, and R. A. Wood, The second Hadley Centre coupled ocean-atmosphere GCM: Model description, spinup and validation, *Clim. Dyn*., *13*, 103–134, 1997.

Key, R. M., WOCE Pacific Ocean radiocarbon program, *Radiocarbon*, *38*, 415–423, 1996.

Kroopnick, P. M., The distribution of ^{13}C of ΣCO$_2$ in the world oceans, *Deep Sea Res*., *32*, 57–84, 1985.

Ledwell, J. R., A. J. Watson, and C. S. Law, Evidence for slow mixing across the pycnocline from an open-ocean tracer-release experiment, *Nature*, *364*, 701–703, 1993.

Ledwell, J. R., A. J. Watson, and C. S. Law, Mixing of a tracer in the pycnocline, *J. Geophys. Res*., *103*, 21,499–21,529, 1998.

Levitus, S., Climatological atlas of the world ocean, *NOAA Prof. Pap*., *13*, 173 pp., U.S. Govt. Print. Off., Washington, D. C., 1982.

Libes, S. M., *An Introduction to Marine Biogeochemistry, 734 pp., John Wiley, New York, 1992.*

Liss, P. S., and L. Merlivat, Air-sea exchange rates: Introduction and synthesis, in *The Role of Air-Sea Exchange in Geochemical Cycling*, edited by P. Buat-Menard, pp. 113–127, D. Reidel, Norwell, Mass., 1986.

Loosli, H. H., ^{39}Ar: A tool to investigate ocean water circulation and mixing, in *Handbook of Environmental Isotope Chemistry*, vol. 3, *The Marine Environment*, edited by P.

Fritz and J. C. Fontes, pp. 385–392, Elsevier Sci., New York, 1989.

Lovelock, J. E., and G. E. Ferber, Exotic tracers for atmospheric studies, *Atmos. Environ., 16*, 1467–1471, 1982.

Lupton, J. E., and H. Craig, A major helium-3 source at 15°S on the East Pacific Rise, *Science*, *214*, 13–18, 1981.

Maier-Reimer, E., Design of a 3D biogeochemical tracer model for the ocean, in *Modelling Oceanic Climate Interactions*, edited D. Anderson and J. Willebrand, *NATO ASI Ser., 111*, 415–464, 1993a.

Maier-Reimer, E., Geochemical cycles in an ocean general circulation model: Preindustrial tracer distributions, *Global Biogeochem. Cycles*, *7*, 645–677, 1993b.

Maier-Reimer, E., and R. Bacastow, Modelling of geochemical tracers in the ocean, in *Climate-Oceanic Interactions, NATO ASI Ser*., edited by M. E. Schlesinger, pp. 233–267, Kluwer Acad., Norwell, Mass., 1990.

Maier-Reimer, E., and K. Hasselmann, Transport and storage of CO$_2$ in the ocean—An inorganic ocean circulation carbon cycle model, *Clim. Dyn*., 63–90, 1987.

Manabe, S., R. J. Stouffer, M. J. Spelman, and K. Bryan, Transient responses of a coupled ocean-atmosphere model to gradual changes of atmospheric carbon dioxide, part I, Annual mean response, *J. Clim*., *4*, 785–818, 1991.

Manabe, S., M. J. Spelman, and R. J. Stouffer, Transient responses of a coupled ocean-atmosphere model to gradual changes of atmospheric carbon dioxide, part II, Seasonal response, *J. Clim*., *5*, 105–126, 1992.

Marotzke, J., Ocean models in climate problems, in *Ocean Processes in Climate Dynamics: Global and Mediterranean Examples*, edited by P. Malanotte-Rizzoli and A. R. Robinson, Norwell, Mass., pp. 79–109, Kluwer Acad., 1994.

McCartney, M. S., Subantarctic mode water, *Deep Sea Res*., *24*, suppl., 103–119, 1977.

McWilliams, J. C., Modeling the oceanic general circulation, *Annu. Rev. Fluid Mech*., *28*, 215–248, 1996.

Meméry, L., and C. Wunsch, Constraining the North Atlantic circulation with tritium data, *J. Geophys. Res*., *95*, 5239–5256, 1990.

Mikolajewicz, U., A meltwater induced collapse of the "conveyor belt" thermohaline circulation and its influence on the distribution of Δ^{14}C and δ^{18}O in the oceans, *Rep. 189*, 25 pp., Germany, Max Planck Inst. für Meteorol., 1996.

Molina, M. J., and F. S. Rowland, Stratospheric sink for chlorofluoromethanes: Chlorine atom catalysed destruction of ozone, *Nature*, *249*, 810–812, 1974.

Najjar, R. J., J. L. Sarmiento, and J. R. Toggweiler, Downward transport and fate of organic matter in the ocean: Simulations with a general circulation model, *Global Biogeochem. Cycles*, *6*, 45–76, 1992.

Orr, J. C., Ocean circulation and the ocean carbon-cycle model intercomparison project, *Int. WOCE Newsl*., *35*, 24–25, 1999.

Orr, J. C., E. Brian, and O. Aumont, Argon-39 as a complementary tracer to evaluate deep-ocean circulation in a 3-D global ocean model (abstract), *Eos Trans. AGU*, *79*(1) Ocean Sci. Meet. Suppl., OS180, 1998.

Orr, J. C., et al., Estimates of anthropogenic carbon uptake from four three-dimensional ocean models, *Global Biogeochem. Cycles*, in press, 2001.

Ostlund, H. G., H. Craig, W. S. Broecker, and D. Spencer, *GEOSECS Atlantic, Pacfic, and Indian Ocean Expeditions: Shorebased Data and Graphics*, vol. 7, U.S. Govt. Print. Off., Washington, D. C., 1987.

Peng, T.-H., E. Maier-Reimer, and W. S. Broecker, Distribution of ^{32}Si in the world ocean: Model compared to observation, *Global Biogeochem. Cycles*, *7*, 463–474, 1993.

Pickart, R. S., N. G. Hogg, and W. M. Smethie, Determining the strength of the Deep Western Boundary Current using

the chlorofluoromethane ratio, *J. Phys. Oceanogr.*, *19*, 940–951, 1989.

Poole, R., and M. Tomczak, Optimum multiparameter analysis of the water mass structure in the Atlantic Ocean thermocline, *Deep Sea Res.*, *46*, 1895–1921, 1999.

Redler, R., and J. Dengg, Spreading of CFCs in numerical models of differing resolution, *Int. WOCE Newsl.*, *35*, 12–14, 1999.

Redler, R., K. Ketelsen, J. Dengg, and C. W. Böning, A high resolution numerical model for the circulation of the Atlantic Ocean, in *Proceedings of the Fourth European SGI/Cray MPP Workshop*, edited by H. Lederer and F. Hertweck, pp. 95–108, Max Planck Inst. for Plasma Stud., Garching, Germany, 1998.

Rhein, M., Ventilation rates of the Greenland and Norwegian Seas derived from distributions of the chlorofluoromethanes F11 and F12, *Deep Sea Res.*, *38*, 485–503, 1991.

Rhein, M., The Deep Western Boundary Current: Tracers and velocities, *Deep Sea Res.*, *41*, 263–281, 1994.

Ribbe, J., Ventilation processes in a Southern Ocean model, Ph.D. thesis, 251 pp., Flinders Univ. of South Aust., Adelaide, Australia, 1996.

Ribbe, J., and M. Tomczak, On convection and the formation of Subantarctic Mode Water in the Fine Resolution Antarctic Model (FRAM), *J. Mar. Syst.*, *13*, 137–154, 1997.

Rintoul, S. R., and M. H. England, Ocean transport dominates air-sea fluxes in driving variability of Subantarctic Mode Water, *J. Phys. Oceanogr.*, in press, 2000.

Robitaille, D. Y., and A. J. Weaver, Validation of subgrid-scale mixing schemes using CFCs in a global ocean model, *Geophys. Res. Lett.*, *22*, 2917–2920, 1995.

Roemmich, D., and C. Wunsch, Apparent changes in the climatic state of the deep North Atlantic Ocean, *Nature*, *307*, 447–450, 1984.

Roether, W., R. Schlitzer, A. Putzka, P. Beining, K. Bulsiewicz, G. Rohardt, and F. Delahoyde, A chlorofluoromethane and hydrographic section across Drake Passage: Deep water ventilation and meridional property transport, *J. Geophys. Res.*, *98*, 14,423–14,435, 1993.

Rogers, K. B., M. A. Cane, and D. P. Schrag, Seasonal variability of sea surface $\Delta^{14}C$ in the equatorial Pacific in an ocean circulation model, *J. Geophys. Res.*, *102*, 18,627–18,639, 1997.

Sabine, C. L., R. M. Key, K. M. Johnson, F. J. Millero, A. Poisson, J. L. Sarmiento, D. W. R. Wallace, and C. D. Winn, Anthropogenic CO_2 inventory of the Indian Ocean, *Global Biogeochem. Cycles*, *13*, 179–198, 1999.

Sarmiento, J. L., A simulation of bomb tritium entry into the Atlantic Ocean, *J. Phys. Oceanogr.*, *13*, 1924–1939, 1983.

Sarmiento, J. L., and C. Le Quéré, Oceanic CO_2 uptake in a model of century-scale global warming, *Science*, *274*, 1346–1350, 1996.

Sarmiento, J. L., J. C. Orr, and U. Siegenthaler, A perturbation simulation of CO_2 uptake in an ocean general circulation model, *J. Geophys. Res.*, *97*, 3621–3645, 1992.

Sarmiento, J. L., R. D. Slater, M. J. R. Fasham, H. W. Ducklow, J. R. Toggweiler, and G. T. Evans, A seasonal three-dimensional ecosystem model of nitrogen cycling in the North Atlantic euphotic zone, *Global Biogeochem. Cycles*, *7*, 417–450, 1993.

Sarmiento, J. L., R. Murnane, and C. Le Quéré, Air-sea CO_2 transfer and the carbon budget of the North Atlantic, *Philos. Trans. R. Soc. London*, *348*, 211–219, 1995.

Schlitzer, R., Assimilation of CFC data into an ocean circulation model, *Int. WOCE Newsl.*, *23*, 23–25, 1996.

Schlosser, P., J. L. Bullister, and R. Bayer, Studies of deep water formation and circulation in the Weddell Sea using natural and anthropogenic tracers, *Mar. Chem.*, *35*, 97–122, 1991.

Schlosser, P., G. Bönisch, B. Kromer, H. H. Loosli, B. Buhler, R. Bayer, G. Bonani, and K. P. Koltermatin, Mid-1980's distribution of tritium, ^{3}He, ^{14}C and ^{39}Ar in the Greenland/Norwegian seas and the Nansen Basin of the Arctic Ocean: Implications for large-scale circulation patterns, *Prog. Oceanogr.*, *35*, 1–28, 1995.

Schmidt, G. A., Oxygen-18 variations in a global ocean model, *Geophys. Res. Lett.*, *25*, 1201–1204, 1998.

Semtner, A. J., and R. M. Chervin, Ocean general circulation from a global eddy-resolving model, *J. Geophys. Res.*, *97*, 5493–5550, 1992.

Shackleton, N. J., Tropical rainforest history and the equatorial Pacific carbonate dissolution cycles, in *The Fate of Fossil Fuel CO_2 in the Oceans*, edited by N. R. Anderson and A. Malahoff, pp. 401–428, Plenum, New York, 1977.

Smethie, W. M., Tracing the thermohaline circulation in the western North Atlantic using chlorofluorocarbons, *Prog. Oceanogr.*, *31*, 51–99, 1993.

Smethie, W. M., and J. H. Swift, The tritium:krypton-85 age of Denmark Strait overflow water and Gibbs fracture zone water just south of Denmark Strait, *J. Geophy. Res.*, *94*, 8265–8275, 1989.

Smethie, W. M., T. T. Takahashi, D. W. Chipman, and J. R. Ledwell, Gas exchange and CO_2 flux in the tropical Atlantic Ocean determined from ^{222}Rn and pCO_2 measurements, *J. Geophys. Res.*, *90*, 7005–7022, 1985.

Smethie, W. M., H. G. Östlund, and H. H. Loosli, Ventilation of the deep Greenland and Norwegian seas: Evidence from krypton-85, tritium, carbon-14, and argon-39, *Deep Sea Res.*, *33*, 675–703, 1986.

Stanev, E. V., K. O. Buesseler, J. V. Staneva, and H. D. Livingston, A comparison of modeled and measured Chernobyl ^{90}Sr distributions in the Black Sea, *J. Environ. Radioact.*, *43*, 187–203, 1999.

Staneva, J. V., K. O. Buesseler, E. V. Stanev, and H. D. Livingston, The application of radiotracers to a study of Black Sea circulation: Validation of numerical simulations against observed weapons testing and Chernobyl ^{137}Cs data, *J. Geophy. Res.*, *104*, 11,099–11,114, 1999.

Stouffer, R. J., S. Manabe, and K. Bryan, Interhemispheric asymmetry in climate response to a gradual increase of atmospheric CO_2, *Nature*, *342*, 660–662, 1989.

Sundermeyer, M. A., and J. F. Price, Lateral mixing and the North Atlantic Tracer Release Experiment: Observations and numerical simulations of Lagrangian particles and a passive tracer, *J. Geophys. Res.*, *103*, 21,481–21,497, 1998.

Taylor, C. B., and W. Roether, A uniform scale for reporting low-level tritium measurements in water, *Int. J. Appl. Radiat. Isot.*, *33*, 377–382, 1982.

Taylor, N. K., Seasonal uptake of anthropogenic CO_2 in an ocean general circulation model, *Tellus, Ser. B*, *47*, 145–169, 1995.

Toggweiler, J. R., K. Dixon, and K. Bryan, Simulations of radiocarbon in a coarse-resolution world ocean model, I, Steady state prebomb distributions, *J. Geophys. Res.*, *94*, 8217–8242, 1989a.

Toggweiler, J. R., K. Dixon, and K. Bryan, Simulations of radiocarbon in a coarse-resolution world ocean model, 2, Distributions of bomb-produced carbon 14, *J. Geophys. Res.*, *94*, 8243–8264, 1989b.

Toggweiler, J. R., K. Dixon, and W.S. Broecker, The Peru upwelling and the ventilation of the South Pacific thermocline, *J. Geophys. Res.*, *96*, 20,467–20,497, 1991.

Tomczak, M., Some historical, theoretical and applied aspects of quantitative water mass analysis, *J. Mar. Res.*, *57*, 275–303, 1999.

Trumbore, S. E., S. S. Jacobs, and W. M. Smethie, Chlorofluorocarbon evidence for rapid ventilation of the Ross Sea, *Deep Sea Res.*, *38*, 845–870, 1991.

Walker, S. J., R. F. Weiss, and P. K. Salameh, Reconstructed histories of the annual mean atmospheric mole fractions for the halocarbons CFC-11, CFC-12, CFC-113, and carbon tetrachloride, *J. Geophys. Res.*, *105*, 14,285–14,296, 2000.

Wallace, D. W. R., and J. R. N. Lazier, Anthropogenic chlorofluoromethanes in newly formed Labrador Sea water, *Nature*, *332*, 61–63, 1988.

Wanninkhof, R., Relationship between wind speed and gas exchange over the ocean, *J. Geophys. Res.*, *97*, 7373–7382, 1992.

Warner, M. J., and R. F. Weiss, Solubilities of chlorofluorocarbons 11 and 12 in water and seawater, *Deep Sea Res.*, *32*, 1485–1497, 1985.

Warner, M. J., and R. F. Weiss, Chlorofluoromethanes in South Atlantic Antarctic Intermediate Water, *Deep Sea Res.*, *39*, 2053–2075, 1992.

Watson, A. J., J. R. Ledwell, and S. C. Sutherland, The Santa Monica Basin Tracer Experiment: Comparison of release methods and performance of perfluorodecalin and sulfur hexafluoride, *J. Geophys. Res.*, *95*, 8719–8725, 1991.

Weaver, A. J., P. B. Duffy, M. Eby, and E. C. Wiebe, Evaluation of ocean and climate models using present-day observations and forcing, *Atmos. Ocean*, *38*, 271–301, 2000.

Weiss, R. F., The solubility of nitrogen, oxygen, and argon in water and sea water, *Deep Sea Res.*, *17*, 721–735, 1970.

Weiss, R. F., Carbon dioxide in water and sea water: The solubility of a nonideal gas, *Mar. Chem.*, *2*, 203–215, 1974.

Weiss, R. F., J. L. Bullister, R. H. Gammon, and M. J. Warner, Atmospheric chlorofluoromethanes in the deep equatorial Atlantic, *Nature*, *314*, 608–610, 1985.

Weiss, W., and W. Roether, The rates of tritium input in the world ocean, *Earth Planet. Sci. Lett.*, *49*, 435–446, 1980.

Woods, J. D., Wave-induced shear instability in the summer thermocline, *J. Fluid Mech.*, *32*, 791–800, 1968.

M. H. England, Centre for Environmental Modelling and Prediction, School of Mathematics, University of New South Wales, Sydney, N. S. W. 2052, Australia. (m.england@unsw.edu.au)

E. Maier-Reimer, Max-Planck-Institut für Meteorologie, Bundesstrasse 55, 20146 Hamburg, Germany.